BIOMEDICAL TESTING BY DIRECT SAMPLING IONIZATION WITH MINIATURE MASS SPECTROMETRY SYSTEMS

by

Spencer Chih-Kai Chiang

A Dissertation

Submitted to the Faculty of Purdue University

In Partial Fulfillment of the Requirements for the degree of

Doctor of Philosophy

Weldon School of Biomedical Engineering

West Lafayette, Indiana

December 2020

THE PURDUE UNIVERSITY GRADUATE SCHOOL
STATEMENT OF COMMITTEE APPROVAL

Dr. Zheng Ouyang, Co-Chair

Weldon School of Biomedical Engineering

Dr. Huang Fang, Co-Chair

School of Aeronautics and Astronautics

Dr. Riyi Shi

Weldon School of Biomedical Engineering

Dr. Yu Xia

Department of Chemistry

Approved by:

Dr. George R. Wodicka

Dedicated to my friends and family.
None of this would be possible without their unyielding
and unwavering support.

ACKNOWLEDGMENTS

My journey through Purdue and subsequently, Tsinghua, was full of twists and turns. Starting from an incredible, yet terrifying experience of relocating across the globe to the strange circumstances that dominated 2020, I can easily say that this has been an experience of a lifetime. As I transition to a new chapter in my life, I will forever be appreciative of the people I met and worked with these last five years.

Firstly, I wish to express my sincere and heartfelt appreciation to my advisor, Professor Zheng Ouyang, who has always been a source of inspiration and opportunity. He is driven, motivated, and enthusiastic; always inspiring me and my fellow peers to be creative and think outside of the box. I would be remiss if I did not mention all of the knowledge he taught me on mass spectrometry and how our research fit into the bigger picture. Without him as my advisor, there would be a countless number of missed opportunities; for all of which, I will always be appreciative.

I would like to thank Dr. Fang Huang for being my co-advisor and co-chair of my committee. Although his research field differs from mine, he was always encouraging and helpful whenever I needed it. I would also like to thank Dr. Riyi Shi and Dr. Yu Xia as my committee members. They offered a lot of help regarding my research and career development.

I wish to give a special acknowledgement to Dr. Wenpeng Zhang. His guidance and advice he gave on my research was impeccable. He was always there to support me throughout my research, answer my questions, and assist in solving any problems that inevitably arose throughout my research. Furthermore, he helped me greatly in transitioning between countries. I am profoundly grateful to have been able to work with him and wish him the best in his future endeavors.

I wish to thank Dr. Yue Ren for guiding me in my research as an undergraduate student at Purdue University. He taught me the basics of research and how to operate the miniature mass spectrometer. Working with him helped me decide to continue research and pursue a graduate career. I would also like to give special thanks to all the group members in Dr. Ouyang's lab at both Purdue and Tsinghua University. It was my pleasure to work with all the talented people there. I would also like to thank all the people at Purspec Technologies for their helpful advice and accommodations for me whenever I suddenly needed to use a Mini β.

Finally, I would like to thank my family and friends; all of whom, have been continually understanding and supportive. It was my father who first taught me about mass spectrometry and encouraged me to pursue a PhD degree, while my mother gave her unyielding support—despite my unintentional decisions to be as far as possible from home. My brother has always been a staunch supporter of me, no matter what I decided to do. I would also like to thank my girlfriend, Yang Jing, for all her love and support. The twists and turns in life are never easy, but she makes every moment worthwhile. For all these reasons and much, much more, I am forever grateful. None of this would be possible without you all. Thank you.

TABLE OF CONTENTS

LIST OF TABLES

LIST OF FIGURES

LIST OF ABBREVIATIONS

In-Text Abbreviations

Abbreviation	Definition
AC	Alternating Current
CID	Collision-Induced Dissociation
CST	Cell Signaling Technology
DAPI	Discontinuous Atmospheric Pressure Interface
ELISA	Enzyme-Linked Immunosorbent Assay
FDA	U.S. Food and Drug Administration
GC	Gas Chromatography
HIPAA	Health Insurance Portability and Accountability Act
IS	Internal Standard
LC	Liquid Chromatography
LIT	Linear Ion Trap
LOD	Limit of Detection
LOQ	Limit of Quantitation
MALDI	Matrix-Assisted Laser Desorption Ionization
MS	Mass Spectrometry
MS/MS	Tandem Mass Spectrometry or MS^2
MSAE	Mass Selective Axial Ejection or Scan-out
MSAT	Mass Selective Axial Transfer
nESI	Nano-Electrospray Ionization
PB	Paternò-Büchi
PCA	Principal Component Analysis
POC	Point-of-Care
PSI	Paper Spray Ionization
RF	Radiofrequency
RSD	Relative Signal Deviation
SEM	Scanning Electron Microscope
SFME	Slug-Flow Microextraction
SISCAPA	Stable Isotope Standards and Capture by Anti-Peptide Antibodies
SWIFT	Stored Waveform Inverse Fourier Transform
T1 Phase	Phase 1 of Translational Medicine
T2 Phase	Phase 2 of Translational Medicine
T2D	Type-2 Diabetes

TAT	Turnaround Time
TB	Tuberculosis
UV	Ultraviolet
WHO	World Health Organization

Chemical List Abbreviations

Abbreviation	Definition
2-EHB	2-ethylhexyl-4-hydroxybenzoate
3-MAPS	3-methacryloxypropyltrimethoxysilane
6-MPC	6-methyl-4-phenyl-2-chromanone
β-CD	β-Cyclodextrin
AA	Acrylamide
AB1	Aflatoxin B1
AB2	Aflatoxin B2
ACN	Acetonitrile
AIBN	2,2'-Azobis(2-methylpropionitrile)
DCM	Dichloromethane
DON	Deoxynivalenol
EA	Ethyl Acetate
EGDMA	Ethylene Glycol Dimethacrylate
FA	Fatty Acid
HDL	High-density Lipoprotein
HEX	Hexakis(1H, 1H, 5H-octafluoropentoxy)-phosphazine
LDL	Low-density Lipoprotein
PC	Phosphatidylcholine
PG	Phosphatidylglycerol
PS	Phosphatidylserine
PSA	Prostate Specific Antigen
ZEAR	Zearalenone

ABSTRACT

Biomedical testing by mass spectrometry (MS) in clinical laboratories is fundamental to providing clinicians with accurate information to confirm their initial diagnoses. However, laboratory-based testing requires careful handling, transport, and complex sample analysis to achieve results with appropriate sensitivities. Patient results are reviewed during the next schedule appointment, hindering the initiation of treatment and adversely affecting patient health outcomes. The introduction of miniature MS systems and its related studies have introduced a basic outline for the implementation of a point-of-care (POC) biomedical testing tool. Current miniature MS systems have been applied to analyzing and monitoring therapeutic drugs and drugs of abuse, using simple sampling procedures. As biomedical testing begins to shift towards analyzing biomolecules, this dissertation seeks to further the applicability of direct sampling ionization with miniature MS systems. Biomolecules with current and emerging diagnostic significance such as proteins, metabolites, and lipids were analyzed using a miniature MS system, integrating both conventional and novel sampling methods.

The first study introduces a protein biomarker analytical workflow using a miniature MS system tied to an immunoaffinity enrichment protocol. A dual linear ion trap miniature MS system was optimized to quantify peptides in solution across a wide mass range, performing high-efficiency tandem MS at a relatively high sensitivity. Amino acid sequences of the digested peptides were identified using several types of collision-induced dissociation (CID). Quantitation of peptides was performed within a solution matrix of similarly digested peptides through the incorporation of internal standards (IS) and product ion monitoring. Finally, the entire workflow was tested by quantifying the targeted *Met* peptide sequence from cell line with a low *Met* protein expression level.

The second study establishes a workflow for lipid profiling of biofluids using a novel direct sampling ionization method with our miniature MS system. Downstream from proteins, lipids represent a class of metabolic biomolecules that directly reflect the biological state. Metabolic diseases cause a distinct perturbation from the norm that is reflected in the lipid profile acquired from comprehensive extraction and analysis. Polymer-coating transfer enrichment was developed to improve the extraction efficiency of lipids from biofluids while eliminating the sample matrix in less than a minute. Photochemical reactions were combined with the novel direct sampling

method for enhanced lipid structure elucidation. Preliminary investigations into the free fatty acid profile of healthy and Type-2 diabetes human patient plasma samples was performed, resulting in several distinct profiles for disease differentiation.

The final study builds a workflow to analyze exogenous metabolites, specifically mycotoxins produced by fungi, in feed and foodstuffs. Mycotoxins pose a significant concern to the world's grain storages, emphasizing the need for constant monitoring to minimize mycotoxin exposure and ingestion. By combining slug-flow microextraction with a miniature MS system, four different mycotoxins were analyzed in different matrices. A surface analysis technique was also proposed, eliminating the need for initial sample preparation before analysis. Trace amounts of mycotoxins could be detected from the surface of a corn kernel without sample destruction. Thus, a universal workflow for continuous monitoring of mycotoxins in grain storages worldwide was outlined in this study.

1. INTRODUCTION

In the modern healthcare landscape, diverse types of diagnostics are available including clinical, imaging, and laboratory-based diagnostics. Each type of diagnostic is important in their own respect; clinical diagnostics providing initial patient assessment of exhibited symptoms, and imaging diagnostics elucidating visual abnormalities within the body. However, laboratory diagnostics is especially important, providing physicians and healthcare professionals with valuable information on the optimal treatment path and confirming their clinical diagnosis.[1] Biomedical testing represents a considerable amount of laboratory diagnostics, representing analytical tests with numerous clinical uses.[2] In most cases, biomedical testing encompasses the testing of various biomolecules to identify disease outcomes. Due to the important of biomedical testing in laboratory diagnostics, these two terms are used interchangeably. Focusing on certain molecular markers such as pharmaceutical drugs[3], drugs of abuse[4], metabolites[5], and protein biomarkers[6], biomedical testing helps achieve numerous clinical objectives such as screening, disease classification, and prognosis, summarized in Table 1-1.[7] Results from biomedical testing can confirm or guide physicians towards the correct treatment paths and highlight any complications that may arise within the individual.

The importance of biomedical testing is exemplified by 29-38% of primary-care physician visits requiring one or more laboratory tests.[8, 9] Based on a study in a single major medical center with over one million patients in a year, 98% of inpatients, 56% of emergency department visits, and 29% of outpatients had laboratory tests to confirm their clinical diagnosis.[10] These modern biomedical advancements provide invaluable data regarding disease type, status, and patient individuality, contributing directly to improving healthcare outcomes.[11] In comparison to the older healthcare model of solely relying upon clinical diagnostics such as physician experience and clinical symptom identification, it is evident that patient quality of life has significantly improved in correlation to improved diagnostics due to a steep decrease in mortality rates.[12, 13] However, as new diseases emerge, biomedical testing has reached a plateau in its ability to improve health outcomes, highlighting several issues within the diagnostics healthcare pathway.

The diagnostic healthcare pathway can be outlined into several steps as seen in Figure 1-1. The entire pathway is initiated by the patient, where individuals begin the healthcare cycle by

Table 1-1. Classification of diagnostic biomolecules and their clinical objectives.[7]

Diagnostic Use	Clinical Objective
Classification	Stratification of a specific disease by one of its subsets
Diagnostics	Confirm or rule-out the presence of a specified disease
Prognosis	Risk-assessment of disease and time to clinical outcome
Prediction	Predict the optimal treatment route with respect to specific individuals
Screening	Predict the optimal treatment route with respect to specific individuals
Treatment Monitoring	Determination of efficacy of therapy and elimination of adverse effects
Post-treatment Monitoring	Prevention of disease recurrence and enforce post-treatment compliance.

entering a hospital or health center with a symptomatic issue. At this point, a clinician will make their initial diagnosis based on the standard visual indicators or basic health examinations, such as heart rate, blood pressure, or auditory/respiratory inspections. Laboratory work specific to the exhibited symptoms are ordered by the clinician for sample collection to occur. Depending on the diagnosis, various sample types can be collected. Peripheral blood[14], venal blood[15], tissue biopsies[16], sputum[17], and saliva[18] are all various common sample types that can be collected for biomedical testing. Afterwards, samples need to be appropriately collected, transported, and delivered to the correct laboratory. Within each designated laboratory, the sample is prepared for analysis by a trained laboratory technician before performing the ordered test. After the results are collected and quickly scanned for obvious errors, a summary is sent back to the hospital following the appropriate Health Insurance Portability and Accountability Act (HIPAA) regulations. Finally, the primary physician interprets and confirms their diagnosis based on the results of the biomedical test. In cases of rarer disease or co-infection of several diseases, several diagnostic cycles may need to occur before initiation of treatment.[19, 20] These delays can easily accumulate and extend into the next scheduled appointment, usually a day to a week later. As a result, treatment initiation is also delayed and hinders timely treatment of more time-sensitive diseases.[21-23] Minimization of the amount of time needed for diagnostics would be a key aspect in establishing prompt treatment and providing patients with the best personalized healthcare.

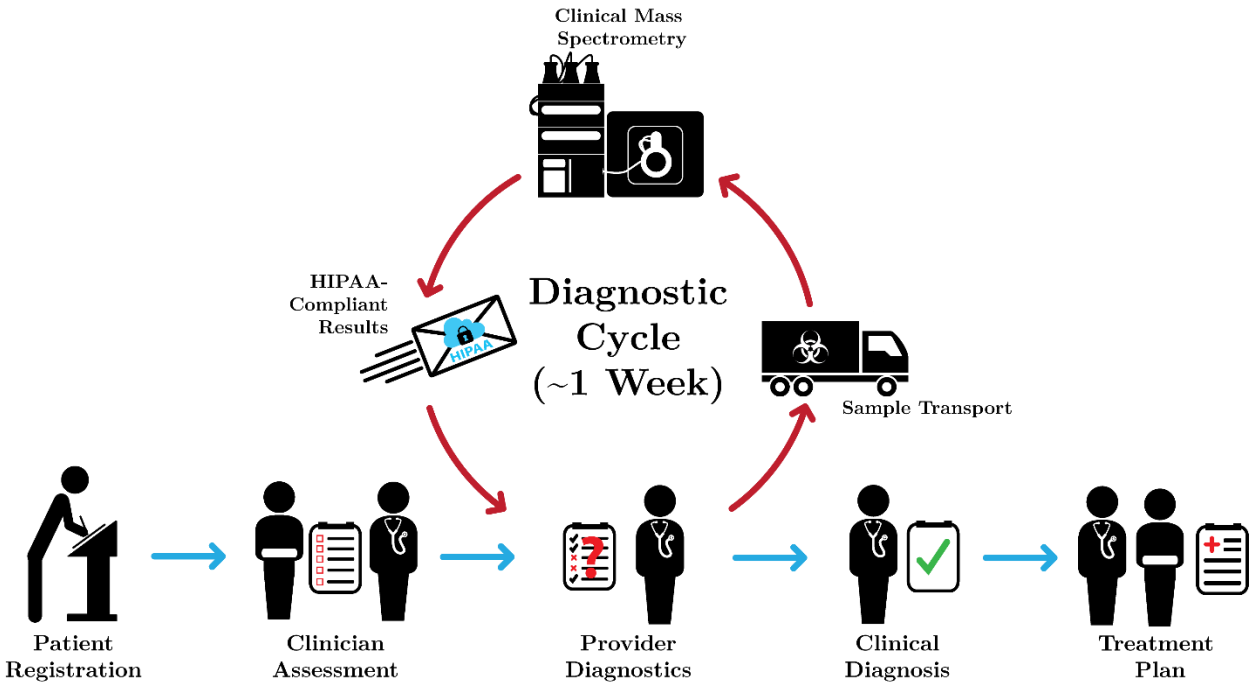

Figure 1-1. Overall workflow of biomedical testing involving clinical mass spectrometry assays.

To minimize the amount of time needed for laboratory diagnostics, studies have measured the efficacy of biomedical tests using turnaround time (TAT).[24, 25] TAT focuses on the time it takes for a sample to be analyzed within the laboratory and is emphasized when developing new laboratory diagnostics. In a study of 657 hospital institutions, a routine blood screening test has a TAT average of 73 minutes.[26] However, TAT is limited in its scope, measuring solely intra-laboratory activities.[27] Other time-consuming activities such as sample delivery and mishandling are unaccounted for. Complex laboratory tests, high patient volumes, and errors in sample collection / delivery can all exponentially increase diagnostic time without affecting the definition of TAT. Another issue that arises is the number of available diagnostic tests. With the current diverse set of sample types and molecular markers, it is impossible for a single laboratory to perform a comprehensive panel of tests. Each different molecule has different targeted effective ranges, various reagents, antibodies, and instrument types that can strain the limited resources available within a clinical laboratory.[28] In response, some laboratories have transitioned into highly specialized laboratories operating research-grade instruments, providing enhanced specificity and sensitivity needed for detection of a specific sample type or molecule.[29-31] Hospitals are required

to contract multiple laboratories to handle different sample types and with different biomedical testing protocols as seen in Figure 1-2.

In order to accommodate the diversity in sample type and laboratories, samples are collected in batches to send to the appropriate laboratory for analysis.[32, 33] This introduces another set of potential pitfalls and delays in treatment initiation. Overall, laboratory diagnostics has become a major bottleneck in the overall healthcare landscape, hindering decision-making downstream. Improvements to modern technology has improved the sensitivity of biomedical tests significantly, but the diversity of unique biomedical devices has also resulted in a patchwork, non-unified system with numerous pitfalls.[34] In order to grasp the scope of biomedical testing, further inspection into the different types of laboratory diagnostics is needed.

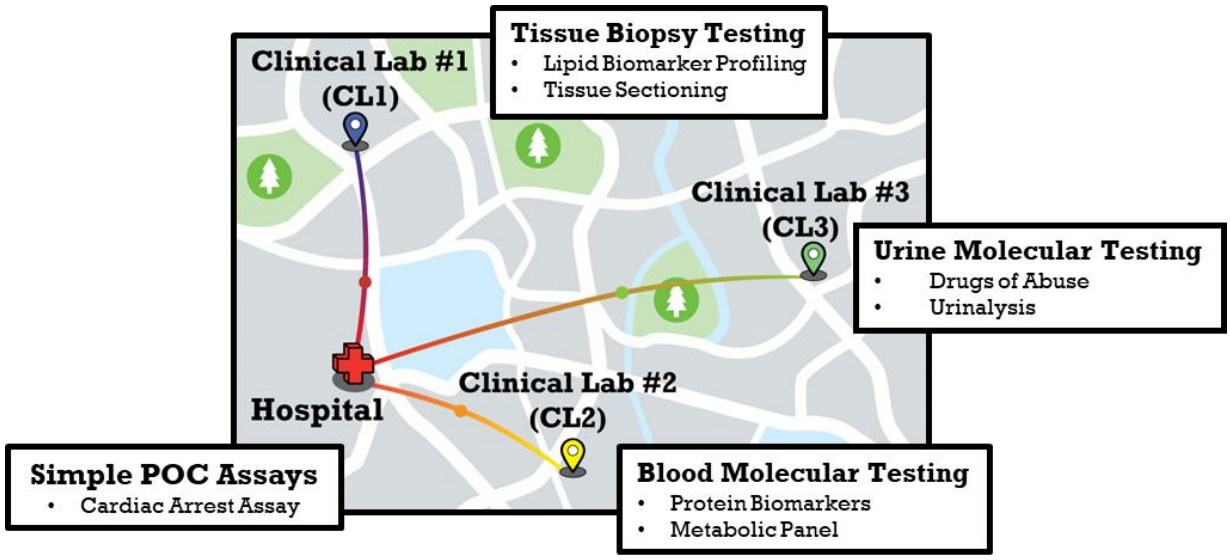

Figure 1-2. Decentralized clinical laboratories for biomedical testing. Different laboratories focus on analyzing varying types of patient samples.

1.1 Instrumentation in Clinical Laboratories

Within a clinical laboratory, there are numerous kinds of instruments available for testing patient samples. However, due to the specificity of clinical laboratories, the instruments available in each laboratory is decided upon the specified sample type analyzed and the targeted volume of patient samples to be analyzed. This can vary from a chemistry-based laboratory analyzing biofluids— blood, urine, fluids— or a microbiology laboratory—tissues and cell cultures. Although each clinical laboratory has its own specific needs, for biomedical testing, clinical

laboratories generally rely upon two major type of analyses: immunoassays[35] and mass spectrometry (MS)[36].

1.1.1 Immunoassays

Immunoassays, mainly enzyme-linked immunosorbent assays (ELISA), have been a standard in analyzing various biomarkers within clinical laboratories.[37-39] Due to its simplicity, reagents and solvents can be pre-allocated including the necessary antibodies for ease-of-use. Several types of antibodies can be used for immunoassays, both of which different in properties that determine its efficacy for clinical use.[40] Polyclonal antibodies are cheap to produce and easy to manufacture but lack specificity, especially with similarly structured molecules that co-exist in complex mixtures. In contrast, monoclonal antibodies are expensive to produce but have a much higher specificity. Currently, there are numerous antibody assays in the market such as ELISA[41], radioimmunoassays[42], and immunofluorescence[43]. These are well-established and have been commonly used to detect analyte presence using methods such as color changes, gamma counters, and fluorescent signals. For immunoassays without a visual indicator, preliminary investigations are done through a spectrophotometer. By measuring the emittance or absorbance of energy, generally within the ultraviolet, visible, and near infrared wavelengths, a relative concentration of analytes can be measured.

Although immunoassays have a near-universal presence across clinical laboratories, there are several significant drawbacks.[44] Firstly, immunoassays are tied in direct correlation to the antibodies used. For diagnostics that require the monitoring of multiple diagnostic molecules, the same number of antibodies must be exposed to the sample. To prevent signal carryover between the multiple antibodies, molecules must also be analyzed separately or using different analytical modalities. In most cases, this means several different fluorescent or colorimetric wavelengths that must be distinctly resolved. Due to this limitation, high-throughput analyses or multiplexing—analyzing multiple analytes in a single run— cannot be performed reliably. Another limitation is the idea that developing a new immunoassay is dependent on developing a complementary antibody / antigen pair. A suitable antibody matched to verified novel biomarkers or unique biomolecules can take months to years to be synthesized and even longer for mass production, with no guarantees in sensitivity and specificity. This is a major limiting factor in the introduction of new diagnostic immunoassays to be used to improve health outcomes. Furthermore, despite the

speed and ease-of-use of immunoassays, it lacks the specificity and quantitative strength for clinical use beyond screening. The possibility of cross-contamination to non-relevant analytes that bind to antibodies result in an elevated limit of detection (LOD), reducing the sensitivity of the overall assay. Similarly, photometry and spectrophotometers are also limited in quantitative capabilities. Quantitative analysis is a key factor that is necessary in improving a biomarker's clinical use, especially for long-term monitoring or early diagnostics. In general, the speed and ease-of-use of immunoassays has resulted in its relegation to a position as a preliminary investigatory tool.

1.1.2 Clinical Mass Spectrometry

In contrast to the use of immunoassays as a preliminary investigative tool for diagnoses, clinical MS has rapidly transitioned into clinical laboratories due to its capabilities in structural identification and quantitative analysis in mixtures.[45] Initially used as a specialized tool for reference-level analyses, MS plays a role in clinical laboratories as a secondary follow-up test after initial in-field or preliminary screening.[46] This role exists due to the lack of sensitivity in immunoassays and the inability of MS to be implemented as a routine screening tool. Preliminary screening by immunoassays can be quickly performed with minimal TAT by providing near instantaneous results, emphasizing its value for resource-limited clinical laboratories or in-field analyses. However, the lower sensitivity of immunoassays can easily result in erroneous results forming false positives and rely upon secondary examinations to confirm an initial diagnosis. In this case, specialized clinical laboratories operating mass spectrometric instruments will perform the relevant tests.

A key component of MS is tandem mass spectrometry (MS/MS). Using this method, analytes undergo mass analysis several times; analyzing both before and after performing dissociation or a chemical gas-phase reaction to change the relevant ion. This method improves the specificity beyond chromatographic and mass separation, while elucidating analyte structure and composition. In most cases, collision-induced dissociation (CID) is commonly performed, where high-energy analytes interact—or collide— with a neutral gas to induce the fragmentation process. As such, this yields various neutral and charged fragments that are observed and analyzed. The resulting fragmentation pattern is unique to the targeted analyte based on its precursor chemical composition and structure. Although there are other dissociation processes that exist, most have a

very specific application that are generally unsuitable outside of research. Similarly, various MS/MS scanning modes have been developed for different applications, all of which can significantly improve sensitivity and specificity. The four main types of MS/MS scan modes are outlined in Figure 1-3, highlighting CID as the main dissociation method.

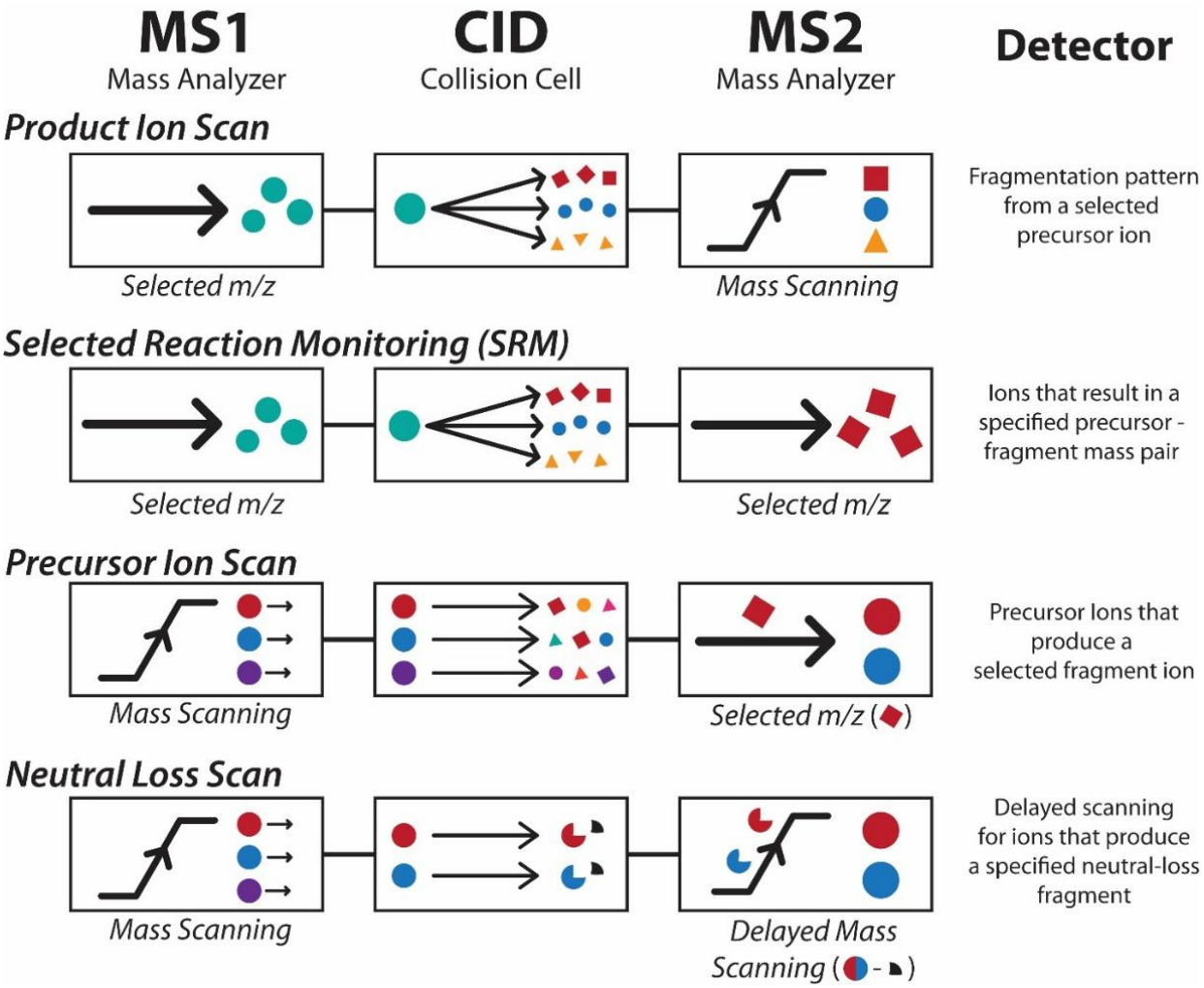

Figure 1-3. MS/MS scan modes using CID performed using a triple-quadrupole mass spectrometer.

Starting from the inception of chromatography-MS for clinical use, quantitative analysis by MS was established into specialized laboratories. Analytes such as pharmaceutical drugs, organic compounds, and metabolites have been analyzed using gas chromatography (GC)-MS in clinical laboratories, but has since expanded into a wide subset of biomolecules with the introduction of liquid chromatography (LC)-MS.[47, 48] Since then, clinical MS has been at the forefront in

establishing novel biomedical testing through translational research in proteomics[49], metabolomics[50], and high-throughput drug discovery[51]. In most cases, clinical MS has become the gold-standard in laboratory testing in both targeted analysis and biochemical profiling. However, MS analysis is limited in availability, mainly in areas that lack resources such as a trained operator, external gas tanks, and multiple reagents for LC use.[52, 53] Similarly, protocol development for a certain analyte is non-standard across clinical laboratories, relying upon in-house research for development, application, and subsequent FDA approval.[54] As such, MS instruments are a significant investment for a clinical laboratory to undertake. It becomes exceedingly hard for MS to be performed continuously, even in clinical laboratories.[55] In turn, clinical laboratories performing such biomedical testing are required to be highly specialized for a specific panel of biomedical tests with higher costs.

1.2 Point-of-Care Diagnostics

Point-of-care (POC) testing was developed as a response to the current state of clinical instruments to provide immediate results in non-traditional settings.[56] In over to overcome the diagnostic bottleneck, POC testing brings laboratory diagnostics closer to the patient by improving throughput and simplifying devices. These tests are required to have a short TAT and provide immediate results to guide clinical diagnostics. However, these POC tests can be targeted for several different applications in the healthcare landscape. In *Section 1.1.1*, it is mentioned that immunoassays are ideal devices for screening the general population. However, improved sensitivity and specificity POC tests have value as a biomedical test to confirm initial diagnoses made by a clinician. To eliminate any confusion, in the scope of this dissertation, POC refers to the latter definition. Other simple, laboratory tests used for screening are referred as *in field* diagnostics.

Both *in field* and POC devices follow a similar fundamental structure, emphasizing ease-of-use and automation / simplification. However, *in field* diagnostics focuses on using quick, rapid tests to scan large populations to help initiate the healthcare pathways. In most cases, these diagnostics devices have appropriate sensitivities for large-scale detection but can result in elevated false-positive rates.[57] Afterwards, more in-depth biomedical testing such as clinical mass spectrometry is used to confirm diagnoses and initiate treatment.[58-60] The development of POC devices that are easy-to-use and can be performed outside of a clinical laboratory has the potential

to revolutionize the healthcare pathway.[61, 62] As a replacement for the traditional sample analysis by a clinical laboratory, these POC biomedical testing devices can assist with clinical diagnosis without significant time delays; within the same appointment and in a patient-care setting.[63] Similarly, these devices can be used for routine treatment monitoring and post-treatment screening for compliance.[64] Patients suffering from chronic diseases can be easily monitored without delay using targeted analysis of specific biomarkers associated with their disease or treatment, further guiding any necessary changes in treatment to optimize health outcomes.

1.2.1 Example Criteria for Point-of-Care Diagnostics

POC diagnostics used for confirmation is subject to a more stringent set of requirements, especially in sensitivity and specificity; albeit with greater access to resources such as electricity and chemical reagents. Since there are no overarching defined criteria for all POC diagnostics, a more 'mature' field with commercialized POC diagnostic instruments was selected for review. Tuberculosis (TB) is one of the world's oldest and most pathogenic diseases, infecting a third of the world's population and persists as one of the top 10 causes of death worldwide. In the current state, the World Health Organization (WHO) recommends a complex algorithm that varies based upon the available resources to provide comprehensive TB diagnostics. Several defined criteria have been published by the WHO for the development of a POC TB screening test including the values based on current clinical laboratory diagnostic tests, all of which are summarized in Table A-2.[65] Based on these criteria, POC devices need to have a high sensitivity and specificity in comparison to the gold standard—bacterial culture— in order to properly 'rule-out' or confirm a TB diagnosis. However, it is evident that current diagnostics cannot match the gold standard in the necessary sensitivity and specificity.[66] This is exemplified by the new POC device 'Xpert MTB/RIF' that utilizes genetic amplification to detect TB-causing mycobacteria.[67] Although it achieves most POC criteria set by the WHO, it still lacks the necessary sensitivity and is more suitable for *in field* diagnostics. However, it also utilizes a separate electronic device that limits its portability in *in field* settings. Unfortunately, POC diagnostics focused on confirming diagnosis emphasizes sensitivity and specificity as two key criteria. Simple workflows, short analytical times and cost efficiency are also necessary, but can be compromised in certain aspects. In order to develop an appropriate POC biomedical test, adopting novel systems that translate clinical laboratory instrumentation should be a main point of focus.[68]

1.2.2 Current Point-of-Care Biomedical Testing Devices

In the current healthcare landscape, there are a limited subset of POC tests which are summarized in Table 1-2.[69] Several different techniques such as electroanalytical chemistry and immunoassays dominate the POC device market based on their simplicity and ease of use. For example, on common POC device is the glucose monitor for diabetic patients. By taking advantage of the chemical conversion of blood glucose into gluconic acid and hydrogen peroxide, the glucose level can be calculated by the measurement of electrical current based on hydrogen peroxide concentration. This device is widely prevalent in use due to its simplicity and sufficient sensitivity to guide self-treatment by diabetics. However, devices such as these are highly specific towards a specific analyte. The electrochemistry-based enzymatic conversion of glucose is unlikely to work for other molecules, even with analytes of similar chemical structures.

Table 1-2. Commonly performed POC biomedical tests.[69] *ER*, emergency room.

Clinical Use	Target Biomolecule	Detection Method	Point-of-Care Testing Instrument Type
Bacterial Infection	Bacteria	Microscopy	Microscope
Blood Clotting Time	Prothrombin	Electrochemistry	Benchtop Analyzer
Cardiac Arrest ER	Troponin I, Troponin A	Immunoassay	Benchtop Analyzer
Compliance Screening	Drugs of Abuse	Immunoassay	Benchtop Analyzer
Diabetes	Glucose	Electrochemistry	Personal use Analyzer
Infectious Agents	Viral Antigens / Antibodies	Immunoassay	Dipstick Immunoassay
Pregnancy	Human Chorionic Gonadotropin	Immunoassay	Benchtop Analyzer
Urine Metabolites	Urinalysis	Spectrophotometry	Dipstick Immunoassay

In contrast, immunoassays are conventionally performed within a clinical laboratory with a wide range of available targets, as discussed in *Section 1.2.1*. Based on the use of an antibody or antigen to bind to the target analyte in samples such as blood, these immunoassays have been

translated for POC and *in field* use through single-stick—otherwise termed dipstick—diagnostics.[70, 71] These diagnostic modalities utilize small strips of substrate that can accept small volumes of patient biofluids. Several layers are present within these assays: the first layer is used to eliminate the cell matrix, while the second layer is present to bind to the target analyte. Lateral-flow immunoassays follow a similar concept but introduce a small-scale chromatographic separation through capillary action along the solid-phase substrate. Many of these single-stick diagnostics follow the mature science of immunoassays such as ELISA, resulting in a well-defined reliability and capability of developed POC devices. Quality control checks are also implemented to ensure accurate use. For analysis, a small optical or fluorescent reader is used to provide qualitative estimates of analyte concentration.[72, 73] Miniaturized CCD cameras or reflectometers exist within these devices to measure the light signals emitted from fluorescent-tagged antibodies.

However, a key limitation of these POC immunoassays is inherited from its clinical laboratory counterpart: sensitivity and specificity. These immunoassays lack the specificity and quantitative capabilities for a 'rule-out' POC biomedical test. Due to the simplified nature of these immunoassays, cross-contamination is an increased concern, further reducing the sensitivity of the overall assay. Similarly, low abundance biomarkers can easily be present at concentrations below the detection limit of these immunoassays. Quantitative analysis is another key component of the diagnostic information needed by clinicians. Increases or decreases to the biomarker concentration can easily elucidate disease progression, revealing information necessary for several diagnostic uses outlined in *Table 1-1*.

1.3 Biomolecule Classes for Biomedical Testing Use

Numerous biomolecules exist within an organism, all of which contribute to a specific disease pathway. Although biomedical testing encompasses a wide range of biomolecules, several classes of biomolecules have recently been highlighted to have clinical significance across various diseases, including proteins, metabolites, and lipids. In recent years, biomedical testing has evolved significantly in tandem with the increasingly powerful research and understanding of the basic sciences. Translational medicine was introduced to streamline the transition from discovery to application. This occurs across several phases: clinical sciences (T1 phase) which involves various large-scale cohort and discovery studies to clinical use (T2 phase).[74] Targeted biomolecules identified for clinical use in the T1 phase encompass an extremely diverse panel of

molecules—such as pharmaceutical drugs, metabolites, lipids and proteins— which can be used for different clinical outcomes.[75-77] Also termed *biomarkers*, molecules of interest with diagnostic capabilities have been the centerpiece of T2 phase research.

1.3.1 Protein Biomarkers

The study of protein biomarkers has significantly expanded in the last decade to characterize the underlying biological pathways and highlight potential therapeutic targets.[78] Since proteins are direct effectors of disease and downstream from the genome, proteins have been molecules of interest. The biomarker pathway is a commonly used workflow in translational medicine to highlight specific proteins that can delineate disease states.[79, 80] Similar to the drug discovery pathway, hundreds of statistically significant proteins are highlighted from a cohort study of several patient sample subsets. This is traditionally done through shotgun proteomics, an untargeted analytical method. By depleting all major proteins such as albumin and hemoglobin from patient samples, proteolytic digestion is performed, and its resulting peptide fragments are molecularly labelled by patient sample. Afterwards, LC-MS/MS is performed with large-scale data analysis to identify any biomarker candidates. At this stage, it is crucial for protein libraries and databases to be available for timely identification and confirmation of its role within the relevant disease pathway. Targeted proteomics is subsequently performed to verify its significance in a larger scale.[81] Top-down proteomics, which looks at intact proteins, identifies the post-translation modifications or protein isoforms.[82] Using this method, targeted proteins can be compared directly to highlight any statistical differences between healthy and diseased patient samples. High-resolution MS instruments are vital throughout this workflow, separating analytes by molecular weights lower than 0.01 Da apart. Another targeted proteomics method commonly performed is bottom-up proteomics. Electrophoresis—commonly, SDS-PAGE— isolates the targeted protein by weight and proteolytically digested before LC-MS/MS analysis.[83] The resulting protein fragments are then analyzed based on its peptide sequences to reveal alterations in amino acid composition.

Despite the well-established biomarker discovery workflow, there is a clinical underutilization of protein biomarkers. The low natural abundance of most validated biomarkers within the body cannot be observed without specialized equipment such as high-resolution mass spectrometry. As such, in the current healthcare state, protein biomarker diagnostics sees limited

use in clinical laboratories. The Food and Drug Administration (FDA) has published several reports on improving the implementation of proteomics-based MS into clinical laboratories, emphasizing key directives such as protocol standardization and larger cohort studies.[84] As a result, the current market utilizing protein biomarkers is heavily limited in diversity and utilizes more traditional methodologies (e.g. immunoassays) when applicable.

Immunoassay Use in Protein-based Biomedical Testing

Several current protein biomarkers are currently in use: troponin[85] and prostate specific antigen (PSA)[86]. Both biomarkers have been utilized clinically with varying degrees of success. Troponin is analyzed through POC immunoassays and have been utilized in the emergency room to 'rule-out' myocardial infarction.[87] Similarly, its use has also been shown for risk stratification and outcome assessment where myocardial injury has occurred and can be extremely useful for clinicians when presented with patients recovering from acute injury.[88] Cardiac troponin immunoassay is one of the most performed emergency room diagnostic tests utilized in hospitals. The immunoassay is based on two specific mouse monoclonal antibodies targeting the central region of human cardiac troponin T. The capture and detection antibodies target to two different amino acid residues—both of which differ between POC immunoassays— within the protein. As a result, the reference limits, limits of detection, and calibrations are non-standard and are not interchangeable among immunoassays.[69] The quality of antibodies also effectively changes the sensitivity and specificity of the immunoassay, stressing the importance of appropriate storage and temperature conditions of these tests. Proteolytic degradation, phosphorylation, complexing with cardiac troponin isoforms, and heparin all play a role in obfuscating the true diagnostic result. Cumulatively, the lack of standardization between assays leads to discrepancies in quantitative measurements and potentially a false positive or negative diagnosis. Furthermore, diverse availability of troponin immunoassays has oversaturated the market with a wealth of different dedicated devices and calibration curves which complicates an otherwise simple POC diagnostic examination. The lack of interchangeability prevents large-scale data collection for subsequent patient studies and affects clinician interpretation of the results based on immunoassay type.

PSA is another blood protein biomarker that is used to screen for prostate cancer.[89] In healthy male patients, PSA circulates in blood at an extremely low concentration, making it undetectable by conventional immunoassay techniques. However, patients with prostate cancer or other

noncancerous diseases, have elevated levels of PSA. During healthcare examinations where prostate cancer is suspected by a primary clinician, these immunoassays are utilized to identify whether there is a significant elevation in circulating PSA. The cross-reactivity of PSA compounded with the possibility of other non-cancerous conditions that elevate PSA result in a lack of information for disease confirmation.[90] The availability of a PSA immunoassay is a stark contrast to the availability of cardiac troponin immunoassays and provides a glimpse into an issue that plagues most validated protein biomarkers. The lack of quantitative capabilities by immunoassays and its high limit of detection result in its use as an initial screening tool at the POC.

Mass Spectrometry Use in Protein-based Biomedical Testing

In addition to the fundamental research performed through MS to identify protein biomarkers, MS also plays a role in the analysis of potential protein biomarkers. For example, two tuberculosis protein biomarkers—ESAT-6 and CFP-10— have been identified as proteins directly derived from the virulence gene in mycobacteria.[91, 92] These protein biomarkers have been targeted by several serological-based immunoassays with varying sensitivity and specificity.[93-95] However, the matrix complexity of blood and the required sample preparation needed to enrich these protein biomarkers result in insufficient sensitivities for POC use. In response, modalities implementing MS with immunoaffinity enrichment have been reported.

The combination of immunoassays with mass spectrometry—called *immunoaffinity multiple-reaction-monitoring* (immuno-MRM)— helps reduce the sample preparation commitment such as chromatography or SDS-PAGE for protein-based diagnostics.[96-98] Monoclonal antibodies are used to capture and elute a specific protein from biofluids before enzymatic digestion. Several significant digested proteins and its major fragments are monitored through MRM using MS. When combining multiple types of monoclonal antibodies to capture a select panel of proteins, multiple precursor/product pairs can be monitored simultaneously. Another immunoaffinity enrichment method—Stable Isotope Standards and Capture by Anti-peptide Antibodies (SISCAPA)— was developed using antibodies to target specific peptide sequences rather than the entire protein.[99] Unlike immuno-MRM, SISCAPA proteolytically digests abundant protein-depleted samples and adds antibodies complementary to the target peptide. Internal standards are spiked into the solution before antibody enrichment for absolute quantitation. The antibodies added within the sample include both native and isotopically labelled peptide antibodies to standardize

peptide capture between sample repeats. The antibody-peptide complexes are recovered and subsequently analyzed through MS/MS analysis. Afterwards, the identified peptide concentration is directly related to protein concentration. A schematic of SISCAPA is provided in Figure 1-4. Overall, both methods are well-established and remain as the gold standard for quantitation of protein biomarkers.

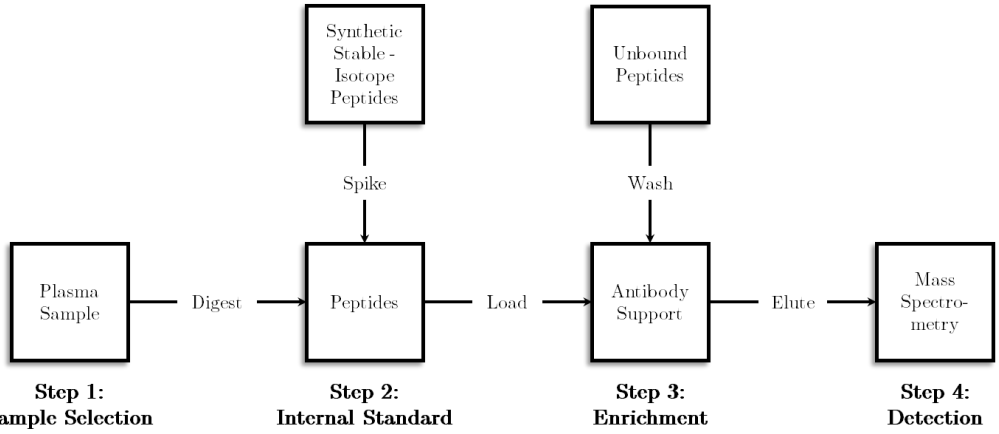

Figure 1-4. Schematic of SISCAPA protocol for peptide quantitation from plasma samples. Reproduced from *Anderson, et. al.*[99]

In comparison to the traditional SDS-PAGE LC-MS/MS method used in the biomarker discovery pathway defined in previously, immunoaffinity enrichment is more suitable for clinical use and have slowly transitioned into clinical laboratories. Technological advancements have been focused on improving the efficacy of the enrichment method by developing automated instruments or using magnetic beads as a binding substrate for antibodies. *Hu et al.* at Arizona State University developed a new porous nanodisk structure to increase the substrate surface area, maximizing the amount of bound peptide antibodies and thus, capture efficiency.[100] Pairing these nanodisks with matrix-assisted laser desorption ionization (MALDI)-MS, direct analysis without chromatographic separation is performed and validated as a clinical TB screening tool, reporting sensitivities and specificities comparable to bacterial culture.

Overall, in comparison to the immunoassays performed for PSA and troponin, immuno-MRM and other MS-based methods are significantly higher in sensitivity and specificity. Further separative capabilities available within the MS system eliminate the risk of cross-reactive proteins when enriched by immunoaffinity methods. The specificity of MS/MS paired to the high resolution of MS provides unparalleled analytical capabilities. However, these instruments cannot be applied

to the POC and is even limited in clinical laboratory settings. As a result, numerous novel protein-based biomarkers are unusable in a clinical setting. Other biomarkers that can potentially be used for diagnostics also face immense challenges in synthesizing a sensitive antigen-antibody pair for immunoassay use. This can take years, which hinders the implementation of new, effective diagnostics.

1.3.2 Screening of Metabolites

Metabolites, in comparison to protein biomarkers, is an even more vast pool of potential disease targets.[5] Biological pathways—such as blood transport, cellular responses, and metabolism— all rely on and produce metabolites. In T1 phase research, significant metabolites are identified through differential screening between biological samples. Disruptions to the biological pathway by disease or pharmaceuticals all produce different metabolites or alter the rate of production. This can include small molecules such as amino acids, nucleotides, antioxidants, or vitamins. Similarly, metabolic pathways such as fatty acid synthesis and glyoxylate cycles are interconnected, resulting in elevated or diminished levels of free fatty acids, lipids, carbohydrates, and other organic acids. Identifying these molecules is an arduous task, encompassing an extensive and expansive list of small molecules under 1 kDa in size. Due to the vast number of metabolites—observed as peaks in MS spectra— comprehensive identification and quantitation of metabolites is impossible to be done manually, emphasizing the need for a comprehensive metabolomic library such as METLIN and Massbank.[101] These databases are dedicated for metabolic profiling, identifying significant metabolites for differentiation of disease states and revealing biological pathways. Major metabolites identified by academic research usually reveals a metabolite low in abundance and relies heavily on LC-MS/MS for isolation and analysis. In current biomedical tests, several metabolites are screened during a routine blood panel such as LDL, HDL, and triglycerides. These tests only semi-quantitatively measures the overall concentration of each class and lacks any further specifics as to the type of metabolite measured. As such, these traditional blood panels still require a trained healthcare professional to correctly interpret the results in tandem with exhibited symptoms; leaving much room for error. [69]

Other metabolite targets can come from organic sources outside of the human body. Sources such as bacteria, fungi, algae, and plants all produce and release metabolites that are disruptive to human health and are regularly screening in clinical laboratories.[102] Whereas endogenous

metabolites focus on analyzing biofluids like blood, urine, and saliva, exogenous metabolites can exist on a diverse set of matrices including surfaces and foodstuffs. Toxins —such as anthrax[103], botulinum[104], and staphylococcal enterotoxin[105]— are a few examples of metabolites detected through relevant immunoassays and bacterial culture, when possible. Samples are carefully collected and sent to designated laboratories for analysis, aware of its potential toxicity. In these cases, POC biomedical testing is critical in minimizing toxic substance exposure and potentially fatal mishandling errors. Several POC immunoassays have been developed for surface detection of these toxins including lateral flow immunoassays. For certain toxins such as mycotoxins that are exposed to animal feed and foodstuffs, the toxin levels are regulated before export and consumption. However, immunoassays have limited sensitivities for the presence of these toxins and can be easily affected by different sample types. Quantitative capabilities are needed to ensure that all foodstuffs fall below the safety threshold for safe consumption. Therefore, developing a more sensitive POC assay or instrument for the analysis of toxin metabolites is a critical point in minimizing toxin exposure and improving human health outcomes.

1.3.3 Profiling of Lipids

Lipidomics is an emerging subdiscipline of metabolomics, focused on understanding and elucidating the lipid distribution—otherwise termed *lipidome*— within the human body. While certain lipids—low-density / high-density lipoprotein (LDL/HDL)— have been commonly used to determine obesity and other obesity-related diseases through routine blood screening, lipid profiling has emerged as a novel clinical laboratory diagnostic tool.[106] Within the body, there are eight different lipid classes that exist.[107] Although each lipid class has a different role, regular metabolic functions within the body maintain a lipid homeostasis. This homeostasis varies slightly based on different factors such as age, genes, and environmental factors as well as individual patients. However, drastic changes can occur under disease onset. These drastic changes are observed by analyzing tissue or biofluid using LC/GC-MS/MS and MALDI-MS.

Several studies have emphasized the use of lipid profiling of patients with Alzheimer's disease.[108] As a common type of dementia with symptoms of progressive memory loss, behavioral disruptions, and cognitive dysfunction, Alzheimer's results from the uncontrolled growth of amyloid plaques within the brain. In early-onset Alzheimer's disruptions to the lipid homeostasis has been observed, especially with the large distribution of cerebral lipids within the brain. Other

neurodegenerative diseases are also commonly associated with changes to the lipidome. Using chromatography MS, several key aspects regarding detection of early onset Alzheimer's was reported, including elevated levels of triglyceride and diacylglycerol. The prevalence of unsaturated fatty acids was also positively associated with the development of neurotic plaques and negatively associated with cognitive performances. Based on the conclusions of various lipidomic studies on Alzheimer's disease, there has been no direct correlation between a single lipid class or type with diagnosis or progression.[107] Thus, for comprehensive insight, multiple lipids need to be monitored over time for accurate diagnosis of Alzheimer's disease.

Unlike proteins and metabolites as a molecular diagnostic biomarker, targeted analysis on a single lipid is insufficient to observe significant changes or statistically confirm disease onset. In most cases, the entire or a major subset of the lipidome is used as a biomarker.[109, 110] However, immunoassays lack the multiplexing capabilities or the ability to separate lipid isomers. Thus, lipid profiling by immunoassay is unlikely to be available. This does not mean that lipids are less important than the other classes, but rather emphasizes the clinical value as a group of potentially significant biomolecules for developing novel biomedical tests. As such, the incorporation of lipid profiling to the POC to assist in clinical diagnosis can revolutionize biomedical tests.

1.4 Addressing Biomedical Testing Needs in the Current Healthcare Landscape

Biomedical testing has grown to become an integral part of a clinician's arsenal for diagnosis, encompassing a wide range of conventional biomolecules such as LDL, PSA, and mycotoxins. These technologies have slowly been implemented into clinical laboratories through the expanding prevalence of MS-based modalities. MS has been heavily involved in developing highly sensitive and specific methods for various laboratory diagnostics—such as therapeutic drug monitoring, drugs of abuse analysis, and newborn metabolite screening. Clinical laboratories are tasked with developing their own in-house diagnostic methods to be approved by the FDA and other federal guidelines.[84] Yet, for POC use, mass spectrometry is unlikely to be implemented due to instrument limitations, maintenance costs, and complexity. The current workflow for MS analysis is relatively slow and limited in throughput, where preparation of samples from its native state to one amenable to MS requires lengthy derivatization that cannot be performed at the POC. Additionally, MS instruments require extensive resources and power such as external gas tanks and turbomolecular pumps. As such, MS is typically performed at clinical or more often, research laboratory level.

However, on the other hand, current POC devices seek to bring these biomedical tests closer to the community, focusing on the development of rapid, simple easy-to-use diagnostic devices with limited sensitivities.[111] In most cases, the end-goal of these devices is for *in field* diagnostics, where community screening is performed routinely. Although these devices are vital in helping initiate the healthcare pathway for patients with underlying symptoms, subsequent confirmatory diagnostics still needs to be performed. This means that the diagnostic bottle neck related to sample preparation and transport remains. Complex laboratory tests, high patient-volume institutions, and errors in sample collection can easily accumulate and elevate TAT. Laboratory diagnostics remains as the main bottleneck in the entire workflow. Furthermore, with more effective *in field* diagnostics initiating the healthcare pathway, more confirmatory biomedical testing is required resulting in a significant increase in sample volume and its relevant diagnostic delays.

In order to address this problem, a biomedical testing tool needs to be made available at the POC with enough sensitivity to 'rule-out' or confirm diagnoses. Although immunoassays have slowly been made available with respect to protein biomarkers, the sensitivities are insufficient for most molecular biomarkers. Similarly, the diversity of molecules utilizes as biomarkers are inherently un-analyzable by POC immunoassays, eliminating an entire class of potentially useful biomarkers.

Miniature mass spectrometry systems are poised as a universal POC solution for biomedical testing. When paired with simple direct sampling ionization methods, miniature MS systems have already shown an immense potential, in analyzing biofluids for illicit and therapeutic drugs and has even been applied for direct tissue analysis. The direct correlation between miniature MS systems and its clinical laboratory counterpart—mass spectrometry— enables a more straightforward translation of conventional and novel MS-based methods for biomedical testing. Thus, MS analysis of various biomolecules, including proteins, metabolites, and lipids, can be performed at the POC with miniature MS systems, overcoming the current diagnostic bottleneck.

1.5 Direct Sampling Ionization Mass Spectrometry

Direct sampling ionization is defined as a minimal extraction method—less than one-minute sample protocol— that can easily produce gas-phase ions from a sample under ambient conditions. These simple and quick ionization modalities are highly amenable at the POC and are meant to overcome chromatographic procedures. The combination of direct sampling ionization with mass

spectrometry enables quantitative analysis of various biomolecules, drugs of abuse, and therapeutic drugs. Several direct sampling ionization methods such a desorption electrospray ionization[112], paper spray ionization (PSI)[113], and extraction nano-electrospray ionization[114] represent the simplicity and rapid aspect of direct sampling that enables POC analysis.

1.5.1 Paper Spray Ionization

Paper spray ionization (PSI) was first introduced in 2010 with various types of derivates reported since.[113, 115-119] This method is most amenable for the analysis of dried blood spots, and is simple and robust to perform, summarized in Figure 1-5. Typically, chromatography paper is used as the substrate and cut into an isosceles triangle to form a sharp tip. By placing a small volume of blood—around 0.4 µL— onto the center of the substrate, the sample matrix is separated from the target analyte. Salts, cell debris and other macromolecules are bound to the substrate when drying. A small amount of solvent is applied to the dried sample spot to elute the analytes. During this solvent application, a high voltage —3 to 5 kV— is applied to initiate an electrospray at the macroscopically formed tip. From this electrospray, ions are introduced into the MS instrument and analyzed. Solid samples such as fingerprint residue[120], powdered drugs[121], and tissue biopsies[122] have all been analyzed by PSI-MS.

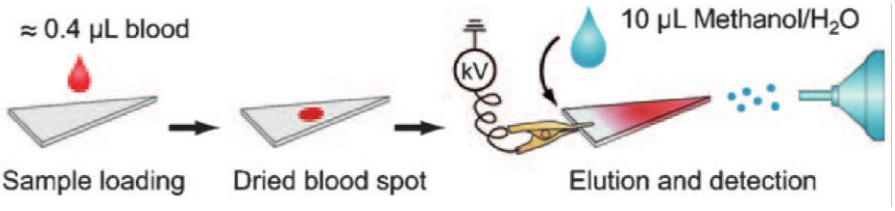

Figure 1-5. Paper Spray Ionization Workflow. Reproduced from *Wang, et. al.*[113]

The simplicity in performing PSI have spurred improvements and research to be performed regarding reproducibility and minimization of background noise due to its non-selective extraction. Standardization incorporation of internal standards has greatly improved the reproducibility of PSI while enabling quantitative analysis. By first pre-loading or even pre-printing internal standards onto the substrate, significant improvements to reproducibility in comparison to the original PSI was observed for therapeutic drug analysis.[123] Furthermore, several studies have outlined the preliminary workflow to quantify multiple drugs simultaneously using

PSI, mimicking the diagnostic methods performed in clinical labs.[114] Table A-1 summarizes the reported quantitative applications of PSI for drugs of abuse and therapeutic drug analysis.[124] The versatility of PSI is also tested by analyzing fingerprints for drug residues collected on a prepared internal standard spiked paper identifying a 99% true-positive and 2.5% false-positive rate for the detection of cocaine.[120] Similarly, PSI for therapeutic drug analysis —such as immunosuppressants— has been extensively analyzed.[125, 126] Clinical validation using an automated PSI source and cartridge for therapeutic drug monitoring was performed and cross-validated with an FDA-approved immunoassay and LC-MS/MS methods. PSI reported a significant correlation and adequate capability in the detection and quantification of immunosuppressants.

1.5.2 Extraction Nano-Electrospray Ionization

Whereas PSI has shown to be capable of fast extraction of analytes and immobilization of complex matrices, the limiting factor in ionization is the erratic formation of ion droplet. This is largely due to the macroscopically formed 'sharp' tip and fibrous nature of the paper substrate. Due to multiple fibers forming their own microscopic tips, droplets of various sizes and aligned in various directions are formed. This limits the number analytes that are introduced into the MS that are appropriately desolvated and aligned leading to low signal intensities. In comparison, nano-electrospray ionization provides a single, nano-sized tip for a homogenous, stable spray. However, there are no extraction capabilities that a paper substrate provides. Extraction nano-electrospray ionization is a combinatory method of paper spray with nano-electrospray ionization, illustrated in Figure 1-6.[127] A small paper slip —0.5mm x 10mm, width x length— is cut and 5 µL of sample is placed onto the paper substrate. After drying, the paper is placed inside the nano-electrospray ionization capillary along with 10 µL of solvent. Analytes are desorbed from the paper into the ionization solvent. A lowered amount of voltage—less than 2 kV— is used to initiate the Taylor cone and form analyte droplets. This direct sampling method was performed to analyze therapeutic drugs in blood and is highly amenable to atmospheric pressure ionization sources and non-heated MS inlets.

In a recent study, extraction nano-electrospray ionization was used for the direct sampling of biological tissues. Due to the abundance of lipids in fatty tissue, the metal electrode used for high voltage application can be used as a direct sampling probe. The metal electrode was placed

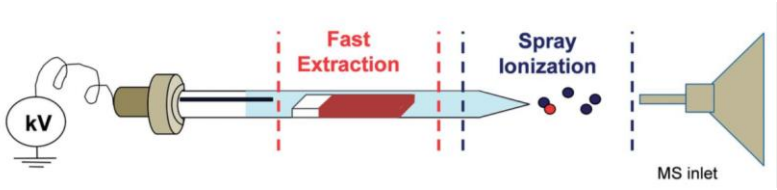

Figure 1-6. Extraction nanospray ionization workflow. Reproduced from *Ma, et. al.*[127]

into the brain, extracting microscopic amounts of tissue. When placed into a capillary filled with the solvent, lipids are extracted and analyzed by MS. Furthermore, photochemical reactions can be performed in-capillary. Paternò-Büchi (PB) reactions with tandem mass spectrometry can elucidate lipid structure and differentiate isomeric lipids.[128] Similarly, extraction nano-electrospray ionization has also been used for the rapid determination of isocitrate dehydrogenase mutation in human gliomas.[129]

1.5.3 Slug-Flow Microextraction

Whereas PS and extraction nano-electrospray ionization utilize paper to immobilize the matrix, slug-flow microextraction (SFME) focuses on the direct analysis of biofluids. This is especially advantageous where samples are frequently collected in a liquid form such as routine blood samples, or when analyzing analytes that easily bind to the paper substrate. SFME is a miniaturized liquid-liquid interaction system, taking advantage of capillary action in a microfluidic format for improved, high-efficiency extraction.[130] Small borosilicate glass capillaries—0.86/1.5 mm i.d./o.d. — are filled with 5 to 10 µL plugs of extraction solvent, placed sequentially. It is critical that both plugs are immiscible to form the liquid-liquid interface. By using an external force—physically tipping the capillary or thru a pipette gun— the two liquid plugs are cycled back and forth. Capillary action forces each plug to cycle within, ensuring that both plugs interact with each other in its entirety. Throughout the cyclic motion, diffusion of select analytes—based on partition coefficient, LogP— occurs across the interface, preventing large matrix proteins and cell debris from entering the extraction solvent phase. From previous experiments, less than 10 cycles are necessary to achieve equilibrium. Thus, several cycles can be performed per second, quickly enriching analytes for direct analysis by MS. After the extraction is complete, the capillary can be used as an electrospray emitter with the addition of a high voltage —around 1.5 kV— realizing on-line analysis.

Through this method, SFME has shown strong analysis of various types of therapeutic drugs in whole blood and serum. However, this method, as with liquid-liquid extraction, is highly dependent on the type of analyte targeted. Analytes with a low solubility in the organic phase will extract much more efficiently in comparison to analytes with high solubility. Despite this limitation, low LODs can still be achieved by MS analysis due to the removal of matrices and salts.

Overall, the direct sampling methods introduced in this section have been developed for easy, direct MS analysis. Samples in both solid and liquid forms can be directly analyzed without complication chromatographic separations and have shown detection limits significantly below the threshold defined by various governing bodies. AS such, the utilization of direct sampling methods is critical for the implementation of miniature MS systems at the POC.

1.6 Miniature Mass Spectrometry Systems

The development of a miniature MS system was largely driven by breakthroughs in successfully reducing the pressure requirements.[131, 132] One significant solution to overcoming the pressure requirements of MS analysis was the use of a discontinuous atmospheric pressure inlet (DAPI). By selectively opening the MS inlet capillary for 15 to 25 ms per scan, a characteristic pressure curve is formed within the chamber. During this time, ion introduction and manipulation can be performed at different pressures depending on the timing before scanning at a chamber pressure of 10^{-5} Torr. Several miniature MS systems utilizing this concept have been developed, starting from the Mini 10, 11, 12, and the current generation—the Mini β.[63, 133, 134] Each of these miniature MS systems are benchtop-sized, lightweight, and easily operated with little to no background in MS. Working in tandem with direct sampling ionization sources, these miniature MS instruments enable POC analysis of therapeutic drugs and drugs of abuse. A sample POC workflow to analyze tissue samples and blood is detailed in Figure 1-7.[113, 135]

Currently, miniature MS systems have been well-established for the analysis of small molecules such as therapeutic drugs and drugs of abuse.[135-137] Direct sampling procedures have also been developed to facilitate the analysis of the same molecules at the POC. However, biomolecules such as proteins, metabolites and lipids have not been analyzed or in a limited fashion, due to further requirements in technological advancement. Throughout the studies performed in this dissertation, we utilize our in-lab developed Mini β system. A DAPI is used for the pulsed ion introduction into the mass analyzer, with several ion traps installed in the z-axis to enable several

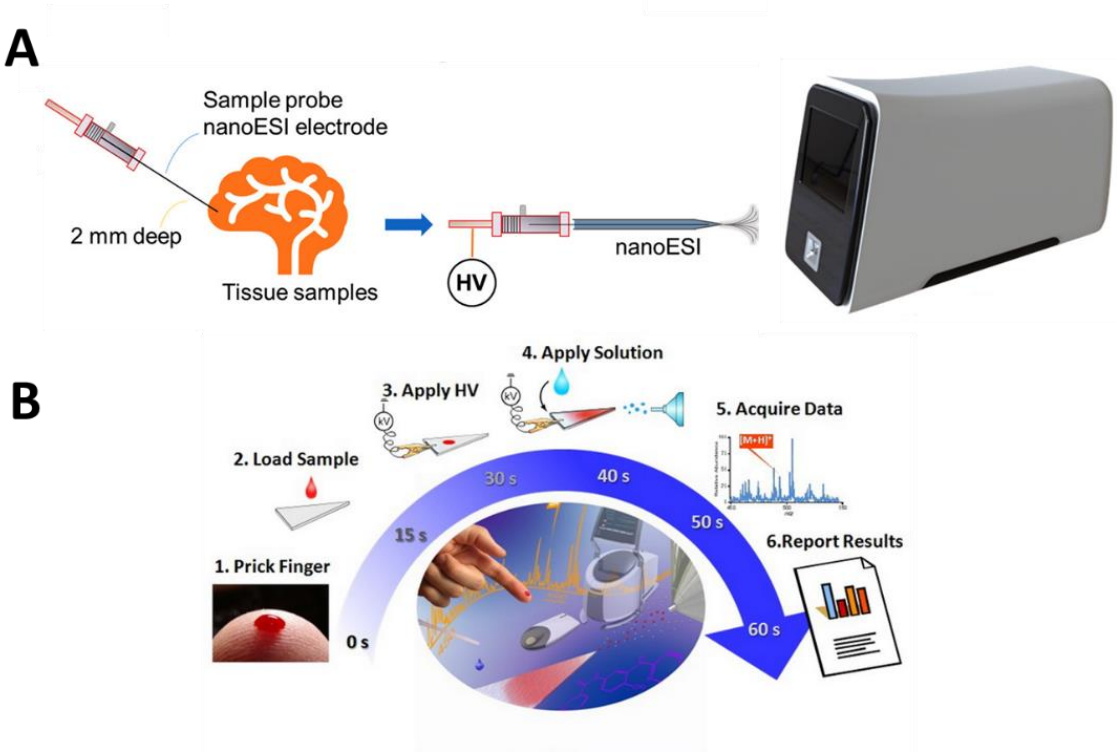

Figure 1-7. Analytical workflows of direct sampling ionization with miniature MS systems. (A) Extraction nano-electrospray ionization of major metabolites and lipids from brain tissue samples. (B) Schematic for POC blood sampling analysis using PSI with a miniature MS system. Redrawn from *Zou, et. al.*[135] and *Wang, et. al.*[113]

MS/MS modalities. An external gas inlet is also made available to control chamber pressure during ion manipulation and optimize MS/MS. Nano-electrospray ionization is used as the standard ionization method to facilitate ease-of-use and quantitative performance. By combining direct sampling ionization with miniature MS systems, comprehensive workflows were developed to introduce MS analysis to the POC.

1.7 Conclusion

The implementation of biomedical testing at the POC is key in improving the healthcare pathway by eliminating diagnostic delays. This requires the utilization of miniature MS systems to provide sensitive and specific MS analysis paired to fast, simple direct sampling ionization techniques for rapid extraction and enrichment. Small biomolecules—such as drugs of abuse and therapeutic drugs— have been analyzed using a combination of direct sampling ionization and miniature MS systems. However, the emerging significance of new biomarkers—proteins,

metabolites, and lipids— are only analyzed within clinical laboratories with insufficient sensitivities or antibodies necessary for translation to the POC. Direct sampling ionization with miniature MS systems represent a universal solution for current and new molecular biomarkers, enabling quantitative analysis and sensitivities appropriate for various diagnostic uses.

To fulfill this demand, several workflows utilizing a miniature MS system was proposed and optimized for the quantitation of proteins, metabolites and lipids. The first study characterizes a new dual ion trap miniature MS instrument to identify the MS techniques that could be utilized. Translation of conventional immunoaffinity enrichment MS techniques was performed to analyze and quantify peptides of different molecular weights and amino acid sequences. The overall workflow was applied to the analysis of the SKBR3 cell line to quantify *Met* protein expression within cells. The second study emphasized the capabilities of a miniature MS system for lipid profiling using a novel direct sampling ionization method—polymer coating transfer enrichment. On-line photochemical reactions were also investigated, elucidating lipid structures and resolving lipid isomers. A preliminary investigation into the free fatty acid profiles of both healthy and type-2 diabetic plasma samples identified several distinct profiles that could be used for disease differentiation. Finally, the last study focused on the analysis of mycotoxins from unique matrices—such as grain and foodstuffs— using SFME as an on-line extraction method. SFME was also adapted into a surface extraction method for the direct extraction of mycotoxins from the surfaces of whole corn kernels, eliminating any sample preparation. Altogether, these studies emphasize the universal capabilities of direct sampling ionization with miniature MS systems to analyze current and novel biomarkers for biomedical testing at the POC.

1.8 References

1. Cannon, B.; Lee, M., Clinical Laboratory Tests: Application to Daily Practice. *J Am Pharm Assoc (Wash)* **1996,** *Ns36* (11), 668-79; quiz 679-81.

2. Woolley, C. F.; Hayes, M. A., Emerging Technologies for Biomedical Analysis. *Analyst* **2014,** *139* (10), 2277-2288.

3. Zuur, M. A.; Bolhuis, M. S.; Anthony, R.; den Hertog, A.; van der Laan, T.; Wilffert, B.; de Lange, W.; van Soolingen, D.; Alffenaar, J. W., Current Status and Opportunities for Therapeutic Drug Monitoring in the Treatment of Tuberculosis. *Expert Opin Drug Metab Toxicol* **2016,** *12* (5), 509-21.

4. Brettell, T. A.; Lum, B. J., Analysis of Drugs of Abuse by Gas Chromatography-Mass Spectrometry (Gc-Ms). *Methods Mol Biol* **2018,** *1810*, 29-42.

5. Cheung, P. K.; Ma, M. H.; Tse, H. F.; Yeung, K. F.; Tsang, H. F.; Chu, M. K. M.; Kan, C. M.; Cho, W. C. S.; Ng, L. B. W.; Chan, L. W. C.; Wong, S. C. C., The Applications of Metabolomics in the Molecular Diagnostics of Cancer. *Expert Rev Mol Diagn* **2019,** *19* (9), 785-793.

6. Moon, J. Y.; Leitao Filho, F. S.; Shahangian, K.; Takiguchi, H.; Sin, D. D., Blood and Sputum Protein Biomarkers for Chronic Obstructive Pulmonary Disease (Copd). *Expert Rev Proteomics* **2018,** *15* (11), 923-935.

7. Graig, L. A.; Phillips, J. K.; Moses, H. L., Biomarker Tests for Molecularly Targeted Therapies: Key to Unlocking Precision Medicine. National Academies Press (US) Copyright 2016 by the National Academy of Sciences. All rights reserved.: Washington (DC), 2016.

8. Hickner, J. M.; Fernald, D. H.; Harris, D. M.; Poon, E. G.; Elder, N. C.; Mold, J. W., Issues and Initiatives in the Testing Process in Primary Care Physician Offices. *The Joint Commission Journal on Quality and Patient Safety* **2005,** *31* (2), 81-89.

9. Plebani, M., Diagnostic Errors and Laboratory Medicine - Causes and Strategies. *EJIFCC* **2015,** *26* (1), 7-14.

10. Ngo, A.; Gandhi, P.; Miller, W. G., Frequency That Laboratory Tests Influence Medical Decisions. *The Journal of Applied Laboratory Medicine* **2017,** *1* (4), 410-414.

11. Keeler, E.; Perkins, M. D.; Small, P.; Hanson, C.; Reed, S.; Cunningham, J.; Aledort, J. E.; Hillborne, L.; Rafael, M. E.; Girosi, F.; Dye, C., Reducing the Global Burden of Tuberculosis: The Contribution of Improved Diagnostics. *Nature* **2006,** *444 Suppl*, 49-57.

12. Abu-Raddad, L. J.; Sabatelli, L.; Achterberg, J. T.; Sugimoto, J. D.; Longini, I. M.; Dye, C.; Halloran, M. E., Epidemiological Benefits of More-Effective Tuberculosis Vaccines, Drugs, and Diagnostics. *Proceedings of the National Academy of Sciences* **2009,** *106* (33), 13980-13985.

13. Frank, S. C.; Cohn, J.; Dunning, L.; Sacks, E.; Walensky, R. P.; Mukherjee, S.; Dugdale, C. M.; Turunga, E.; Freedberg, K. A.; Ciaranello, A. L., Clinical Effect and Cost-Effectiveness of Incorporation of Point-of-Care Assays into Early Infant Hiv Diagnosis Programmes in Zimbabwe: A Modelling Study. *Lancet HIV* **2019,** *6* (3), e182-e190.

14. Lee, A. C., Haematologist-Reviewed Peripheral Blood Smear in Paediatric Practice. *Singapore Med J* **2018,** *59* (2), 64-68.

15. Coventry, L. L.; Jacob, A. M.; Davies, H. T.; Stoneman, L.; Keogh, S.; Jacob, E. R., Drawing Blood from Peripheral Intravenous Cannula Compared with Venepuncture: A Systematic Review and Meta-Analysis. *J Adv Nurs* **2019,** *75* (11), 2313-2339.

16. Halonen, S.; Kari, J.; Ahonen, P.; Kronström, K.; Hyttinen, J., Real-Time Bioimpedance-Based Biopsy Needle Can Identify Tissue Type with High Spatial Accuracy. *Ann Biomed Eng* **2019,** *47* (3), 836-851.

17. Gaspar, P. C.; Rudolf-Oliveira, R. C. M.; Wildner, L. M.; de Moraes, A. C. R.; Reis, M. L.; da Silva, R. M.; Gonçalves, J.; Bazzo, M. L.; Santos-Silva, M. C., Evaluation of Leucocytes from Sputum Samples of Pulmonary Tuberculosis Patients Using Flow Cytometry. *Int J Tuberc Lung Dis* **2018,** *22* (9), 1071-1076.

18. Niedrig, M.; Patel, P.; El Wahed, A. A.; Schädler, R.; Yactayo, S., Find the Right Sample: A Study on the Versatility of Saliva and Urine Samples for the Diagnosis of Emerging Viruses. *BMC Infect Dis* **2018,** *18* (1), 707.

19. Platt, L.; Easterbrook, P.; Gower, E.; McDonald, B.; Sabin, K.; McGowan, C.; Yanny, I.; Razavi, H.; Vickerman, P., Prevalence and Burden of Hcv Co-Infection in People Living with Hiv: A Global Systematic Review and Meta-Analysis. *Lancet Infect Dis* **2016,** *16* (7), 797-808.

20. Tavares, A. M.; Fronteira, I.; Couto, I.; Machado, D.; Viveiros, M.; Abecasis, A. B.; Dias, S., Hiv and Tuberculosis Co-Infection among Migrants in Europe: A Systematic Review on the Prevalence, Incidence and Mortality. *PLoS One* **2017,** *12* (9), e0185526.

21. Kompelli, A. R.; Li, H.; Neskey, D. M., Impact of Delay in Treatment Initiation on Overall Survival in Laryngeal Cancers. *Otolaryngol Head Neck Surg* **2019,** *160* (4), 651-657.

22. Htun, Y. M.; Khaing, T. M. M.; Yin, Y.; Myint, Z.; Aung, S. T.; Hlaing, T. M.; Soonthornworasiri, N.; Silachamroon, U.; Kasetjaroen, Y.; Kaewkungwal, J., Delay in Diagnosis and Treatment among Adult Multidrug Resistant Tuberculosis Patients in Yangon Regional Tuberculosis Center, Myanmar: A Cross-Sectional Study. *BMC Health Serv Res* **2018,** *18* (1), 878.

23. Bleicher, R. J., Timing and Delays in Breast Cancer Evaluation and Treatment. *Ann Surg Oncol* **2018,** *25* (10), 2829-2838.

24. Khan, M.; Khalid, P.; Al-Said, Y.; Cupler, E.; Almorsy, L.; Khalifa, M., Improving Reports Turnaround Time: An Essential Healthcare Quality Dimension. *Stud Health Technol Inform* **2016,** *226*, 205-8.

25. Tabak, Y. P.; Vankeepuram, L.; Ye, G.; Jeffers, K.; Gupta, V.; Murray, P. R., Blood Culture Turnaround Time in U.S. Acute Care Hospitals and Implications for Laboratory Process Optimization. *J Clin Microbiol* **2018,** *56* (12).

26. Hawkins, R. C., Laboratory Turnaround Time. *The Clinical biochemist. Reviews* **2007,** *28* (4), 179-94.

27. Bossuyt, X.; Verweire, K.; Blanckaert, N., Laboratory Medicine: Challenges and Opportunities. *Clinical chemistry* **2007,** *53* (10), 1730-3.

28. Balog, J.; Kumar, S.; Alexander, J.; Golf, O.; Huang, J.; Wiggins, T.; Abbassi-Ghadi, N.; Enyedi, A.; Kacska, S.; Kinross, J.; Hanna, G. B.; Nicholson, J. K.; Takats, Z., In Vivo Endoscopic Tissue Identification by Rapid Evaporative Ionization Mass Spectrometry (Reims). *Angewandte Chemie International Edition* **2015,** *54* (38), 11059-11062.

29. Rochat, B.; Kottelat, E.; McMullen, J., The Future Key Role of Lc-High-Resolution-Ms Analyses in Clinical Laboratories: A Focus on Quantification. *Bioanalysis* **2012,** *4* (24), 2939-58.

30. Clarke, N. J.; Hoofnagle, A. N., Mass Spectrometry Continues Its March into the Clinical Laboratory. *Clin Lab Med* **2011,** *31* (3), ix-xi.

31. Annesley, T. M.; Cooks, R. G.; Herold, D. A.; Hoofnagle, A. N., Clinical Mass Spectrometry-Achieving Prominence in Laboratory Medicine. *Clin Chem* **2016,** *62* (1), 1-3.

32. Sánchez-Romero, M. I.; García-Lechuz Moya, J. M.; González López, J. J.; Orta Mira, N., Collection, Transport and General Processing of Clinical Specimens in Microbiology Laboratory. *Enferm Infecc Microbiol Clin* **2019,** *37* (2), 127-134.

33. Heireman, L.; Van Geel, P.; Musger, L.; Heylen, E.; Uyttenbroeck, W.; Mahieu, B., Causes, Consequences and Management of Sample Hemolysis in the Clinical Laboratory. *Clin Biochem* **2017,** *50* (18), 1317-1322.

34. Vesper, H. W.; Myers, G. L.; Miller, W. G., Current Practices and Challenges in the Standardization and Harmonization of Clinical Laboratory Tests. *Am J Clin Nutr* **2016,** *104 Suppl 3* (Suppl 3), 907s-12s.

35. Zhang, Z.; Hu, W.; Li, L.; Ding, H.; Li, H., Therapeutic Monoclonal Antibodies and Clinical Laboratory Tests: When, Why, and What Is Expected? *J Clin Lab Anal* **2018,** *32* (3).

36. Fung, A. W. S.; Sugumar, V.; Ren, A. H.; Kulasingam, V., Emerging Role of Clinical Mass Spectrometry in Pathology. *J Clin Pathol* **2020,** *73* (2), 61-69.

37. Hendrickson, O. D.; Chertovich, J. O.; Zherdev, A. V.; Sveshnikov, P. G.; Dzantiev, B. B., Ultrasensitive Magnetic Elisa of Zearalenone with Pre-Concentration and Chemiluminescent Detection. *Food Control* **2018,** *84*, 330-338.

38. Stephen, L., Multiplex Immunoassay Profiling. *Methods Mol Biol* **2017,** *1546*, 169-176.

39. Uljon, S.; Kataria, Y.; Flood, J. G., Vortioxetine Use May Cause False Positive Immunoassay Results for Urine Methadone. *Clin Chim Acta* **2019,** *499*, 1-3.

40. Wootla, B.; Denic, A.; Rodriguez, M., Polyclonal and Monoclonal Antibodies in Clinic. *Methods Mol Biol* **2014,** *1060*, 79-110.

41. Aydin, S., A Short History, Principles, and Types of Elisa, and Our Laboratory Experience with Peptide/Protein Analyses Using Elisa. *Peptides* **2015,** *72*, 4-15.

42. Kennaway, D. J., A Critical Review of Melatonin Assays: Past and Present. *J Pineal Res* **2019,** *67* (1), e12572.

43. Shoemark, A.; Frost, E.; Dixon, M.; Ollosson, S.; Kilpin, K.; Patel, M.; Scully, J.; Rogers, A. V.; Mitchison, H. M.; Bush, A.; Hogg, C., Accuracy of Immunofluorescence in the Diagnosis of Primary Ciliary Dyskinesia. *Am J Respir Crit Care Med* **2017,** *196* (1), 94-101.

44. Tighe, P. J.; Ryder, R. R.; Todd, I.; Fairclough, L. C., Elisa in the Multiplex Era: Potentials and Pitfalls. *Proteomics. Clinical Applications* **2015,** *9* (3-4), 406-406.

45. French, D., Advances in Clinical Mass Spectrometry. *Adv Clin Chem* **2017,** *79*, 153-198.

46. Jannetto, P. J.; Fitzgerald, R. L., Effective Use of Mass Spectrometry in the Clinical Laboratory. *Clinical chemistry* **2016,** *62* (1), 92-8.

47. Couchman, L.; Fisher, D. S.; Subramaniam, K.; Handley, S. A.; Boughtflower, R. J.; Benton, C. M.; Flanagan, R. J., Ultra-Fast Lc-Ms/Ms in Therapeutic Drug Monitoring: Quantification of Clozapine and Norclozapine in Human Plasma. *Drug Test Anal* **2018,** *10* (2), 323-329.

48. Ramoo, B.; Funke, M.; Frazee, C.; Garg, U., Comprehensive Urine Drug Screen by Gas Chromatography/Mass Spectrometry (Gc/Ms). *Methods Mol Biol* **2016,** *1383*, 125-31.

49. Aebersold, R.; Mann, M., Mass Spectrometry-Based Proteomics. *Nature* **2003,** *422* (6928), 198-207.

50. Kim, Y. M.; Heyman, H. M., Mass Spectrometry-Based Metabolomics. *Methods Mol Biol* **2018,** *1775*, 107-118.

51. Cuyckens, F., Mass Spectrometry in Drug Metabolism and Pharmacokinetics: Current Trends and Future Perspectives. *Rapid Commun Mass Spectrom* **2019,** *33 Suppl 3*, 90-95.

52. Chong, Y. K.; Ho, C. C.; Leung, S. Y.; Lau, S. K. P.; Woo, P. C. Y., Clinical Mass Spectrometry in the Bioinformatics Era: A Hitchhiker's Guide. *Comput Struct Biotechnol J* **2018,** *16*, 316-334.

53. Clarke, W., Mass Spectrometry in the Clinical Laboratory: Determining the Need and Avoiding Pitfalls. *Mass Spectrometry for the Clinical Laboratory* **2017**, 1-15.

54. Clarke, W.; Rhea, J. M.; Molinaro, R., Challenges in Implementing Clinical Liquid Chromatography-Tandem Mass Spectrometry Methods - Seeing the Light at the End of the Tunnel. *Journal of Mass Spectrometry* **2013,** *48* (7), 755-767.

55. van den Broek, I., Proteins and Clinical Mass Spectrometry: A Fairy Tale? *Clin Chem* **2019,** *65* (2), 220-221.

56. Goble, J. A.; Rocafort, P. T., Point-of-Care Testing. *J Pharm Pract* **2017,** *30* (2), 229-237.

57. Iovine, N. M.; Ison, T.; Payton, T.; Morris, J. G., Jr.; Rand, K., High Percentage of False-Positive Results for Influenza B Obtained with a Rapid Influenza Point-of-Care Test. *Clin Infect Dis* **2014,** *59* (4), 604-5.

58. Wabuyele, S. L.; Colby, J. M.; McMillin, G. A., Detection of Drug-Exposed Newborns. *Ther Drug Monit* **2018,** *40* (2), 166-185.

59. Loke, S. Y.; Lee, A. S. G., The Future of Blood-Based Biomarkers for the Early Detection of Breast Cancer. *Eur J Cancer* **2018,** *92*, 54-68.

60. Ombrone, D.; Giocaliere, E.; Forni, G.; Malvagia, S.; la Marca, G., Expanded Newborn Screening by Mass Spectrometry: New Tests, Future Perspectives. *Mass Spectrom Rev* **2016,** *35* (1), 71-84.

61. Lindholm, C.; Altimiras, J., Point-of-Care Devices for Physiological Measurements in Field Conditions. A Smorgasbord of Instruments and Validation Procedures. *Comp Biochem Physiol A Mol Integr Physiol* **2016,** *202*, 99-111.

62. Quesada-González, D.; Merkoçi, A., Nanomaterial-Based Devices for Point-of-Care Diagnostic Applications. *Chem Soc Rev* **2018,** *47* (13), 4697-4709.

63. Li, L.; Chen, T.-C.; Ren, Y.; Hendricks, P. I.; Cooks, R. G.; Ouyang, Z., Mini 12, Miniature Mass Spectrometer for Clinical and Other Applications—Introduction and Characterization. *Analytical Chemistry* **2014,** *86* (6), 2909-2916.

64. Taylor, K. S.; Verbakel, J. Y.; Feakins, B. G.; Price, C. P.; Perera, R.; Bankhead, C.; Plüddemann, A., Diagnostic Accuracy of Point-of-Care Natriuretic Peptide Testing for Chronic Heart Failure in Ambulatory Care: Systematic Review and Meta-Analysis. *Bmj* **2018,** *361*, k1450.

65. Denkinger, C.; Kik, S.; Casenghi, M., High-Priority Target Product Profiles for New Tuberculosis Diagnostics: Report of a Consensus Meeting. *WHO Meeting Report* **2014,** (April 2014), 1-98.

66. Pai, M.; Schito, M., Tuberculosis Diagnostics in 2015: Landscape, Priorities, Needs, and Prospects. *Journal of Infectious Diseases* **2015,** *211* (Suppl 2), S21-S28.

67. Pai, M.; Ramsay, A.; O'Brien, R., Evidence-Based Tuberculosis Diagnosis. *PLoS Medicine* **2008,** *5* (7), 1043-1049.

68. Pai, M.; Nicol, M. P.; Boehme, C. C., Tuberculosis Diagnostics: State of the Art and Future Directions. *Microbiol Spectr* **2016,** *4* (5).

69. Luppa, P. B.; Müller, C.; Schlichtiger, A.; Schlebusch, H., Point-of-Care Testing (Poct): Current Techniques and Future Perspectives. *TrAC Trends in Analytical Chemistry* **2011,** *30* (6), 887-898.

70. Anfossi, L.; Di Nardo, F.; Cavalera, S.; Giovannoli, C.; Baggiani, C., Multiplex Lateral Flow Immunoassay: An Overview of Strategies Towards High-Throughput Point-of-Need Testing. *Biosensors (Basel)* **2018,** *9* (1).

71. Lattanzio, V. M.; Nivarlet, N.; Lippolis, V.; Della Gatta, S.; Huet, A. C.; Delahaut, P.; Granier, B.; Visconti, A., Multiplex Dipstick Immunoassay for Semi-Quantitative Determination of Fusarium Mycotoxins in Cereals. *Anal Chim Acta* **2012,** *718*, 99-108.

72. Bheemavarapu, L. P.; Shah, M. I.; Joseph, J.; Sivaprakasam, M., Multi-Cartridge Fluorescence Reader for Quantitative Immunoassays. *Conf Proc IEEE Eng Med Biol Soc* **2019,** *2019*, 5447-5450.

73. Joseph, J.; Vasan, J. K.; Shah, M.; Sivaprakasam, M.; Mahajan, L., Iquant™ Analyser: A Rapid Quantitative Immunoassay Reader. *Conf Proc IEEE Eng Med Biol Soc* **2017,** *2017*, 3732-3736.

74. Woolf, S. H., The Meaning of Translational Research and Why It Matters. *JAMA* **2008,** *299* (2), 211-213.

75. Fu, Z.; Zhang, R.; Li, P.; Jia, M., Translational Epidemiology: The Powerful Tool for Precision Cancer Medicine. *J Cancer Res Ther* **2019,** *15* (2), 269-271.

76. Fernández-Figueroa, E. A.; Lino-Silva, S.; Peña-Velasco, J. E.; Rangel-Escareño, C., Pharmaco-Geno-Proteo-Metabolomics and Translational Research in Cancer. *Adv Exp Med Biol* **2019,** *1168*, 1-7.

77. Aronson, J. K.; Ferner, R. E., Biomarkers-a General Review. *Curr Protoc Pharmacol* **2017,** *76*, 9.23.1-9.23.17.

78. Geyer, P. E.; Holdt, L. M.; Teupser, D.; Mann, M., Revisiting Biomarker Discovery by Plasma proteomics. *Mol Syst Biol* **2017,** *13* (9), 942.

79. Geyer, P. E.; Kulak, N. A.; Pichler, G.; Holdt, L. M.; Teupser, D.; Mann, M., Plasma Proteome Profiling to Assess Human Health and Disease. *Cell Syst* **2016,** *2* (3), 185-95.

80. Zhao, Y.; Brasier, A. R., Qualification and Verification of Protein Biomarker Candidates. *Adv Exp Med Biol* **2016,** *919*, 493-514.

81. Vidova, V.; Spacil, Z., A Review on Mass Spectrometry-Based Quantitative Proteomics: Targeted and Data Independent Acquisition. *Anal Chim Acta* **2017,** *964*, 7-23.

82. Cai, W.; Tucholski, T. M.; Gregorich, Z. R.; Ge, Y., Top-Down Proteomics: Technology Advancements and Applications to Heart Diseases. *Expert Rev Proteomics* **2016,** *13* (8), 717-30.

83. Goldman, A. R.; Beer, L. A.; Tang, H. Y.; Hembach, P.; Zayas-Bazan, D.; Speicher, D. W., Proteome Analysis Using Gel-Lc-Ms/Ms. *Curr Protoc Protein Sci* **2019,** *96* (1), e93.

84. Lathrop, J. T.; Jeffery, D. A.; Shea, Y. R.; Scholl, P. F.; Chan, M. M., Us Food and Drug Administration Perspectives on Clinical Mass Spectrometry. *Clinical chemistry* **2016,** *62* (1), 41-7.

85. Jarolim, P., High Sensitivity Cardiac Troponin Assays in the Clinical Laboratories. *Clin Chem Lab Med* **2015,** *53* (5), 635-52.

86. Park, D. J.; Kim, Y.; Lee, H. K.; Lee, J.; Han, K.; Kwon, H. J., Multicenter Comparison of Four Automated Immunoassay Analyzers for Prostate Specific Antigen. *Ann Lab Med* **2019,** *39* (4), 406-410.

87. Rodenko, O.; Eriksson, S.; Tidemand-Lichtenberg, P.; Troldborg, C. P.; Fodgaard, H.; van Os, S.; Pedersen, C., High-Sensitivity Detection of Cardiac Troponin I with Uv Led Excitation for Use in Point-of-Care Immunoassay. *Biomed Opt Express* **2017,** *8* (8), 3749-3762.

88. Kozinski, M.; Krintus, M.; Kubica, J.; Sypniewska, G., High-Sensitivity Cardiac Troponin Assays: From Improved Analytical Performance to Enhanced Risk Stratification. *Crit Rev Clin Lab Sci* **2017,** *54* (3), 143-172.

89. Makarov, D. V.; Carter, H. B., The Discovery of Prostate Specific Antigen as a Biomarker for the Early Detection of Adenocarcinoma of the Prostate. *J Urol* **2006,** *176* (6 Pt 1), 2383-5.

90. Grossman, D. C.; Curry, S. J.; Owens, D. K.; Bibbins-Domingo, K.; Caughey, A. B.; Davidson, K. W.; Doubeni, C. A.; Ebell, M.; Epling, J. W., Jr.; Kemper, A. R.; Krist, A. H.; Kubik, M.; Landefeld, C. S.; Mangione, C. M.; Silverstein, M.; Simon, M. A.; Siu, A. L.; Tseng, C. W., Screening for Prostate Cancer: Us Preventive Services Task Force Recommendation Statement. *Jama* **2018,** *319* (18), 1901-1913.

91. Ganguly, N.; Giang, P. H.; Gupta, C.; Basu, S. K.; Siddiqui, I.; Salunke, D. M.; Sharma, P., Mycobacterium Tuberculosis Secretory Proteins Cfp-10, Esat-6 and the Cfp10:Esat6 Complex Inhibit Lipopolysaccharide-Induced Nf-Kappab Transactivation by Downregulation of Reactive Oxidative Species (Ros) Production. *Immunology and cell biology* **2008,** *86* (1), 98-106.

92. Guinn, K. M.; Hickey, M. J.; Mathur, S. K.; Zakel, K. L.; Grotzke, J. E.; Lewinsohn, D. M.; Smith, S.; Sherman, D. R., Individual Rd1 -Region Genes Are Required for Export of Esat-6/Cfp-10 and for Virulence of Mycobacterium Tuberculosis. *Molecular Microbiology* **2004,** *51* (2), 359-370.

93. Leng, J.; Ding, Y.; Shou, C.; Wu, Z.; Zhuo, G.; Wang, K.; Shen, J.; Huang, S., Development of a Novel Anti Esat-6 Monoclonal Antibody for Screening of Mycobacterium Tuberculosis. *International Journal of Clinical and Experimental Medicine* **2014,** *7* (11), 4238-4243.

94. Li, F.; Xu, M.; Qin, C.; Xia, L.; Xiong, Y.; Xi, X.; Fan, X.; Gu, J.; Pu, J.; Wu, Q.; Lu, S.; Wang, G., Recombinant Fusion Esat6-Cfp10 Immunogen as a Skin Test Reagent for Tuberculosis Diagnosis: An Open-Label, Randomized, Two-Centre Phase 2a Clinical Trial. *Clinical Microbiology and Infection* **2016,** *22* (10), 889.e9-889.e16.

95. Yuan, K.; Wu, X.; Zhang, Q.; Zhong, Z.; Chen, J., Enzyme-Linked Immunospot Assay Response to Recombinant Cfp-10/Esat-6 Fusion Protein among Patients with Spinal Tuberculosis: Implications for Diagnosis and Monitoring of Surgical Therapy. *International Journal of Infectious Diseases* **2013,** *17* (9), e733-e738.

96. Boström, T.; Takanen, J. O.; Hober, S., Antibodies as Means for Selective Mass Spectrometry. *Journal of Chromatography B* **2016,** *1021*, 3-13.

97. De Marchi, T.; Kuhn, E.; Carr, S. A.; Umar, A., Antibody-Based Capture of Target Peptides in Multiple Reaction Monitoring Experiments. 2015; Vol. 1293, pp 123-135.

98. Schoenherr, R. M.; Saul, R. G.; Whiteaker, J. R.; Yan, P.; Whiteley, G. R.; Paulovich, A. G., Anti-Peptide Monoclonal Antibodies Generated for Immuno-Multiple Reaction Monitoring-Mass Spectrometry Assays Have a High Probability of Supporting Western Blot and Elisa. *Molecular & Cellular Proteomics* **2015,** *14* (2), 382-398.

99. Anderson, N. L.; Anderson, N. G.; Haines, L. R.; Hardie, D. B.; Olafson, R. W.; Pearson, T. W., Mass Spectrometric Quantitation of Peptides and Proteins Using Stable Isotope Standards and Capture by Anti-Peptide Antibodies (Siscapa). *Journal of proteome research* **2004,** *3* (2), 235-44.

100. Liu, C.; Zhao, Z.; Fan, J.; Lyon, C. J.; Wu, H.-J.; Nedelkov, D.; Zelazny, A. M.; Olivier, K. N.; Cazares, L. H.; Holland, S. M.; Graviss, E. A.; Hu, Y., Quantification of Circulating Mycobacterium Tuberculosis Antigen Peptides Allows Rapid Diagnosis of Active Disease and Treatment Monitoring. *Proceedings of the National Academy of Sciences of the United States of America* **2017,** *114* (15), 3969-3974.

101. Zhu, Z.-J.; Schultz, A. W.; Wang, J.; Johnson, C. H.; Yannone, S. M.; Patti, G. J.; Siuzdak, G., Liquid Chromatography Quadrupole Time-of-Flight Mass Spectrometry Characterization of Metabolites Guided by the Metlin Database. *Nature Protocols* **2013,** *8* (3), 451-460.

102. Choi, J. R.; Yong, K. W.; Choi, J. Y.; Cowie, A. C., Emerging Point-of-Care Technologies for Food Safety Analysis. *Sensors (Basel)* **2019,** *19* (4).

103. Cohen, N.; Mechaly, A.; Mazor, O.; Fisher, M.; Zahavy, E., Rapid Homogenous Time-Resolved Fluorescence (Htrf) Immunoassay for Anthrax Detection. *J Fluoresc* **2014,** *24* (3), 795-801.

104. Singh, A. K.; Stanker, L. H.; Sharma, S. K., Botulinum Neurotoxin: Where Are We with Detection Technologies? *Crit Rev Microbiol* **2013,** *39* (1), 43-56.

105. Benkerroum, N., Staphylococcal Enterotoxins and Enterotoxin-Like Toxins with Special Reference to Dairy Products: An Overview. *Crit Rev Food Sci Nutr* **2018,** *58* (12), 1943-1970.

106. Bandu, R.; Mok, H. J.; Kim, K. P., Phospholipids as Cancer Biomarkers: Mass Spectrometry-Based Analysis. *Mass Spectrom Rev* **2018,** *37* (2), 107-138.

107. Kawatsuki, A.; Morita, S. Y.; Watanabe, N.; Hibino, E.; Mitsuishi, Y.; Sugi, T.; Murayama, S.; Nishimura, M., Lipid Class Composition of Membrane and Raft Fractions from Brains of Individuals with Alzheimer's Disease. *Biochem Biophys Rep* **2019,** *20*, 100704.

108. Zarrouk, A.; Debbabi, M.; Bezine, M.; Karym, E. M.; Badreddine, A.; Rouaud, O.; Moreau, T.; Cherkaoui-Malki, M.; El Ayeb, M.; Nasser, B.; Hammami, M.; Lizard, G., Lipid Biomarkers in Alzheimer's Disease. *Curr Alzheimer Res* **2018,** *15* (4), 303-312.

109. Sans, M.; Zhang, J.; Lin, J. Q.; Feider, C. L.; Giese, N.; Breen, M. T.; Sebastian, K.; Liu, J.; Sood, A. K.; Eberlin, L. S., Performance of the Masspec Pen for Rapid Diagnosis of Ovarian Cancer. *Clinical chemistry* **2019,** *65* (5), 674-683.

110. Zhang, J.; Katta, N.; Suliburk, J.; Rector, J.; Garza, K. Y.; Sans, M.; Zahedivash, A.; Ludolph, B.; Bensussan, A.; Giese, N.; Syed, A.; Yu, W.; Liu, J.; Nagi, C.; Young, J. H.; Eberlin, L. S.; Sorace, A. G.; Lin, J. Q.; DeHoog, R. J.; Milner, T. E., Nondestructive Tissue Analysis for Ex Vivo and in Vivo Cancer Diagnosis Using a Handheld Mass Spectrometry System. *Science Translational Medicine* **2017,** *9* (406), eaan3968-eaan3968.

111. Caliendo, A. M.; Gilbert, D. N.; Ginocchio, C. C.; Hanson, K. E.; May, L.; Quinn, T. C.; Tenover, F. C.; Alland, D.; Blaschke, A. J.; Bonomo, R. A.; Carroll, K. C.; Ferraro, M. J.; Hirschhorn, L. R.; Joseph, W. P.; Karchmer, T.; MacIntyre, A. T.; Reller, L. B.; Jackson, A. F.; Infectious Diseases Society of, A., Better Tests, Better Care: Improved Diagnostics for Infectious Diseases. *Clinical infectious diseases : an official publication of the Infectious Diseases Society of America* **2013,** *57 Suppl 3* (Suppl 3), S139-S170.

112. Takáts, Z., Mass Spectrometry Sampling under Ambient Conditions with Desorption Electrospray Ionization. **2009,** *471* (2004), 10-13.

113. Wang, H.; Liu, J.; Cooks, R. G.; Ouyang, Z., Paper Spray for Direct Analysis of Complex Mixtures Using Mass Spectrometry. *Angewandte Chemie* **2010,** *122* (5), 889-892.

114. Espy, R. D.; Teunissen, S. F.; Manicke, N. E.; Ren, Y.; Ouyang, Z.; Van Asten, A.; Cooks, R. G., Paper Spray and Extraction Spray Mass Spectrometry for the Direct and Simultaneous Quantification of Eight Drugs of Abuse in Whole Blood. *Analytical Chemistry* **2014,** *86* (15), 7712-7718.

115. Hecht, M.; Evard, H.; Takkis, K.; Veigure, R. t.; Aro, R.; Lohmus, R.; Herodes, K.; Leito, I.; Kipper, K., Sponge Spray—Reaching New Dimensions of Direct Sampling and Analysis by Ms. *Analytical Chemistry* **2017,** *89* (21), 11592-11597.

116. Wang, T.; Zheng, Y.; Wang, X.; Austin, D. E.; Zhang, Z., Sub-Ppt Mass Spectrometric Detection of Therapeutic Drugs in Complex Biological Matrixes Using Polystyrene-Microsphere-Coated Paper Spray. *Analytical Chemistry* **2017,** *89* (15), 7988-7995.

117. Zargar, T.; Khayamian, T.; Jafari, M. T., Immobilized Aptamer Paper Spray Ionization Source for Ion Mobility Spectrometry. *Journal of Pharmaceutical and Biomedical Analysis* **2017,** *132*, 232-237.

118. Zhou, X.; Pei, J.; Huang, G., Reactive Paper Spray Mass Spectrometry for in Situ Identification of Quinones. *Rapid Communications in Mass Spectrometry* **2014,** *29* (1), 100-106.

119. Sarkar, D.; Som, A.; Pradeep, T., Catalytic Paper Spray Ionization Mass Spectrometry with Metal Nanotubes and the Detection of 2,4,6-Trinitrotoluene. *Analytical Chemistry* **2017,** (2), acs.analchem.7b02288-acs.analchem.7b02288.

120. Costa, C.; Webb, R.; Palitsin, V.; Ismail, M.; De Puit, M.; Atkinson, S.; Bailey, M. J., Rapid, Secure Drug Testing Using Fingerprint Development and Paper Spray Mass Spectrometry. *Clinical Chemistry* **2017,** *63* (11), 1745-1752.

121. Ren, Y.; Wang, H.; Liu, J.; Zhang, Z.; McLuckey, M. N.; Ouyang, Z., Analysis of Biological Samples Using Paper Spray Mass Spectrometry: An Investigation of Impacts by the Substrates, Solvents and Elution Methods. *Chromatographia* **2013,** *76* (19-20), 1339-1346.

122. Wang, H.; Manicke, N. E.; Yang, Q.; Zheng, L.; Shi, R.; Cooks, R. G.; Ouyang, Z., Direct Analysis of Biological Tissue by Paper Spray Mass Spectrometry. *Analytical Chemistry* **2011,** *83* (4), 1197-1201.

123. Manicke, N. E.; Abu-Rabie, P.; Spooner, N.; Ouyang, Z.; Cooks, R. G., Quantitative Analysis of Therapeutic Drugs in Dried Blood Spot Samples by Paper Spray Mass Spectrometry: An Avenue to Therapeutic Drug Monitoring. *Journal of the American Society for Mass Spectrometry* **2011,** *22* (9), 1501-1507.

124. Chiang, S.; Zhang, W.; Ouyang, Z., Paper Spray Ionization Mass Spectrometry: Recent Advances and Clinical Applications. *Expert Review of Proteomics* **2018,** *15* (10), 781-789.

125. Shi, R.-Z.; El Gierari, E. T. M.; Manicke, N. E.; Faix, J. D., Rapid Measurement of Tacrolimus in Whole Blood by Paper Spray-Tandem Mass Spectrometry (Ps-Ms/Ms). *Clinica chimica acta; international journal of clinical chemistry* **2015,** *441*, 99-104.

126. Shi, R. Z. R. Z.; El Gierari, E. T. M.; Faix, J. D.; Manicke, N. E., Rapid Measurement of Cyclosporine and Sirolimus in Whole Blood by Paper Spray-Tandem Mass Spectrometry. *Clinical Chemistry* **2016,** *62* (1), 295-297.

127. Ma, Q.; Bai, H.; Li, W.; Wang, C.; Cooks, R. G.; Ouyang, Z., Rapid Analysis of Synthetic Cannabinoids Using a Miniature Mass Spectrometer with Ambient Ionization Capability. *Talanta* **2015,** *142*, 190-6.

128. Ma, X.; Chong, L.; Tian, R.; Shi, R.; Hu, T. Y.; Ouyang, Z.; Xia, Y., Identification and Quantitation of Lipid C=C Location Isomers: A Shotgun Lipidomics Approach Enabled by Photochemical Reaction. *Proceedings of the National Academy of Sciences* **2016,** *113* (10), 2573-2578.

129. Pu, F.; Alfaro, C. M.; Pirro, V.; Xie, Z.; Ouyang, Z.; Cooks, R. G., Rapid Determination of Isocitrate Dehydrogenase Mutation Status of Human Gliomas by Extraction Nanoelectrospray Using a Miniature Mass Spectrometer. *Analytical and Bioanalytical Chemistry* **2019,** *411* (8), 1503-1508.

130. Ren, Y.; McLuckey, M. N.; Liu, J.; Ouyang, Z., Direct Mass Spectrometry Analysis of Biofluid Samples Using Slug-Flow Microextraction Nano-Electrospray Ionization. *Angewandte Chemie International Edition* **2014,** *53* (51), 14124-14127.

131. Gao, L.; Cooks, R. G.; Ouyang, Z., Breaking the Pumping Speed Barrier in Mass Spectrometry: Discontinuous Atmospheric Pressure Interface. *Analytical Chemistry* **2008,** *80* (11), 4026-4032.

132. Zhai, Y.; Feng, Y.; Wei, Y.; Wang, Y.; Xu, W., Development of a Miniature Mass Spectrometer with Continuous Atmospheric Pressure Interface. *Analyst* **2015,** *140* (10), 3406-3414.

133. Gao, L.; Song, Q.; Patterson, G. E.; Cooks, R. G.; Ouyang, Z., Handheld Rectilinear Ion Trap Mass Spectrometer. *Analytical Chemistry* **2006,** *78* (17), 5994-6002.

134. Liu, X.; Wang, X.; Bu, J.; Zhou, X.; Ouyang, Z., Tandem Analysis by a Dual-Trap Miniature Mass Spectrometer. *Analytical Chemistry* **2019,** *91* (2), 1391-1398.

135. Zou, R.; Cao, W.; Chong, L.; Hua, W.; Xu, H.; Mao, Y.; Page, J.; Shi, R.; Xia, Y.; Hu, T. Y.; Zhang, W.; Ouyang, Z., Point-of-Care Tissue Analysis Using Miniature Mass Spectrometer. *Analytical Chemistry* **2019,** *91* (1), 1157-1163.

136. Kirby, A. E.; Lafrenière, N. M.; Seale, B.; Hendricks, P. I.; Cooks, R. G.; Wheeler, A. R., Analysis on the Go: Quantitation of Drugs of Abuse in Dried Urine with Digital Microfluidics and Miniature Mass Spectrometry. *Analytical Chemistry* **2014,** *86* (12), 6121-6129.

137. Pu, F.; Zhang, W.; Bateman, K. P.; Liu, Y.; Helmy, R.; Ouyang, Z., Using Miniature Ms System with Automatic Blood Sampler for Preclinical Pharmacokinetics Study. *Bioanalysis* **2017,** *9* (21), 1633-1641.

2. TARGETED PROTEIN AND PEPTIDE QUANTITATION BY IMMUNOAFINITY ENRICHMENT WITH A MINIATURE MASS SPECTROMETRY SYSTEM

2.1 Introduction

Mass spectrometry (MS) is a powerful tool in proteomics that allows for the identification and quantitation of proteins.[1] In the last decade, proteomics has expanded significantly in coordination with MS for the study of biological systems at a molecular level.[2-7] The wide application of proteomics in the study of biological system allows for the discovery of mechanisms of biological processes and protein biomarkers related to disease states and progression.[3, 8-13] These applications rely on the development of quantitation methods with reliable workflows, such as utilizing immunoaffinity enrichment or molecular tags.[14-16] The combination of immunoaffinity enrichment and chromatography techniques with MS enables quantitation of proteins to be routinely performed by detecting specified digested peptides.[8, 17, 18] However, the transfer of proteomic methods for clinical analysis requires further simplification of the traditionally complicated and time-consuming sample pretreatment. Modifications of enzyme onto nanomaterials—such as NanoDisks[19]— have been shown to improve the immunoaffinity enrichment and throughput. The immobilization of proteases onto functional materials can also accelerate the digestion of proteins significantly. These methods have been tested extensively on clinical samples and have been shown to be promising for screening biomarkers.[20, 21] Some ambient ionization techniques have also been applied for the analysis of proteins such as desorption electrospray ionization[22-24], paper spray[25], electrospray ionization-assisted laser desorption ionization[26], and radio-frequency acoustic desorption ionization[27], all of which avoid chromatographic separation and minimize sample pretreatment procedures.

The miniaturization of MS systems is an important endeavor for implementing MS analysis into clinical and point-of-care (POC) applications.[28-30] Miniature MS instruments are a promising solution for the direct analysis of peptides or proteins and critical towards the development of an integrated system for POC proteome analysis. These miniature MS systems have previously shown strong performances in quantitative analysis of drugs in biofluids.[25, 31, 32] However, protein and peptide analysis has not been realized by miniature MS systems. Several spectra of protein standards have been reported previously, but only using high concentration standards.[29] Challenges

that have currently hindered protein analysis by miniature MS instruments are the limited mass ranges by a linear ion trap and inefficient tandem MS analysis around the 1 kDa mass range for quantitative analysis.

In this work, we investigate the capabilities of our prototype Mini β for high-mass molecular analysis using a variety of standards. Several notable improvements over the previous system include the addition of a second linear ion trap, pressure control through an external gas inlet, and improved radiofrequency (RF) and alternating current (AC) electronics. A wide range of standards including peptides and small proteins were analyzed by nano-electrospray ionization (nESI) and the Mini β. Several notable improvements over the previous system—Mini 12— include the mass range, resolution and accuracy. Large molecular weight standards were used to characterize the capabilities of our prototype by several tandem MS (MS/MS) modalities in conjunction with pressure control to optimize collision-induced dissociation (CID) efficiency. Finally, improved isolation and analyte multiplexing is investigated as potential features to enhance high-throughput analysis by our miniature MS instrument. Results identified that our prototype Mini β is amenable for the analysis of large molecular weight molecules and can be potentially be used as a POC biomedical testing tool for protein biomarker diagnostics.

After fully characterizing the capabilities of our prototype miniature MS instrument, a workflow was developed for the quantification of peptides using various synthetic peptides in collaboration with Cell Signaling Technology (CST). Peptides of different molecular weights and amino acids— ranging from 800 Da to 1800 Da— were analyzed by both in-trap and beam-type MS/MS to identify significant peptide fragments. Afterwards, the *Met* peptide—m/z 1046— and its internal standard were selected as the target peptide for further workflow development. MS^3 analysis—performing MS/MS twice— was performed to verify the sequence of the major fragment of the *Met* peptide. Further development was performed to optimize mass analysis of the targeted peptide by the miniature MS instrument. Quantitative linearity ranging from 50 nM to 5 μM was identified, with a limit of detection at 10 nM. As a preliminary examination of the proposed workflow, SKBR3 cell lysate was analyzed by performing immunoaffinity enrichment to quantify the *Met* peptide. The combination of immunoaffinity enrichment with miniature MS systems provides a strong basis for the development of a POC biomedical testing tool; however, investigations on real immunoaffinity enriched SKBR samples reveal the capability of detecting, but not quantitation, from 1 mg of cell lysate.

2.2 Experimental Methods

Ultra-high purity water, methanol, acetonitrile, ammonia, acetic and formic acid were purchased from ThermoFisher Scientific (Waltham, MA, USA). Peptide standards and immunoaffinity enriched samples were provided by Cell Signaling Technology (Beverly, MA, USA). Peptide standards used in this experiment include: STAT6 (Sequence: GY*VPATIK, 928 Da), SMAD2 (Sequence: VLTQM(ox)GSPSvR, 1196 Da), FGFR4 (Sequence: GvHHIDY*Y*KK, 1418 Da), AKT (Sequence:RPHFPQfS*YSASGA, 1732 Da), Met (Sequence: YVNDFFNK, 1046 Da), isotopically-labelled Met (Sequence: YVNDFfNK, 1056 Da), and Met2 (Sequence: VFPNSAPlEGGTR, 1350 Da). Addition of isotopic amino acid is depicted in lowercase. M(ox) represents oxidized Methionine. Phosphorylated amino acids are followed by *. Peptide standard solutions provided were stored in acetonitrile/water/trifluoroacetic acid (TFA) (60/40/1; *v/v/v*) at a concentration of 25 µM. Several exceptions are the *Met* and *isotopically labelled Met* standards which were provided at a concentration of 414 µM and 313 µM, respectively. Resulting peptide solutions were diluted in methanol:water (1/1; *v/v*) when analyzed in negative ion mode. Formic acid was added was added to the dilution solution—methanol:water:formic acid (50/50/1; *v/v/v*) — for positive ion mode analysis. *Met* proteins from SKBR3 cell lysate were first treated with dithiothreitol to reduce disulfides before trypsin digestion. Digestion was stopped using an acetonitrile/water/TFA solution (60/40/1; *v/v/v*) and dried before analysis. The immunoaffinity enriched sample was reconstituted in methanol water (1/1; *v/v*) before analysis by the miniature MS instrument.

Borosilicate glass capillaries of 0.86 mm inner diameter (i.d) and 1.5 mm outer diameter (o.d.) were purchased from Sutter Instruments (Novato, CA, USA) and used to fabricate nESI tips using a micropipette puller (Model P-1000, Sutter Instrument, CA). All miniature MS spectra and calibration curves were processed in OriginPro 2019b (OriginLab, Northampton, MA).

Immunoaffinity Enrichment Protocol

The anti-*Met* antibody M14-4186—5 µg per immunoaffinity precipitation (IAP)— was conjugated in PBS (10 mM Na_2HPO_4, 10 mM NaH_2PO_4, 150 mM NaCl) overnight to 10 µL packed Protein A agarose beads (Roche, Basel, Switzerland) at 4 °C, and the unbound antibody was removed by washing 4 times with 1.4 mL of ice-cold PBS. Tryptic, lyophilized peptides

derived from 5 mg of Balb-C mouse liver tissue were resuspended in MOPS IAP buffer (50mM MOPS pH 7.2, 10 mM KH_2PO_4, 50 mM NaCl) and centrifuged at 12,000 rpm for 5 minutes to remove insoluble materials in an Eppendorf 5415D centrifuge (Eppendorf, NY, USA). Solubilized peptides were combined with antibody/bead slurries and subjected to end-over-end rotation for 2 h at 4 °C. Beads were pelleted by centrifugation at 5,400 rpm for 1 min in a Galaxy minispin (VWR, PA, USA) microcentrifuge at 20 °C. Beads were washed twice with 1 mL MOPS IAP buffer and four times with 1 mL water (Honeywell Burdick and Jackson, NJ, USA). Peptides were eluted from beads with 0.15% TFA—sequential elution of 65 µL followed by 55 µL, 10 min each at room temperature. Eluted peptides were desalted over tips packed with Empore C18 (Sigma-Alrich, MO, USA) and eluted with acetonitrile:water (40/60; *v/v*; 0.1% TFA) and dried under vacuum.

Miniature Mass Spectrometry Instrument Analysis

The miniature mass spectrometer used in this experiment is a modified Mini β (PURSPEC Technologies, IN, USA) equipped with a discontinuous atmospheric pressure interface (DAPI) for the introduction of ions from a pulsed nanoESI source and two linear ion traps (LIT).[30, 33] Both linear ion traps are fitted co-axially and use an axial ejection method for both ion transfer and mass scanning.[34] The electric field radius for both linear ion traps are 4 mm and 51 mm for r_0 and length, respectively. A second pinch valve was fitted off-axis as a gas inlet to control the induction of air into the chamber. MS/MS analysis was performed on all peptide standards to identify significant peptide chain fragments. The National Institute of Standards and Technology peptide fragment calculator (NIST, MD, USA) was utilized to identify the theoretical peptide fragments.

For miniature MS analysis, peptides were isolated using a ramped RF sweep. A 20 ms AC sweep from 10 kHz to 50 kHz was used to eject the background high mass ions. Beam-type CID was performed by setting a voltage gradient between the two linear ion traps—1.2 kV, LIT1; 2.5 kV, LIT2. In-trap CID for *Met*—m/z 1046— was set to a frequency of 80 to 98 kHz. A wide frequency range was used to fragment the precursor ion and the produced b_8 fragment—loss of H_2O. Mass selective axial ejection (MSAE) was performed by setting the LIT1 AC frequency to 55.5 kHz with a low amount of energy applied for analyte excitation. Mass scanning—otherwise called scan-out— was performed in LIT2 by ramping the RF from 0.5 kV to 5 kV across 300 ms with an AC frequency of 330 kHz. Gate 3 was set with a slightly positive voltage—20 V— to

facilitate the formation of the ejection cone necessary for axial ejection. Lastly, the timing of each segment—including the DAPI opening time and ion cooling times— were optimized. Comparison spectra were collected using a Bruker Maxis Impact Q-TOF mass spectrometer (Bruker Daltonics, Bremen, Germany) or an Orbitrap Fusion Lumos Tribrid mass spectrometer coupled to an EASY-nLC 1200 (ThermoFisher, MA, USA).

2.3 Results and Discussion

2.3.1 Mass Range, Accuracy, and Resolution

Characterization of our miniature MS instrument was performed by using a wide variety of large molecular weight analytes, peptides and small proteins. Nano-electrospray ionization (nESI) was the ionization method used to analyze all standard samples. Borosilicate glass capillaries were pulled to a nanotip—2 to 5 nm— and 10 µL of solution was placed within. The nESI electrode holder is used to apply a high voltage—1.5 to 2 kV— to initiate solution ionization. A schematic of our modified miniature MS instrument is shown in Figure 2-1. After ionization by nESI, ions are trapped in the LIT1 and transferred to LIT2 for mass analysis. Due to improved RF and AC electronics, a wider mass range and high-mass ions can be identified. Cytochrome C is a 12 kDa protein that forms numerous charge states when using ESI and is used as the model analyte to characterize the working mass range (Figure B-1). Charge states from +20—m/z 619— to +8—m/z 1548— were identified using our miniature MS instrument. This signifies a wide working range for biologically significant peptides, especially with the formation of multiply charged ions.

Before mass analysis, calibration of our miniature mass spectrometer is key in identifying accurate mass weights of compounds in unknown samples. Other factors such as non-linear RF ramps or AC wobble can easily affect the calibration of our miniature MS instrument, thus further characterization of mass accuracy is needed. Using an in-house calibration standard, we use several low mass peaks—m/z 466,578— and four high mass peaks—m/z 1021,1121,1221,1321— from the UltraMark calibration standard to draw a calibration curve. A linear regression line was generated using OriginPro, with the slope and intercept placed into the software for calibration. Using these six points, a strong linearity was observed with a r^2 value of nearly one (Figure 2-2a, *insert*). Calibration was performed three times and averaged. In order to test the mass accuracy of the instrument, Angiotensin I and II were used as the sample analyte.

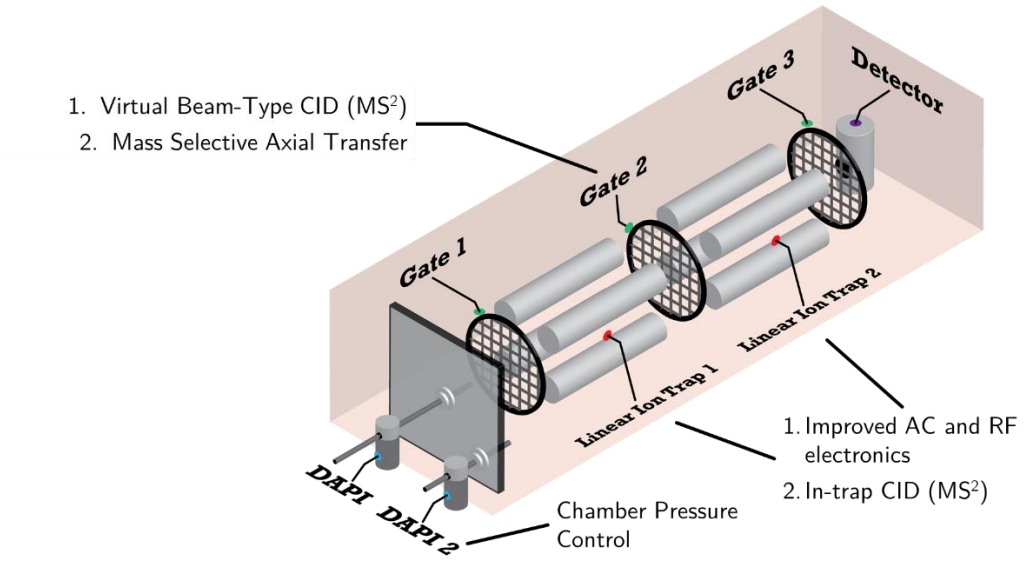

Figure 2-1. Schematic and listed improvements of the modified Mini β. *DAPI*, discontinuous atmospheric pressure interface; *CID*, collisional-induced dissociation; *AC*, alternating current; *RF*, radiofrequency.

During nESI, both single and doubly charged analytes are produced and used to characterize mass accuracy (Figure 2-2b, c). All mass peaks—*Angiotensin I*, m/z 648.9,1297.6; *Angiotensin II*, m/z 523.77,1046.54— were shifted by less than 0.1% and accurate within 1 Da. Although for proteomic applications, a shift of 1 Da is wide, the use of MS/MS helps improve the specificity of our analytical method.

Finally, mass resolution is characterized by achieving unit-resolution of Hexakis(1H, 1H, 5H-octafluoropentoxy)-phosphazine (HEX). The scan-out RF was narrowed to a mass range of 1000 Da and the scan-out speed was decreased—from 5000 Da/s to 1500 Da/s. All three isotopic peaks of HEX were clearly resolved (Figure B-2). As a result, the improvements to mass range, accuracy, and resolution of the modified miniature MS instrument shows a strong potential for high-mass analysis.

2.3.2 Pressure Optimization and Tandem Mass Spectrometry Capabilities

With the addition of a second ion trap, a fundamental aspect of the miniature MS instrument is the ion transfer between traps. Further characterization of the miniature MS system is necessary to highlight the capabilities of a dual ion trap system. Initial investigations have been performed previously by *Liu, et al.* translating several commercial MS instrument scan modes into the dual ion trap system used.[30] In this study, we utilize the *Met* peptide —m/z 1046— as our target.

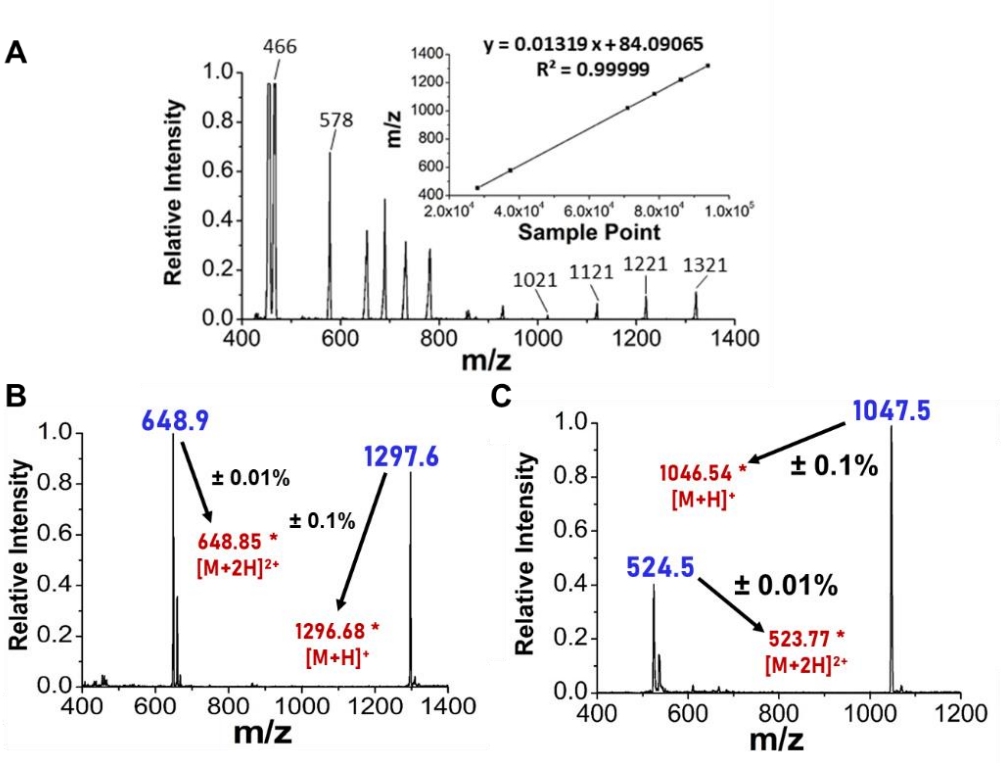

Figure 2-2. (a) Full scan of the in-house calibration solution spiked with UltraMark calibration solution. (a, insert) Linear calibration curve drawn from the calibration solution with an r^2 value of 1. (b) Angiotensin I and (c) angiotensin II at a concentration of 0.1 µg mL^{-1} was used to quantify the accuracy of the mass calibration using our standard solution. * represents the m/z published on the Human Metabolome Database.

For ion manipulations within the vacuum chamber, the ideal pressure is at 10^{-2} to 10^{-3} Torr. In order to maintain this pressure with the secondary gas inlet, the length of a pinhole metal inlet capillary was adjusted to 42 cm. Before the ion transfer, the gas inlet was opened to normalize the chamber pressure to 10^{-2} Torr and held open throughout. Comparisons between the two pressure curves formed during each scan is shown in Figure 2-3.

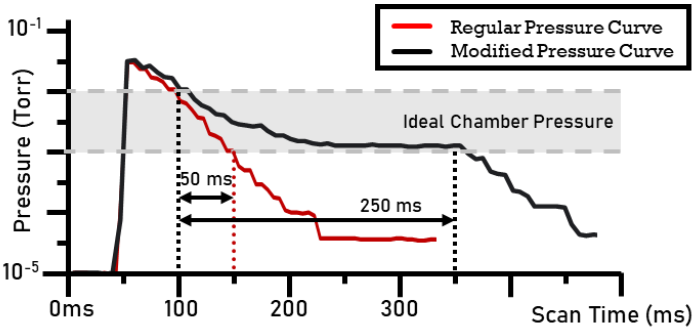

Figure 2-3. Pressure curves when opening (*black)* or closing (*red)* the off-axis gas inlet. The amount of time within the ideal chamber pressure range is increased by a factor of 5.

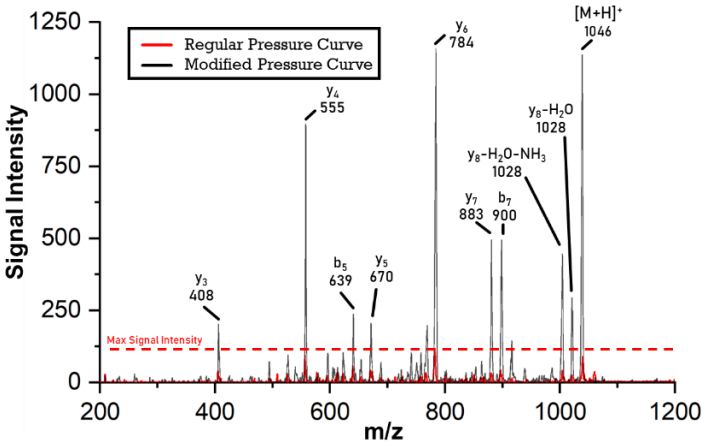

Figure 2-4. Tandem mass spectra of the *Met* peptide using the regular (*red*) and gas-inlet assisted (*black*) pressure curve. The signal intensity is increased 10-fold, highlighting major peptide fragment peaks.

By opening the gas inlet, a significant increase in SNR due to the improved ion transfer and MS/MS efficiency was observed (Figure 2-4). Coincidentally, the higher pressure is also beneficial when performing beam-type CID. As a more energetically powerful dissociation method in comparison to in-trap CID, the resulting MS/MS spectra produces a wider variety of ion fragments. A voltage gradient was formed by setting the float direct current (DC) voltages of each ion trap to 2.5 kV and 1.2 kV, respectively. In Figure B-3, MS/MS spectra are shown using the two different CID methods, illustrating different *y* and *b* peptide fragments as well as a more preferential formation of low mass fragment ions by beam-type CID.

2.3.3 Peptide Multiplexing using Dual Linear Ion Traps

As a proof-of-concept study, peptide multiplexing was performed using our miniature MS instrument. This is especially important for disease diagnostics to improve sensitivity and specificity. In diseases such as tuberculosis (TB), *Li et al.* reported a significant increase in their MS-based diagnostic method by observing two proteins —both CFP-10 and ESAT-6.[19] Similarly, the second peptide can help validate the presence of a protein, especially after tryptic digestion of sample. Therefore, a preliminary method for peptide multiplexing was developed. Trypsin-digested mouse liver peptides —1 mg— was reconstituted in 10 mL of methanol:water (1/1; *v/v*; 1% formic acid) to mimic a desalted trypsin-digest solution. Both *Met* and *Met 2*—peptide fragments from the *Met* protein— were spiked at a concentration of 10 µM for peptide multiplexing (Figure 2-5).

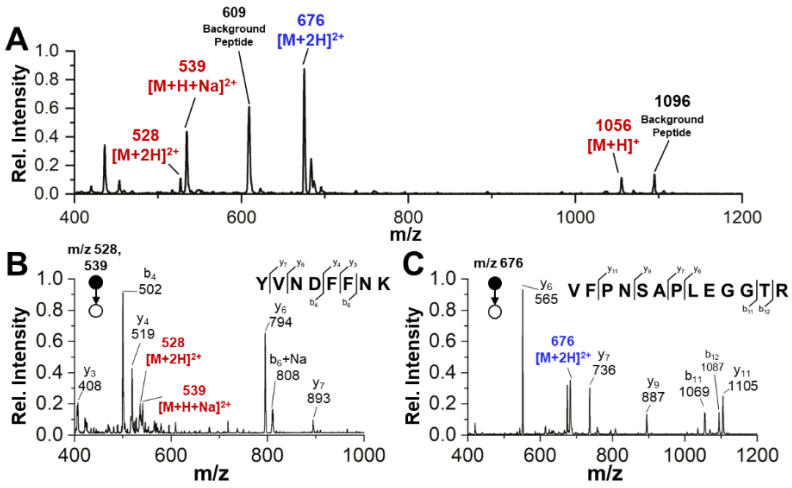

Figure 2-5. Two different synthetic *Met* peptides were spiked into a trypsin-digested mouse liver peptide solution reconstituted in methanol:water (1/1;*v/v*; 1% formic acid). Both *Met* peptides are observed in the (a) full scan spectra by directly scan-out from LIT1. Peptide multiplexing was performed by sequentially and selectively transferring *Met* and *Met2* from LIT1 to LIT2 for MS/MS analysis by in-trap CID. MS/MS spectra of (b) *Met* and (c) *Met2* were obtained from the same scan function and sample. *LIT*, linear ion trap; *MS/MS*, tandem mass spectrometry; *CID*, collision-induced dissociation.

The miniature MS method for peptide multiplexing was developed for several scans to occur with only a single ion introduction. The samples are introduced into the first ion trap through nESI. During ion transfer, instead of setting Gate 2 to 0V, the voltage is set to 30V. With the application of the ion-specific resonant frequency— a similar AC frequency for in-trap CID— only ions that are resonated can be transferred into LIT2. This method is used to selectively transfer the doubly-charged *Met* peptide and its sodium adduct—m/z 528,539 respectively— before in-trap CID and scan-out by LIT2. After scan-out of the *Met* peptide, another resonant frequency—tuned to *Met2,* m/z 676— was set on LIT1 to initiate transfer to the now-empty LIT2. During each transfer, the gas inlet is opened with a similar timing as shown in *Section 2.3.2* to maximize ion transfer efficiency. This method allows for several ions to be MS/MS analyzed with the same ion introduction, with inconsequential delays to the overall scan time. Furthermore, variations in sample introduction is overcome, revealing the importance of multiplexing that can be achieved using a miniature MS system.

2.3.4 Tandem Mass Spectrometry Analysis of Four Peptide Standards

Performance of our miniature MS system was evaluated using peptides—masses ranging from 800 Da to 1800 Da— provided by CST (Figure 2-6). Peptides were ionized by nESI with 1.5 kV

in positive ion mode. The peptide ions were trapped in the first linear ion trap and then isolated using RF-AC sweeps. Afterwards, ions were non-selectively transferred to the second ion trap for in-trap CID. MS/MS analysis of all four peptides resulted in *b* or *y* peptide fragments with the loss of ammonia or water. These losses are specific to certain amino acids and considered when labelled. Dehydration occurs on lysine, arginine, glutamine, and asparagine, while deamination occurs on serine and tyrosine. Peptide fragment prediction software was used to annotate MS/MS spectra and highlight the fragmentation pattern of all four peptides. In all four peptide standards, the doubly charged ions were selected to be fragmented to produce a richer MS/MS profile. In accordance to the results in the previous study, peptide analysis by our instrument is amenable.

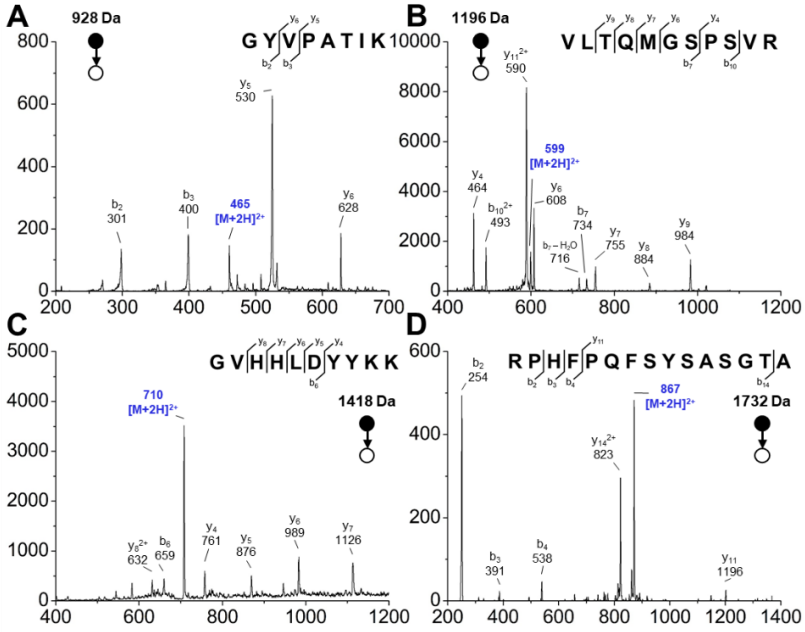

Figure 2-6. MS/MS spectra of four different synthetic peptide standards at a concentration of 10 µM provided by Cell Signaling Technology. (a) STAT6, (b) SMAD2, (c) FGFR4 and (d) AKT peptide.

2.3.5 Major Fragment Analysis of the *Met* Peptide

The *Met* peptide —sequence: YVNDFFNK— was used as the target molecule for quantitative studies, a major tryptic peptide fragment from the *C-Met* protein.[35] This peptide can be analyzed under both positive and negative ion modes which was observed by the addition or loss of a proton, respectively. However, in positive ion mode, it was observed that the sodium adduct of *Met* peptide was present along with numerous other background peaks. Due to this matrix-like effect in positive ion mode, low concentration analysis of *Met* peptide results in diminished ion intensity. Negative

ion mode analysis eliminates the presence of most background peaks observed in positive ion mode, along with improved signal intensities. Experiments represented henceforth were performed in negative ion mode unless stated otherwise.

In order to further characterize the *Met* peptide, MS/MS was performed by both beam-type and in-trap CID (Figure B-4). It was observed that the doubly charged peptide requires less energy for fragmentation in comparison to the single charged peptide. Further increases in the fragmentation voltage results in an increase in low mass fragments. However, excessive AC energy or increased voltage gradients between the LIT DC float result in extensive fragment losses. Positive ion mode MS/MS results in a much richer fragmentation profile in comparison to negative ion mode, most likely due to the fragments being positively charged. Both fragmentation types result in a major peptide fragment—m/z 633, sequence:DFFNK— with the loss of two amines on asparagine and lysine. It is noted that when using in-trap CID, the *Met* peptide will first preferentially form the b_8 fragment—loss of a water molecule— and must be fragmented again to form the m/z 633 peak. Due to the prevalence of the y_5 fragment—m/z 633—, this peak is used as the target for quantitation by MS/MS analysis.

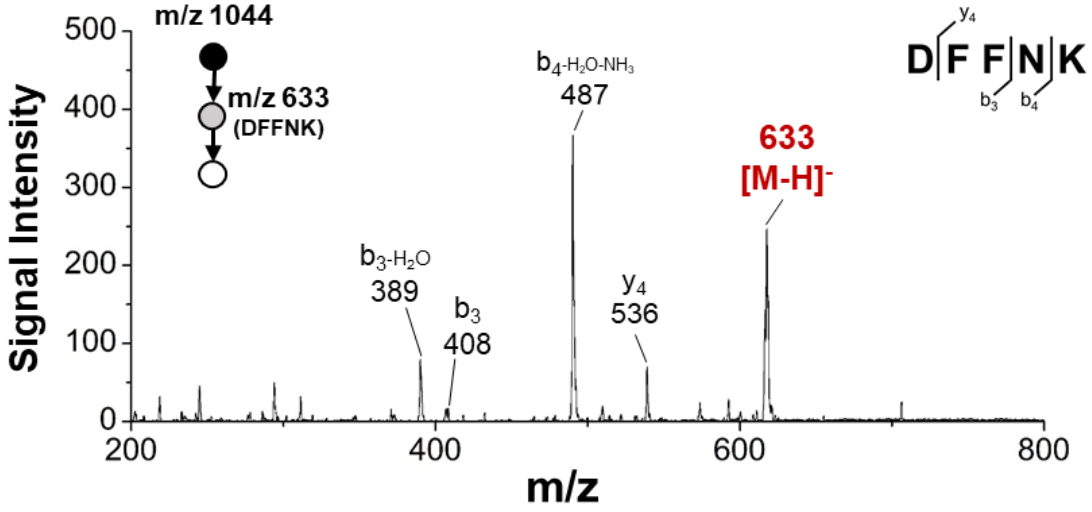

Figure 2-7. MS^3 analysis of the major peptide y_5 fragment to verify amino acid sequence.

MS^3 characterization was performed to ensure correct sequence profiling of the y_5 peptide fragment. As with the previous study, 10 µM of *Met* peptide standard in methanol:water (1/1;*v/v*) was analyzed in negative ion mode. The peptide was isolated in LIT1 and beam-type CID was performed during ion transfer at a pressure of 4.7 mTorr. Another isolation at m/z 633 was

performed in LIT2 before in-trap CID at a frequency of 300 kHz, resulting in peaks correlated to its amino acid composition (Figure 2-7).

2.3.6 Quantitation Curve using the Optimized Miniature MS Method

Optimization of experimental and instrument parameters was performed to maximize signal intensity and eliminate errors during the drawing of the calibration curve. Experimental parameters include the dilution of all standard peptide solutions with methanol:water (1/1; *v/v*) along with an ionization voltage of 1.4 kV. A standard MS method—identified *scan function*— was developed using a 100 ms long gas inlet opening to maintain a pressure of 4.7 mTorr during ion transfer. Ions are introduced via the DAPI for 15 ms and trapped at a q-value of 0.3 in the first LIT. Quantitation is performed by monitoring the peak signal intensity of m/z 633 and the internal standard fragment, m/z 643—from the regular and isotopically labelled peptides. After transferring the ions to the second ion trap, an AC frequency of 75 to 80 kHz was applied for 20 ms and a second AC frequency of 85-90 kHz was applied to fragment the b_8 fragment for another 10 ms. Ion transitions from m/z 1044 to m/z 633 and m/z 1054 to m/z 633 were monitored to identify the ratios between the two signal intensities. A quantitation curve drawn using peptide standards is shown in Figure 2-8. The linear range is from 50 nM to 5 µM with an r^2 value of 0.9989.

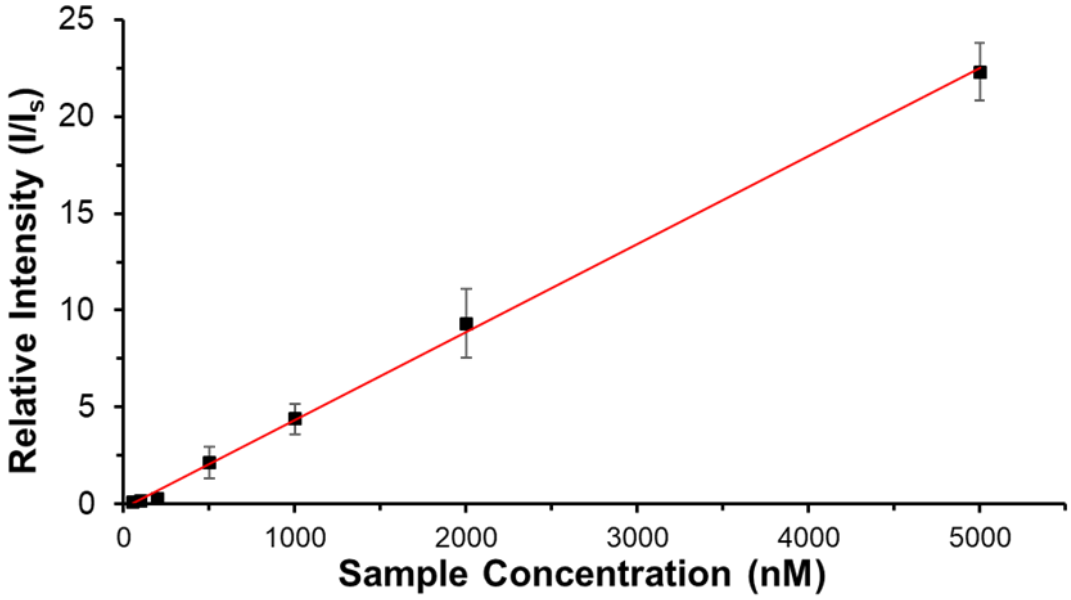

Figure 2-8. Peptide standard calibration curve using optimized miniature MS method. Linearity is drawn from 10 nM to 5 µM with an r^2 value of 0.9989.

2.3.7 Effect of Background Peptides on Signal Intensity

After pretreatment by immunoaffinity enrichment, the presence of background peptides is common and is the prevalent reason in why immunoassays have lowered sensitivities.[18, 36, 37] These background peptides can easily affect ionization efficiency and quantitative performance during peptide analysis. This effect is investigated by using the trypsin-digested mouse liver peptide solution from the peptide multiplexing study. Various concentrations of mouse liver peptide solution ranging from 100 ppb to 10 ppm were spiked with 1 µM of *Met* peptide and its internal standard. The ratios of peak signal intensity between the *Met* peptide and its internal standard was investigated and identified no significant changes throughout the sample between the different concentrations of mouse liver peptide solution. When the background peptide solution concentration was increased to greater than 10 ppm, a significant drop in *Met* peptide signal intensity was observed. This establishes a limit on the amount of background peptide present after immunoaffinity enrichment.

Several blank immunoaffinity enriched samples—produced by using non-targeted antibodies— from CST were analyzed for its overall signal intensity and its approximation to the different concentrations of mouse liver peptide solutions. It was observed that the signal intensity was on par with the background peptide solution concentrations between 10 ppb and 1 ppm, thus concluding that the co-eluting peptides from an immunoaffinity enrichment protocol has no significant effect. However, when this sample was compared to a standard solution of *Met* peptide and its internal standard, the signal intensity ratio was diminished by a factor of 4.

2.3.8 Modification of the Miniature MS Method for Matrix-Matched Quantitation Curve

Due to the significant difference of *Met* peptide ionization *in solution* and *in matrix*—mouse liver peptide solution, 100ppb— another quantitation curve was drawn with all samples diluted in a mouse liver peptide solution. The internal standard used for this quantitation curve was at a concentration of 500 nM and varied from 10 nM to 5 µM. The method was modified to take advantage of mass-selective axial transfer (MSAT), as well as other small parameter changes as part of the re-optimization. A schematic of the defined protocol is shown in *Figure 2-9.* The resulting calibration curve again showed strong linearity in the linear range of 10 nM to 5 µM. Relative signal deviations (RSDs) of all six points were calculated to be less than 22.4%

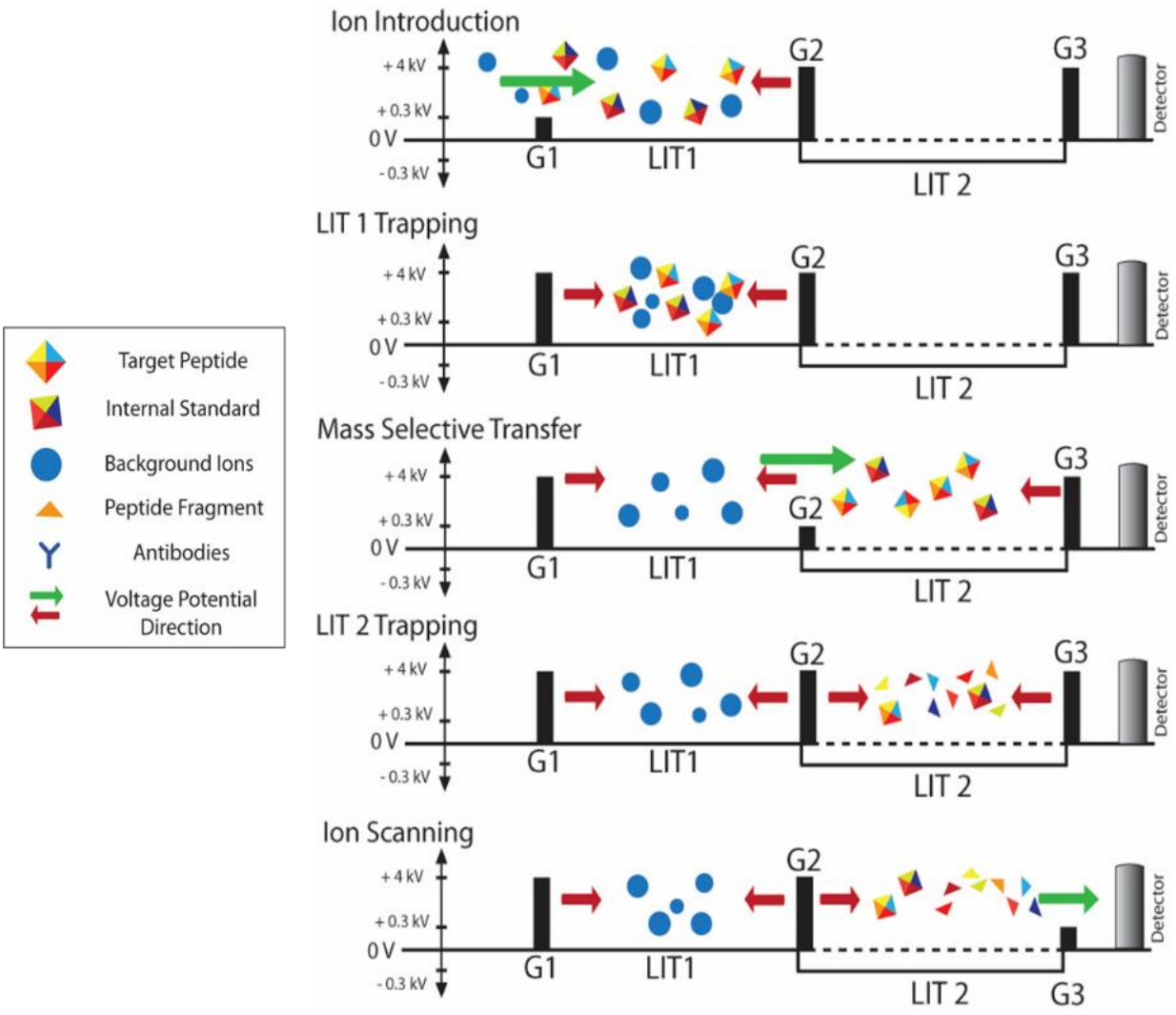

Figure 2-9. Schematic of the scan function used in the miniature MS instrument. The overall scan time is less than 2 seconds after ion introduction.

across all samples with a limit of detection and quantitation like the standard calibration curve (Figure B-5). As mentioned previously, the signal intensity ratio was diminished by a factor of 4.

2.3.9 Preliminary Study of *Met* Peptide Quantification in SKBR3 Cell Lysate

The same miniature MS method was applied to quantify the *Met* peptide from immunoaffinity enriched cell lysate (Figure 2-10). The *C-Met* protein exists in cells as a tyrosine kinase receptor that is correlated with poor patient prognosis and invasive cancer phenotypes.[38, 39] Several series of biological activities are driven by the activation of this receptor, promoting the phosphorylation

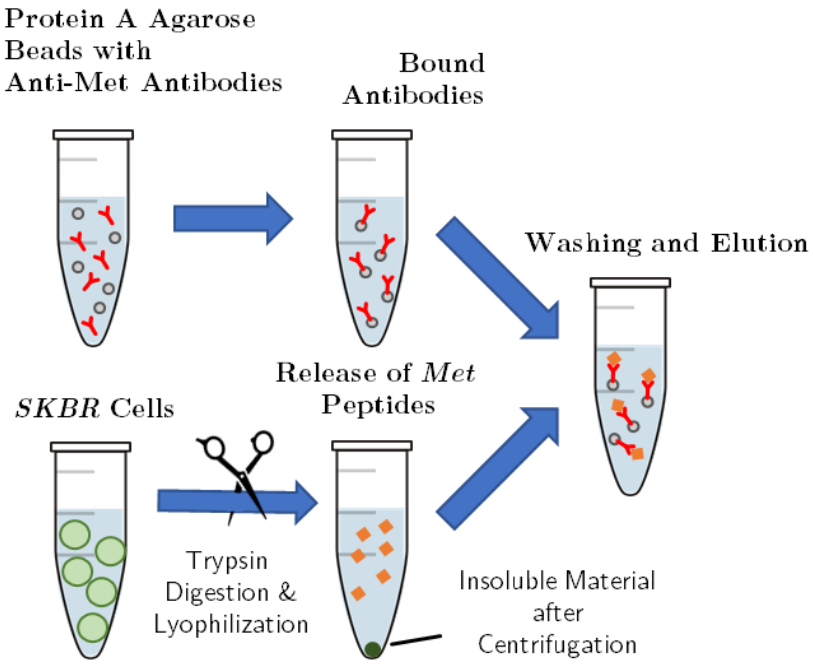

Figure 2-10. Immunoaffinity enrichment workflow for the quantitation of SKBR3 cells before miniature MS analysis.

of downstream proteins. Quantitative studies evaluating *Met* expression has the potential to elucidate oncogenic signaling pathways and be used for drug efficacy evaluations.[40] Trypsin digested cell lysate—1mg— were desalted using C18 tips and dried. Before MS analysis, dried samples were reconstituted in 50 µL of methanol:water (1/1; *v/v*) and spiked with the internal standard for a final concentration of 500 nM. The resulting MS spectra identified several peaks associated with the internal standard and a very minimal peak of the *Met* peptide (Figure 2-11).

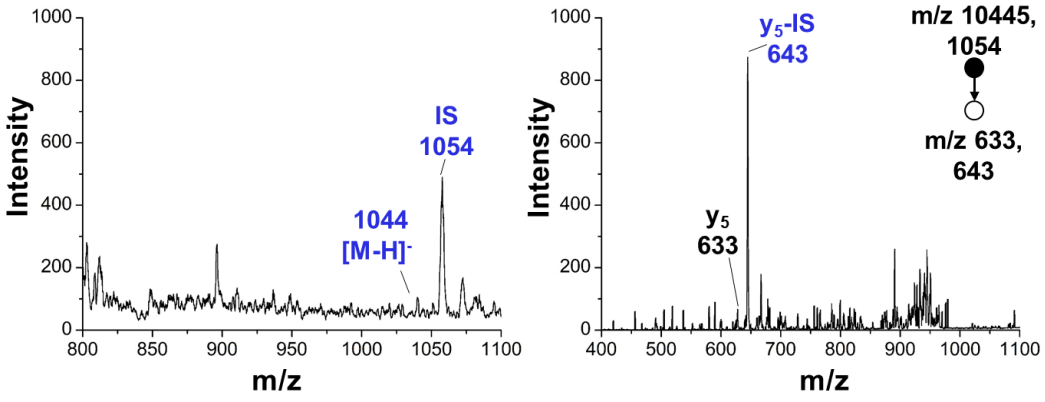

Figure 2-11. Full scan (*left*) and MS/MS *(right)* spectra of immunoaffinity enriched SKBR cell lysate for the *Met* peptide.

Five scans were averaged to eliminate background noise in both full scan and MS/MS scans. Using the matrix-matched quantitation curve, the *Met* peptide was calculated to have a concentration of 125 nM. However, this is inconsistent with the previous findings using LC-MS/MS performed by CST which identified a concentration of 4 nM. This concentration is outside of the linear range defined by our calibration curve and lower than the calculated limit of detection, resulting in an erroneous quantitation. However, detection of the *Met* peptide was achieved from a cell line with a low expression of the *C-Met* protein.

2.4 Conclusion

The analysis of peptides and proteins using our novel prototype dual ion trap miniature MS system was achieved. Protein biomarkers find a limited use in biomedical testing, in part due to the lack of appropriate sensitivities in current POC devices. Miniature mass spectrometry systems are a viable alternative, streamlining the translation of extensive preclinical research on protein biomarkers done with MS. Targeted proteomic techniques including immunoaffinity enrichment and immuno-MRM are several techniques that can be performed at the POC. Characterization of advancements to the miniature MS instrument such as mass accuracy, mass range, and CID efficiency were necessary as a preliminary investigation to the possibility of analyzing large biomolecules. A workflow utilizing conventional immunoaffinity enrichment techniques with our miniature MS instrument was successfully applied to the analysis of a signaling protein expressed in SKBR3 cells. As a result, the developed workflow enables quantitative protein analysis at the POC with a high level of sensitivity and specificity necessary for the application of novel protein biomarkers.

2.5 References

1. Cravatt, B. F.; Simon, G. M.; Yates Iii, J. R., The Biological Impact of Mass-Spectrometry-Based Proteomics. *Nature* **2007,** *450* (7172), 991-1000.
2. Aebersold, R.; Mann, M., Mass Spectrometry-Based Proteomics. *Nature* **2003,** *422* (6928), 198-207.
3. Kim, J. J.; Savas, J. N.; Miller, M. T.; Hu, X.; Carromeu, C.; Lavallée-Adam, M.; Freitas, B. C. G.; Muotri, A. R.; Yates, J. R.; Ghosh, A., Proteomic Analyses Reveal Misregulation of Lin28 Expression and Delayed Timing of Glial Differentiation in Human Ips Cells with Mecp2 Loss-of-Function. *PLOS ONE* **2019,** *14* (2), e0212553-e0212553.
4. Wysocki, V. H.; Resing, K. A.; Zhang, Q.; Cheng, G., Mass Spectrometry of Peptides and Proteins. *Methods* **2005**.
5. Syka, J. E. P.; Coon, J. J.; Schroeder, M. J.; Shabanowitz, J.; Hunt, D. F., Peptide and Protein Sequence Analysis by Electron Transfer Dissociation Mass Spectrometry. *Proceedings of the National Academy of Sciences of the United States of America* **2004,** *101* (26), 9528-33.
6. Gillet, L. C.; Leitner, A.; Aebersold, R., Mass Spectrometry Applied to Bottom-up Proteomics: Entering the High-Throughput Era for Hypothesis Testing. *Annu Rev Anal Chem (Palo Alto Calif)* **2016,** *9* (1), 449-72.
7. Artigues, A.; Nadeau, O. W.; Rimmer, M. A.; Villar, M. T.; Du, X.; Fenton, A. W.; Carlson, G. M., Protein Structural Analysis Via Mass Spectrometry-Based Proteomics. 2016.
8. Park, H. M.; Satta, R.; Davis, R. G.; Goo, Y. A.; Leduc, R. D.; Fellers, R. T.; Greer, J. B.; Romanova, E. V.; Rubakhin, S. S.; Tai, R.; Thomas, P. M.; Sweedler, J. V.; Kelleher, N. L.; Patrie, S. M.; Lasek, A. W., Multidimensional Top-Down Proteomics of Brain-Region-Specific Mouse Brain Proteoforms Responsive to Cocaine and Estradiol. *Journal of Proteome Research* **2019,** *18* (11), 3999-4012.
9. Shaw, J. B.; Li, W.; Holden, D. D.; Zhang, Y.; Griep-Raming, J.; Fellers, R. T.; Early, B. P.; Thomas, P. M.; Kelleher, N. L.; Brodbelt, J. S., Complete Protein Characterization Using Top-Down Mass Spectrometry and Ultraviolet Photodissociation. *Journal of the American Chemical Society* **2013,** *135* (34), 12646-12651.
10. Zhou, M.; Wysocki, V. H., Surface Induced Dissociation: Dissecting Noncovalent Protein Complexes in the Gas Phase. *Accounts of Chemical Research* **2014**.
11. Harvey, S. R.; Seffernick, J. T.; Quintyn, R. S.; Song, Y.; Ju, Y.; Yan, J.; Sahasrabuddhe, A. N.; Norris, A.; Zhou, M.; Behrman, E. J.; Lindert, S.; Wysocki, V. H., Relative Interfacial Cleavage Energetics of Protein Complexes Revealed by Surface Collisions. *Proceedings of the National Academy of Sciences of the United States of America* **2019,** *116* (17), 8143-8148.
12. Dowd, S. E.; Mustroph, M. L.; Romanova, E. V.; Southey, B. R.; Pinardo, H.; Rhodes, J. S.; Sweedler, J. V., Exploring Exercise- and Context-Induced Peptide Changes in Mice by Quantitative Mass Spectrometry. *ACS Omega* **2018,** *3* (10), 13817-13827.

13. Gillette, M. A.; Carr, S. A., Quantitative Analysis of Peptides and Proteins in Biomedicine by Targeted Mass Spectrometry. *Nature Methods* **2013,** *10* (1), 28-34.

14. Frost, D. C.; Buchberger, A. R.; Li, L., Mass Defect-Based Dimethyl Pyrimidinyl Ornithine (Dipyro) Tags for Multiplex Quantitative Proteomics. *Analytical Chemistry* **2017,** *89* (20), 10798-10805.

15. Frost, D. C.; Greer, T.; Li, L., High-Resolution Enabled 12-Plex Dileu Isobaric Tags for Quantitative Proteomics. *Analytical Chemistry* **2015,** *87* (3), 1646-1654.

16. Xiang, F.; Ye, H.; Chen, R.; Fu, Q.; Li, L., N,N-Dimethyl Leucines as Novel Isobaric Tandem Mass Tags for Quantitative Proteomics and Peptidomics. *Analytical Chemistry* **2010,** *82* (7), 2817-2825.

17. Brockmann, A.; Annangudi, S. P.; Richmond, T. A.; Ament, S. A.; Xie, F.; Southey, B. R.; Rodriguez-Zas, S. R.; Robinson, G. E.; Sweedler, J. V., Quantitative Peptidomics Reveal Brain Peptide Signatures of Behavior. *Proceedings of the National Academy of Sciences of the United States of America* **2009,** *106* (7), 2383-2388.

18. Kuhn, E.; Addona, T.; Keshishian, H.; Burgess, M.; Mani, D. R.; Lee, R. T.; Sabatine, M. S.; Gerszten, R. E.; Carr, S. A., Developing Multiplexed Assays for Troponin I and Interleukin-33 in Plasma by Peptide Immunoaffinity Enrichment and Targeted Mass Spectrometry. *Clinical Chemistry* **2009,** *55* (6), 1108-1117.

19. Liu, C.; Zhao, Z.; Fan, J.; Lyon, C. J.; Wu, H. J.; Nedelkov, D.; Zelazny, A. M.; Olivier, K. N.; Cazares, L. H.; Holland, S. M.; Graviss, E. A.; Hu, Y., Quantification of Circulating Mycobacterium Tuberculosis Antigen Peptides Allows Rapid Diagnosis of Active Disease and Treatment Monitoring. *Proceedings of the National Academy of Sciences of the United States of America* **2017**.

20. Wilcken, B.; Wiley, V.; Hammond, J.; Carpenter, K., Screening Newborns for Inborn Errors of Metabolism by Tandem Mass Spectrometry. *New England Journal of Medicine* **2003**.

21. Hoofnagle, A. N.; Becker, J. O.; Wener, M. H.; Heinecke, J. W., Quantification of Thyroglobulin, a Low-Abundance Serum Protein, by Immunoaffinity Peptide Enrichment and Tandem Mass Spectrometry. *Clinical Chemistry* **2008**.

22. Dulay, M. T.; Eberlin, L. S.; Zare, R. N., Protein Analysis by Ambient Ionization Mass Spectrometry Using Trypsin-Immobilized Organosiloxane Polymer Surfaces. *Analytical Chemistry* **2015,** *87* (24), 12324-12330.

23. Garza, K. Y.; Feider, C. L.; Klein, D. R.; Rosenberg, J. A.; Brodbelt, J. S.; Eberlin, L. S., Desorption Electrospray Ionization Mass Spectrometry Imaging of Proteins Directly from Biological Tissue Sections. *Anal. Chem* **2018,** *90*, 22-22.

24. Ferguson, C. N.; Benchaar, S. A.; Miao, Z.; Loo, J. A.; Chen, H., Direct Ionization of Large Proteins and Protein Complexes by Desorption Electrospray Ionization-Mass Spectrometry. *Analytical Chemistry* **2011,** *83* (17), 6468-6473.

25. Zhang, C.; Manicke, N. E., Development of a Paper Spray Mass Spectrometry Cartridge with Integrated Solid Phase Extraction for Bioanalysis. *Analytical Chemistry* **2015,** *87* (12), 6212-6219.

26. Peng, I. X.; Ogorzalek Loo, R. R.; Margalith, E.; Little, M. W.; Loo, J. A., Electrospray-Assisted Laser Desorption Ionization Mass Spectrometry (Eldi-Ms) with an Infrared Laser for Characterizing Peptides and Proteins. *Analyst* **2010,** *135* (4), 767-772.

27. Dixon, R. B.; Sampson, J. S.; Muddiman, D. C., Generation of Multiply Charged Peptides and Proteins by Radio Frequency Acoustic Desorption and Ionization for Mass Spectrometric Detection. *Journal of the American Society for Mass Spectrometry* **2009,** *20* (4), 597-600.

28. Li, L.; Chen, T. C.; Ren, Y.; Hendricks, P. I.; Cooks, R. G.; Ouyang, Z., Mini 12, Miniature Mass Spectrometer for Clinical and Other Applications - Introduction and Characterization. *Analytical Chemistry* **2014**.

29. Gao, L.; Song, Q.; Patterson, G. E.; Cooks, R. G.; Ouyang, Z., Handheld Rectilinear Ion Trap Mass Spectrometer. *Analytical Chemistry* **2006,** *78* (17), 5994-6002.

30. Liu, X.; Wang, X.; Bu, J.; Zhou, X.; Ouyang, Z., Tandem Analysis by a Dual-Trap Miniature Mass Spectrometer. *Analytical Chemistry* **2019,** *91* (2), 1391-1398.

31. Pu, F.; Chiang, S.; Zhang, W.; Ouyang, Z., Direct Sampling Mass Spectrometry for Clinical Analysis. *The Analyst* **2019,** *144* (4), 1034-1051.

32. Su, Y.; Wang, H.; Liu, J.; Wei, P.; Cooks, R. G.; Ouyang, Z., Quantitative Paper Spray Mass Spectrometry Analysis of Drugs of Abuse. *The Analyst* **2013,** *138* (16), 4443-4443.

33. Xu, W.; Charipar, N.; Kirleis, M. A.; Xia, Y.; Ouyang, Z., Study of Discontinuous Atmospheric Pressure Interfaces for Mass Spectrometry Instrumentation Development. *Analytical Chemistry* **2010,** *82* (15), 6584-6592.

34. Londry, F. A.; Hager, J. W., Mass Selective Axial Ion Ejection from a Linear Quadrupole Ion Trap. *Journal of the American Society for Mass Spectrometry* **2003,** *14* (10), 1130-1147.

35. Organ, S. L.; Tsao, M.-S., An Overview of the C-Met Signaling Pathway. *Therapeutic Advances in Medical Oncology* **2011,** *3* (1 Suppl), S7-S7.

36. Li, G.; Ma, F.; Cao, Q.; Zheng, Z.; DeLaney, K.; Liu, R.; Li, L., Nanosecond Photochemically Promoted Click Chemistry for Enhanced Neuropeptide Visualization and Rapid Protein Labeling. *Nature Communications* **2019,** *10* (1).

37. Liu, R.; Huang, Y.; Xu, H.; Zheng, Y.; Liu, Y.; Han, S.; Yang, M.; Xie, Y.; Wang, K.; Duan, J. a.; Li, L., A Strategy for Identifying Species-Specific Peptide Biomarkers in Deer-Hide Gelatin Using Untargeted and Targeted Mass Spectrometry Approaches. *Analytica Chimica Acta* **2019,** *1092*, 32-41.

38. Bottaro, D. P.; Rubin, J. S.; Faletto, D. L.; Chan, A. M. L.; Kmiecik, T. E.; Vande Woude, G. F.; Aaronson, S. A., Identification of the Hepatocyte Growth Factor Receptor as the C-Met Proto-Oncogene Product. *Science* **1991,** *251* (4995), 802-804.

39. Abounader, R.; Reznik, T.; Colantuoni, C.; Martinez-Murillo, F.; Rosen, E. M.; Laterra, J., Regulation of C-Met-Dependent Gene Expression by Pten. *Oncogene* **2004,** *23* (57), 9173-9182.

40. Christensen, J. G.; Schreck, R.; Burrows, J.; Kuruganti, P.; Chan, E.; Le, P.; Chen, J.; Wang, X.; Ruslim, L.; Blake, R.; Lipson, K. E.; Ramphal, J.; Do, S.; Cui, J. J.; Cherrington, J. M.; Mendel, D. B., A Selective Small Molecule Inhibitor of C-Met Kinase Inhibits C-Met-Dependent Phenotypes in Vitro and Exhibits Cytoreductive Antitumor Activity in Vivo. *Cancer Research* **2003,** *63* (21), 7345-7355.

3. PROFILING POTENTIAL LIPID BIOMARKERS IN BIOFLUIDS USING POLYMER COATING TRANSFER ENRICHMENT WITH MINIATURE MASS SPECTROMETRY SYSTEMS

3.1 Introduction

Lipids are a significant class of biomolecules, representing and facilitating various functions within the cell.[1, 2] As a structural component of cell membranes, source of cell energy, and intermediate in the metabolic signaling processes, lipids play a prevalent, yet significant role within the body. The prevalence of lipids within cells and its respective macromolecular constituents such as tissue and biofluids result in an attractive target for biomedical testing. Numerous studies have focused on profiling the distribution of lipids—otherwise termed *lipidome*— in association with diseases such as cancer and Alzheimer's to reveal statistically significant lipid profiles.[3-5] Mass spectrometry (MS) is a powerful tool based on its identification—i.e. specificity— and quantitation—i.e. sensitivity. The analytical capability of MS instruments is furthered by the addition of photodissociation and photochemical derivatization to enable a more detailed structural analysis of lipids.[6-8] These methods have also been utilized to highlight the discovery of novel lipid biomarkers.[9, 10]

However, conventional lipid analysis has been limited in its use of matrix-assisted laser desorption ionization (MALDI)-MS[11, 12] or chromatography—GC or LC— MS[13, 14]. MALDI-MS utilizes a chemical matrix to cover thin tissue sections before using a high-energy laser to induce ion desorption and ionization. There are several drawbacks to this method, including a significant presence of chemical matrix in the ions produced. This method is also more amenable for the analysis of solid samples—e.g. tissue sections or biopsies— rather than biofluids. Thus, lipid sampling and testing through these methods are reserved for post-operative patients. More recently, the advent of ambient ionization methods has emphasized the possibility of MS lipid analysis in real-time—within surgery rooms— utilizing methods such as desorption electrospray ionization[15] and MasSpec Pen.[16, 17] Other direct sampling techniques such as extraction spray have also shown the possibility of directly analyzing tissue samples through swabs or probes paired to a miniature MS instrument.[18]

For more routine screening methods, biofluid-based lipid biomarkers are a more attractive option for analysis, with consideration to the standardized protocols regarding collection of patient

samples. In this regard, chromatography-MS is the gold standard for lipid profiling. Plasma and its native counterpart—whole blood—are a composition of numerous biological molecules including the anti-coagulant used during sample transport. This results in an incredibly complex sample matrix. Extraction of lipids relies upon an initial sample purification or extraction procedure to eliminate the abundant proteins, cells, and cell debris. However, unlike the targeted extraction of immunoaffinity enrichment, lipid profiling requires an untargeted approach. Several classes of lipids must be equivalently enriched, representative of the natural lipidome within the sample. Several ambient ionization methods have been introduced previously for lipid analysis without chromatography— paper spray[19] and coated-blade spray[20]. Through these methods, lipids remain poorly desorbed through these methods due to strong matrix effects. Solid phase microextraction (SPME) has become a strong alternative for sample treatment.[21] SPME of biological fluids have shown good matrix removal capabilities along with analyte extraction. However, the limiting factor for SPME is its surface area—i.e. extraction capacity. The small amount of absorbent available results in a minimal amount of analyte being extracted and detected.[22] Thus, high resolution MS is a necessary component for comprehensive lipid quantitative analysis.

A novel direct sampling ionization technique was introduced as an alternative to SPME.[23] By forming the absorbent polymer along the interior of a capillary, both enrichment, photochemical derivatization, and internal standard addition can be combined for sensitive and quantitative analysis. This method—polymer coating transfer enrichment (PCTE)— enables the translation of lipid biomarker profiling into the POC when combined with miniature mass spectrometry systems. In this study, in-depth characterization of the polymer, mathematical studies on the enrichment capabilities of PCTE, and comparison studies of the selectivity of slug-flow microextraction (SFME) to PCTE are performed. Lipid and fatty acid standards were analyzed by the miniature MS instrument to identify the fragmentation pattern. Finally, preliminary investigations using the Paternò-Büchi (PB) photochemical reaction were performed on sample extracts of whole blood to highlight major diagnostics ions and minor fragments of lipid isomers. The potential for PCTE paired with miniature MS instruments enables the direct sampling of whole blood samples for lipid biomarker profiling of various diseases such as diabetes and cancer.

3.2 Experimental Methods

3.2.1 Materials

HPLC-grade solvents including water, ethyl acetate, acetone, methanol, dimethyl sulfoxide (DMSO), acetonitrile (ACN), and formic acid were all purchased from ThermoFisher Scientific (Waltham, MA, USA). Lipid standards were purchased from Avanti Polar Lipids, Inc (Alabaster, AL, USA) and fatty acid (FA) standards were purchased from Cayman Chemical (Ann Arbor, MI, USA). Standard solutions were diluted using methanol water (1/1; *v/v*). Oleic acid-d9—deuterated FA 18:1— was used as an internal standard for quantitative studies. Rabbit blood samples were purchased from Innovative Research (Novi, MI, USA) and stored at 4ºC.

3.2.2 Polymer Coating for Lipid Enrichment

3-methacryloxypropyltrimethoxysilane (3-MAPS) was purchased from Alfa Aesar (Haverhill, MA, USA) and diluted with methanol (1/1; *v/v*). Ethylene glycol dimethacrylate (EGDMA) and acrylamide monomer (AA) was purchased from TCI Chemicals (Portland, OR, USA). 2-2'-Azobis(2-methylpropionitrile) (AIBN) was purchased from Aladdin Reagent (Shanghai, China).

Borosilicate capillaries—0.86/1.5mm i.d./o.d. (Sutter Instruments, Novato, CA, USA)— were washed using methanol and water (3 times, sequentially) to ensure clean surfaces for modification. Glass capillaries were activated by washing using a 5% NaOH solution (*w/v*) under room temperature overnight. Afterwards, capillaries were silanized using the 3-MAPS solution for 12h in 40 ºC water bath. Capillaries were washed thoroughly using methanol after silanization and dried in an oven at 70 ºC for another 2 hours.

The polymer solution was prepared using acrylamide and EGDMA as the monomer and cross-linker—10 mg of AA, 3 mg of AIBN, and 100 µL of EGDMA dissolved in ACN:DMSO (9/1;*v/v*). The solution was sonicated for 10 minutes to eliminate dissolved gases from the solution before use. A plug of 5 µL of polymer solution was placed inside of a silanized capillary and moved towards the center. Both ends were plugged using homemade rubber plugs and placed into a 70 ºC oven. Capillaries were rotated after 10 minutes to ensure even heat-distribution for the heat-initiated radical polymerization. A monolithic polymer structure is formed within the capillary after another 10 minutes in the oven—20 minutes overall. When cooled to room temperature,

unbound polymers are removed under a flow of nitrogen gas at 20 psi. The remaining polymer structure bound to the glass capillaries form the thin capillary coating used for lipid enrichment. The polymer-coated glass capillaries were washed with ACN, water, and methanol—3 times, each— before drying in a 70 ºC oven and storing at room temperature for later use.

3.2.3 Lipid Enrichment by Polymer Coating Transfer Enrichment

Enrichment by PCTE follows a non-equilibrium solid phase microextraction process. Several liquid plugs are placed inside of the polymer coated capillary: biofluid and extraction solvent—10 µL, each. The liquid plugs are separated by a small air plug— approximately 5 to 10 mm— to prevent unwanted liquid-liquid interaction. Using a pipette gun, both liquid plugs are cycled back and forth through capillary action. The aliphatic nature of the polymer helps absorb lipids into the polymer coating when interacting with the biofluid. Afterwards, the extraction solvent releases the captured lipids for analysis by MS. Although a single capillary-action driven interaction of the liquid plugs is minimal and does not reach equilibrium, repeated processes result in a near-complete extraction in a short amount of time. Plugs are cycled 40 to 60 times to ensure maximum enrichment efficiencies were obtained. For MS analysis, the extraction solvent is removed from the capillary and placed into a nano-electrospray ionization (nESI) tip.

3.2.4 Lipid Enrichment by Slug-Flow Microextraction

Slug-flow microextraction (SFME) is a process that relies upon a liquid-liquid interaction between the sample and extraction solvent plugs. The overall procedure is identical to PCTE except for the polymer coating and plug of air. Two liquid plugs—sample and extraction solvent—are cycled by capillary action. This action results in the entire sample interacting with the extraction solvent at the formed liquid-liquid interface. Polar analytes from the sample plug are transferred into the extraction solvent after cycling for 60 s. For MS analysis, the extraction solvent is removed from the capillary placed into a nESI tip.

3.2.5 Paternò-Büchi Reaction for Photochemical Lipid Analysis

PB reactions were performed to investigate the elucidation of lipid structure in both lipid standards and whole blood. This photochemical reaction utilizes acetone for the addition of an

acetone molecule to the C=C bond in unsaturated lipids. Solution exposure to the photons emitted by an ultraviolet (UV) lamp excite the carbonyl group in lipids, resulting in a cycloaddition reaction to occur with acetone (Figure C-1). During tandem MS (MS/MS) analysis, this bond is easily broken, releasing the acetone molecule to reveal a characteristic 58 Da loss along with the two lipid fragments. Isomeric lipids with C=C bonds at different positions along the lipid chain can be separated using this reaction by observing the lipid fragment masses. PB reactions were performed online using a 254 nm UV lamp onto nESI tip. After transferring the elution solvent into a nESI tip, an additional 10 µL of acetone:water (4/1; *v/v*) was added. The tip was placed near — around 1 cm— the UV lamp to induce PB reaction for a minute.

3.2.6 Miniature Mass Spectrometry Instrument Analysis

A single ion trap miniature mass spectrometer (Mini β, PURSPEC Technologies, Beijing, China) was used to evaluate standards and whole blood. The discontinuous atmospheric pressure interface (DAPI) was used to introduce a packet of ions to be captured by the linear ion trap. A linear ion trap —r_0: 4 mm; length: 51 mm— is used for MS analysis. No external gas is needed; instead, opening the DAPI for a second time during ion manipulation is used to increase the chamber pressure. Thus, the DAPI is opened twice during a single scan: first, to introduce ions, and second, to increase the chamber pressure for improved MS/MS analysis. MS/MS analysis was performed on several lipids using negative ion mode. ‘

For full scan analysis in the negative ion mode, the scan function was set to a mass range of m/z 100 to 800 to minimize space charge. During this scan, alternating current (AC) was applied to eject high mass ions—ions with a molecular weight greater than 500 Da. Scan-out was performed by the axial ejection method towards the detector. Stored Waveform Inverse Fourier Transform (SWIFT) was used to isolate the selected peak at a high q-value with MS/MS performed at a q-value of 0.2. For analysis in positive ion mode, the mass range was set from m/z 200 to 1200. A q-value of 0.3 was used to identify phosphatidylcholine (PC), phosphatidylserine (PS), and phosphotidylglycerol (PG) lipid species and analyzed through MS/MS. All major fragments were confirmed using a commercial q-ToF instrument (Maxis Impact, Bruker Daltonics, Bremen, Germany).

3.3 Results and Discussion

3.3.1 Polymer Coating Characterization

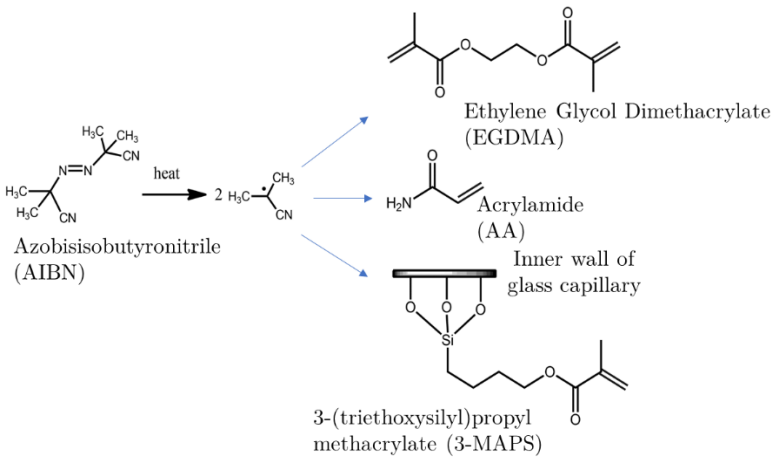

Figure 3-1. Principle components of the polymer coating solution. 3-MAPS is used as an anchor to the inner wall of the glass capillaries, while AA and EGDMA are the monomer and cross-linker. AIBN initiates polymerization by releasing free radicals when heated.

Heat-initiated radical polymerization was employed to synthesize poly (acrylamide-ethylene glycol dimethacrylate) within pre-modified borosilicate glass capillaries (Figure 3-1). After polymerization for 20 to 30 minutes, cross-linking was stopped by removing the capillaries from the oven and using nitrogen to blow out the unbound polymers. A thin and homogenous polymer layer was formed on the glass capillaries. The resulting chemical structure of the polymer results in several functional groups complementary to the lipid structure. The aliphatic bore of the porous polymer (Figure C-2, *red*) preferentially interacts with the aliphatic group of lipids. In contrast, the amide groups (Figure C-2, *green*) formed by the acrylamide backbone reduce the hydrophobicity of the polymer, assisting in improving sample contact with the polymer. Nitrogen adsorption experiments were also performed to verify the presence of micropores and mesopores (Figure 3-2, *right*). During PCTE analysis, the mesopores help increase the flow of whole blood—a more viscous sample type— throughout the polymer, while the micropores could assist in enhancing *van der Waals* forces between the polymer and analyte. Both infrared (Figure C-3) and scanning electron microscopy (Figure 3-2) studies were previously performed to visualize the

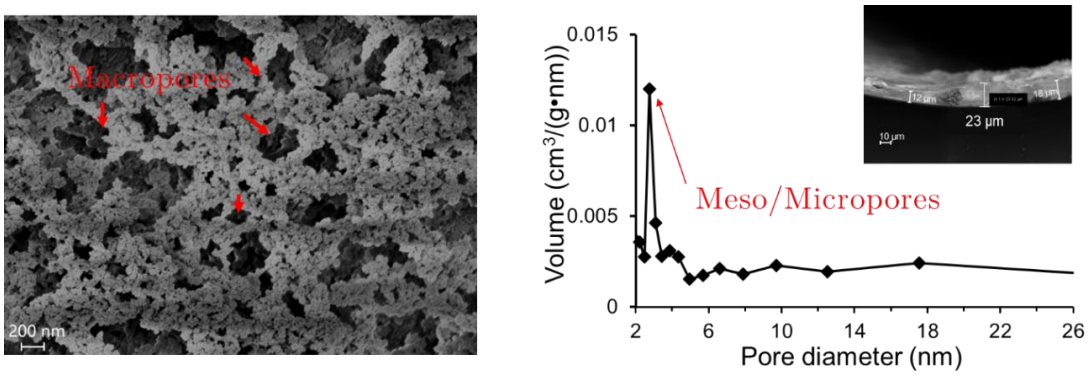

Figure 3-2. *(left)* SEM image of polymer surface. Macropores are easily visualized and prominent throughout the polymer coating. *(right)* Barret-Joyner-Halenda plot for micropore distribution within the poly (AA-EGDMA) coating. (*right, insert*). Cross-sectional image of formed polymer.

polymer composition and physical characteristics. SEM analysis identified a porous surface with a thickness of 20 µm (Figure 3-2, *insert*).

3.3.2 Mathematical Modeling of PCTE

The enrichment strategy by PCTE is justified as a discontinuous, repeatable, and nonequilibrium microextraction process. Within each capillary-action driven cycle, only a portion of the sample plug interacts with the polymer at a short amount of time. In this short period, diffusion of lipids into—and out of— the polymer occurs, carrying a small number of lipids. By repeating this process multiple times, lipids are consistently transferred until diffusion towards the polymer can no longer occur. This differs fundamentally from SPME, which relies upon equilibrium to occur to maximize enrichment. In order to evaluate the improved efficacy of PCTE compared to SPME, a mathematical model was created. Several assumptions were made to simplify the model. The first assumption is that the polymer coating has the same surface area of SPME. This is to ensure that a consistent comparison can be made between the two different modalities. The second assumption is that for PCTE, the extractions are consistent across each cycle. Several constants such as the diffusion and partition coefficients are selected based on a previously published SPME article. The time constant is also assumed to be the same between each method. The third assumption is that desorption from the polymer to the extraction solvent is complete. No lipids remain on the polymer during desorption and is completely eluted into the extraction solvent. Another assumption is that the elution solvent acts as an infinite reservoir for

the absorption of lipids. Due to the relatively large volume of extraction solvent, lipids that have been previously extracted can be safely assumed to have no effect on subsequent elution. This assumption can be further expanded to assume that all lipids captured by the polymer are eluted into the extraction solvent. This is justified due to the equivalent amounts of time spent by the sample-polymer and polymer-extraction solvent interfaces.

The general equation for a liquid-solid mass transfer equation was used as a starting point. The number of analytes—defined as *n*— absorbed by a solid-phase with respect to time—defined as *t*— is shown as:

Equation 3-1. $n_t = n_0(1 - e^{-at})$

In this equation, n_0 represents the initial number of analytes in the sample; n_t represents the number of analytes after *t* amount of time. First, the inverse exponential is substituted by a single variable—defined as r_1. *Equation 3-2* defines the first number of analytes extracted by the *first* extraction cycle.

Equation 3-2. $n_1 = n_0 r_1$

In the second cycle, the number of available analytes is diminished by n_1 resulting in the updated equation:

Equation 3-3. $n_2 = (n_0 - n_1) r_2$

Assuming that each cycle is the same amount of time, *t* is substituted with *k*—defined as the number of cycles. After a *k* number of cycles, the equation becomes:

Equation 3-4. $n_k = (n_0 - n_1 - n_2 - \cdots - n_{k-1})\, r_k$

In *Equation 3-4*, r_k and its constituents—r_1, r_2, ..., r_k— are defined as the ratio of analytes to be extraction in each extraction cycle. Based on the assumptions made initially, this means that the ratio of analytes captured from the biofluid plug remains constant.

Equation 3-5. $r_1 \approx r_2 \approx r_3 \approx \cdots \approx r_k = r$

After setting the time for each cycle to be 1 s and combining it with *Equation 3-1* and *Equation 3-2*:

Equation 3-6. $r = \frac{n_1}{n_0} = 1 - e^{-at} = 1 - e^{-a}$

A summation of the total analytes becomes:

Equation 3-7. $n_{total} = \sum_{k=1}^{\infty} n_1 + n_2 + n_3 + \cdots + n_k \approx n_0[1-(1-r)^k]$

$$= V_s C_0 (1 - e^{-ak})$$

where, V_s represents the volume of the sample solution and C_0 is the initial concentration of analytes. Combined, this represents the number of analytes in the liquid plug. The final equation remains very similar to *Equation 3-1*. However, instead of *t*, the PCTE process is directly related to the number of cycles performed. With enough cycles, a complete extraction of analytes from the sample plug can be achieved.

In contrast, SPME has been previously modelled. These studies have defined the amount of analyte extracted by the sorbents under equilibrium conditions to be:

Equation 3-8. $n_e = \frac{K_e V_c V_s}{K_e V_c + V_s} C_0 \approx K_e V_f C_0$

K_e represents the distribution coefficient of the analyte between the coating and the sample matrix. V_c is the volume of the coating layer. Based on these two equations with the assumptions made in the beginning of the section, extraction kinetic curves were drawn. As a result, it is evident that SPME is limited by the distribution coefficient, and thus can only extract a certain percentage of the total number of analytes. However, in PCTE, *Equation 3-7* is less limited by the diffusion coefficient in the exponential, resulting in a larger percentage of analytes being extracted (*Figure 3-3).*

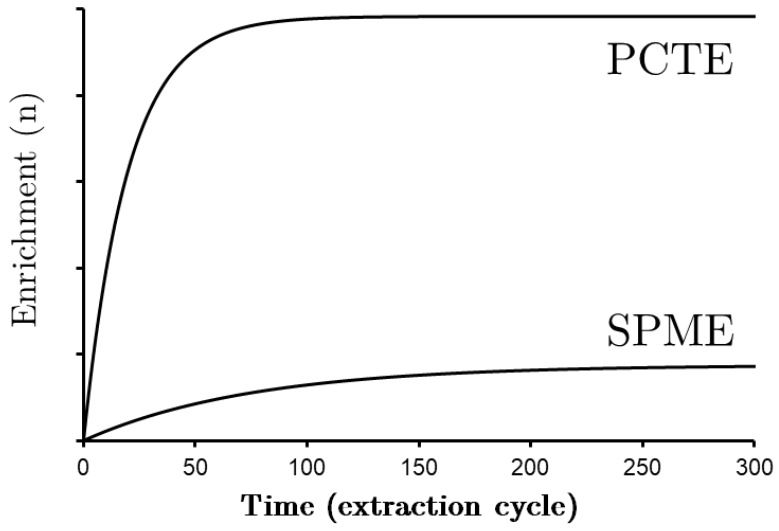

Figure 3-3. Mathematical modelling for the comparison of SPME to PCTE modalities. *PCTE,* polymer coating transfer enrichment; *SPME,* solid phase microextraction.

3.3.3 Polymer Coating Transfer Enrichment Analysis by Mass Spectrometry

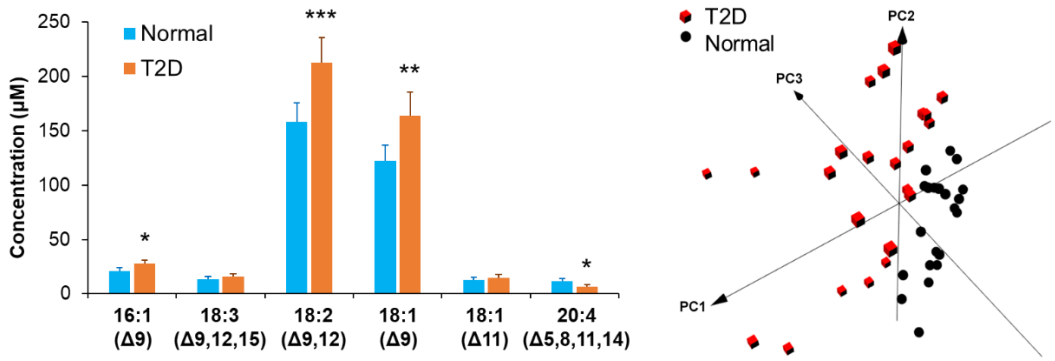

Figure 3-4. PCTE analysis of clinical samples by mass spectrometry. *(left)* Comparative analysis of major free FAs in both healthy and T2D-affected patients. *(right)* 3D PCA plot of the major free FAs in human blood samples (N = 23 for T2D; N = 22 for normal). *PCTE*, polymer coating transfer enrichment; *T2D*, type-2 diabetes; *PCA*, principle component analysis; *FA*, fatty acid. Reproduced from *Zhang, Chiang, et al.*[23]

In a previous study, PCTE was utilized as a direct sampling ionization method for clinical analysis using a commercial mass spectrometer. Quantitation of free fatty acids was performed through the coupling of PCTE with the photochemical PB reaction. When performing MS/MS on the PB products, a neutral loss of 58—an acetone molecule— could be observed and used for quantitative screening (Figure C-4). Clinical analysis of patient samples with type-2 diabetes (T2D) was performed by analyzing free fatty acids through PB-MS/MS (Figure 3-4). Isomeric FA18:1 (Δ9 / Δ11) were differentiated and detected throughout the samples. Comparative analysis between healthy and type-2 diabetes patient samples resulted in the identification of select FAs with significantly different concentrations. Principal component analysis (PCA) analysis was also performed on abundant major free fatty acids, resulting in a clear separation between T2D and healthy patient samples. This result can be attributed to the disturbed FA metabolism due to insulin resistance in patients afflicted with T2D.

3.3.4 Lipid and Fatty Acid Analysis using a Miniature Mass Spectrometry System

A single ion trap miniature MS system was used to analyze several lipid standards at a concentration of 10 ppm to characterize whether different species of lipids could be analyzed. Phosphatidylserine (PS), phosphatidylglycerol (PG), and phosphatidycholine (PC) were chosen as the three main phospholipids to be analyzed using the miniature MS system (Figure C-5). PS is an anionic phospholipid that is prevalent in most cell membranes and involved in cell signaling. A

common PS standard—PS 16:0 / 18:1; colloquially known as POPS— was used as a lipid standard to characterize the lipid fragmentation pattern. PG is another lipid class that is prominent in bacterial membranes. With a glycerol in the substitution site, PG is a prominent component of lung surfactants and is easily seen in bodily fluids such as amniotic fluid. PG 16:0 / 18:1 was used as the second lipid standard. Finally, PC is a dominant lipid standard found throughout all biofluids as an integral component of cell membranes and is commonly studied in numerous biofluids. Both PS and PG were analyzed in the negative ion mode, while PC was predominant in the positive ion modes. Although PS and PG showed small peaks in a commercial q-ToF when analyzed in the positive ion mode, the ion peak was more clearly defined in the negative ion mode. In the case of PS, sodiated peaks were most prominent when analyzed in positive ion mode, revealing little to no fragment peaks when MS/MS analysis was performed. The analysis of PC was performed in positive ion mode with the addition of 1% formic acid to the standard solution to improve the ionization. PC was easily observed, however, its fragment peak at m/z 185 was hard to observe. Due to the mass range transition from m/z 760 to m/z 185, it is challenging to capture the low mass fragment. By lowering the q-value during MS/MS analysis to less than 0.2, the m/z 185 fragment of PC can be observed, revealing the necessity of optimizing the MS method.

Another class of standards that were analyzed are FAs. FAs are the constituents of lipids, consisting of a hydrocarbon chain that is straight—saturated— or bent—unsaturated, with a carboxyl group at one end. In general, MS/MS analysis cannot be performed on fatty acids, producing no significant peaks. This can limit the specificity during mass analysis, especially in lower-resolution instruments. However, relative quantitation can be performed on multiple fatty acids to observe ratios between different types of saturated and unsaturated fatty acids (Figure 3-5). SFME using 10 µL of whole rabbit blood and ethyl acetate as the extraction solvent was performed. Analysis of free fatty acids was performed in the negative ion mode to isolate FA18:0, FA18:1,18:2 peaks (Figure 3-5, *insert*). It can be clearly seen that the resolution by the miniature MS instrument is enough to resolve the characteristic FA 18 peaks. Further limit-of-detection (LOD) studies were performed on an isotopically labelled fatty acid—FA18:1-d17. Signal intensities of a FA18:1 in whole blood extract spiked with 2.5 ppm of IS and one without IS were compared to calculate the LOD. The LOD of FA18:1 was calculated to be 2 ppm with relative signal deviations (RSDs) to be under 25%.

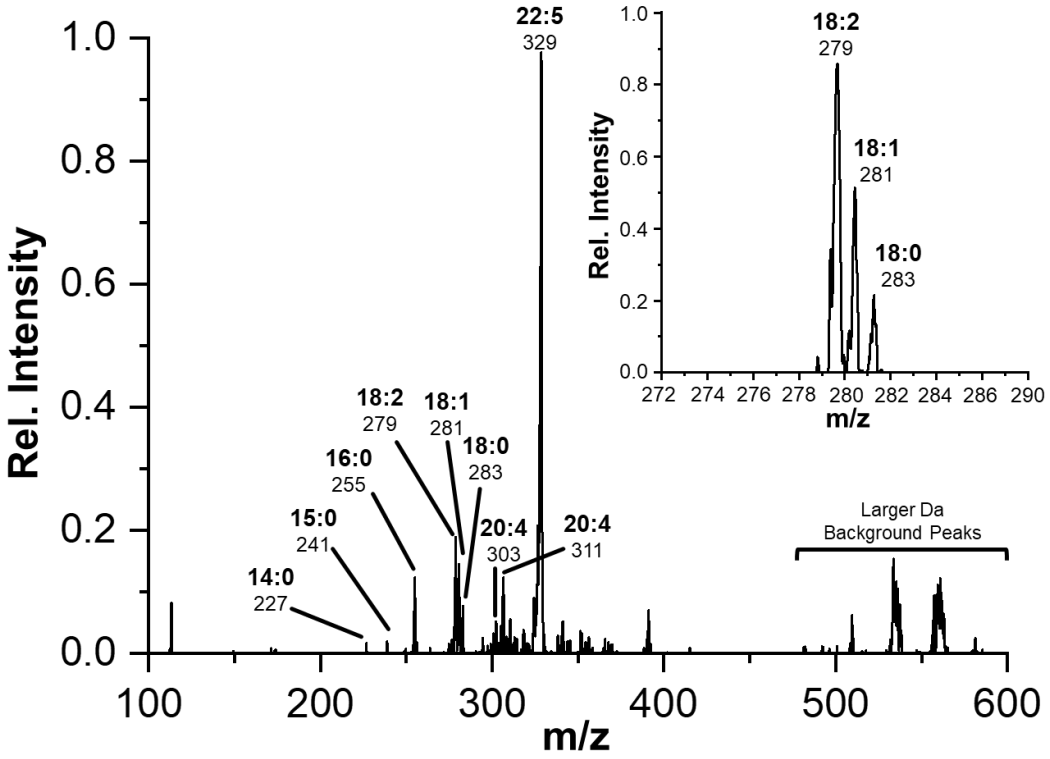

Figure 3-5. Preliminary investigation of full scan MS for fatty acid analysis using a miniature MS instrument. Fatty acids were enriched from whole rabbit blood using SFME. (*insert*) Isolation of FA 18:0, 18:1, 18:2 to ensure resolution is enough to resolve the three different FA peaks. *MS*, mass spectrometry; *SFME*, slug-flow microextraction; *FA*, fatty acid.

3.3.5 Extraction of Lipids from Whole Rabbit Blood using Direct Sampling Ionization

Several direct sampling techniques —PCTE and SFME— were used as a comparative study for the efficacy of the polymer coating. Slug-flow microextraction was first used to extract lipids from 10 µL of whole blood. Due to the low solubility of lipids in water—a large constituent of blood— as defined by a high LogP value, fatty acids should be easily extracted into the extraction solvent. In this study, ethyl acetate was the main extraction solvent used. Both plugs were cycled for 30s before removal of the extraction solvent and placement into a nESI tip for analysis. For analysis in positive ion mode, an additional 10 µL of methanol:water (1/1; *v/v*; 1% formic acid) was directly added. In the negative ion mode, 8 different types of fatty acids could be identified on m/z alone (Figure 3-6b). The characteristic triple peak at m/z 279, 281, 283 associated with linoleic acid, oleic acid, and steric acid, respectively, were identified in the spectra. However, a significant number of background peaks were also present. In positive ion mode, the only major

peak identified was the PC 18:1 / 16:0 peak at m/z 760 (Figure 3-6d). Unidentified background peaks were heavily dominant in a lower mass range, at around m/z 600 to 700.

PCTE capillaries were also utilized under similar conditions to SFME. Ethyl acetate was utilized as the extraction solvent, however, a gap of air—5 mm wide— was added to minimize the liquid-liquid interaction from the two plugs. This ensures that the transfer of analyte only occurs through the polymer and not from the liquid-liquid interface. In order to maintain the gap of air between each plug, each cycle was slower than each cycle in SFME. However, even with the slower cycle time, extraction was still performed within one minute and enough to achieve the max enrichment. Again, the extraction solvent was direct analyzed in both negative (Figure 3-6a) and positive (Figure 3-6c) mode. A distinct comparison between the positive and negative mode spectra collected by the two direct sampling ionization methods resulted in a significant difference in the number of background peaks present in the spectra.

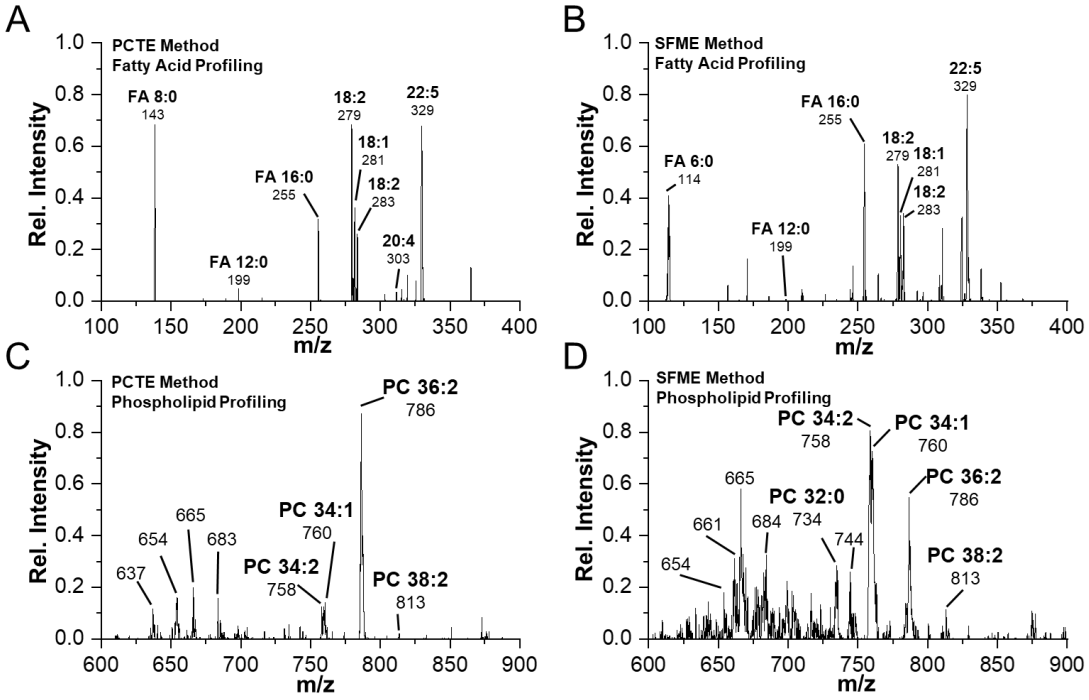

Figure 3-6. Full scan MS spectrum in negative ion mode of fatty acids extracted by (a) PCTE and (b) SFME. (c) PCTE and (d) SFME extracts of lipids in the positive ion mode are also compared, showing an overall cleaner spectrum profile by PCTE.

The overall signal intensity from PCTE was lowered in comparison to SFME, most likely due to the more selective nature of the polymer coating for the capture and desorption of lipids. This selectivity is confirmed by the direct improvement of intensity ratio—signal intensity to highest

background peak— in PCTE when compared to SFME—termed *no coating* (Figure C-6). While a similar fatty acid profile was achieved through both methods, PCTE provides a cleaner, less convoluted spectrum. In the positive ion mode, a similar conclusion can be made. PC peaks with less background noise is observed, especially for the unknown background molecules at a lower m/z range. The elevated intensity of PC16:1 / 18:0 by SFME is different from what was expected, potentially due to the co-extraction of other nonpolar analytes during extraction. Although the elevated signal intensity can be beneficial for analysis, excessively elevated SNR can result in space charge effects causing peak widening and reducing spectra resolution. In comparison, PCTE presents a more expected distribution. As such, it becomes increasingly clear the benefits of using a more specific rapid direct sampling ionization method such as PCTE, especially for lipid profiling.

In this case, the use of a dual-ion trap miniature MS system would be highly beneficial, providing tandem MS spectra for PC confirmation. The use of a virtual beam-type collision induced dissociation (CID) would help set the second ion trap with a low q-value to capture the m/z 185 fragment. Similarly, pseudo MS/MS methods could be established to analyze the lipidome, such as neutral loss scan and precursor ion scan, as previously defined by *Liu et al.*[24]

3.3.6 Evaluating the Quantitation of Fatty Acids using Full Scan MS

The inability for fatty acids to be analyzed by conventional MS/MS methods leads to a concern regarding quantitative capabilities due to the variation in matrix effects between samples. Generally, this is not a concern due to the use of high-resolution mass spectrometry, except for lipid isomers. However, for miniature MS systems, quantitation based on full scan MS can still be performed if the relative signal deviation (RSD) between patient samples is within an acceptable range. Three different blood samples of rabbit whole blood were used and compared to each other by both SFME and PCTE, with the extraction procedures identical to the previous section. The three characteristic fatty acids—FA18:0, 18:1, 18:2— were monitored throughout this experiment. After extraction, 1 µL of oleic acid-d17 at a concentration of 50 ppm was added before analysis to act as the internal standard.

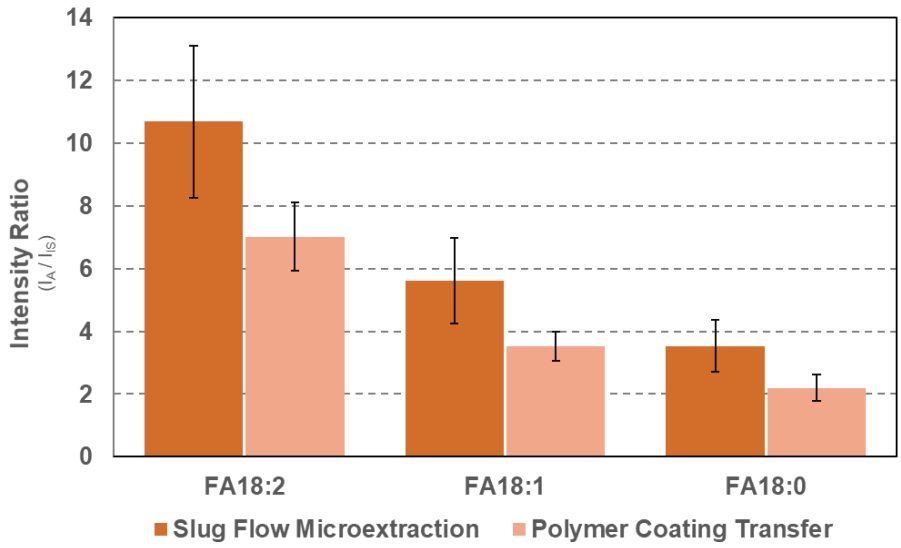

Figure 3-7. Comparison of SFME and PCTE for full scan relative quantitation of FA 18:0, 18:1, 18:2 enriched by PCTE with a spiked internal standard of FA 18:0-d17. Signal intensities were normalized by the internal standard. *SFME*, slug-flow microextraction; *PCTE*, polymer coating transfer enrichment; *FA*, fatty acid.

Relative quantitation was performed by normalizing signal peak intensities—at m/z 279, 281, 283— to the internal standard (Figure 3-7). It was observed that the RSD of all three peaks were relatively constant—under <20%— between all rabbit samples and extraction methods. However, the signal intensity ratios are significantly different between PCTE and SFME, as expected due to the different enrichment fundamentals. SFME has a higher intensity ratio, but an elevated RSD. In comparison, PCTE with its standardized protocol in IS spiking, results in much better RSDs when performing full scan MS profiling.

3.3.7 Paternò-Büchi Reactions for Analysis of Fatty Acids in Whole Blood

In this study, PB reactions were performed on both SFME and PCTE extracts. Following the extraction protocol,10 µL of acetone:water solution (4/1; *v/v*) was added into an nESI tip. A 254 nm UV lamp was used with the nESI tip placed 1 cm away from the bulb. Reaction were performed for 1 minute before analysis. This reaction was optimized in a previous study to minimize any unwanted cross reactions (Figure 3-8). After PB reaction, unsaturated lipids and fatty acids react with the acetone to form an acetone-adduct —characterized by the addition of 58 Da. This photochemical reaction was first performed on lipid standards (Figure C-7). Since the characteristic fragment peak of PC lipids provides minimal information regarding the structure,

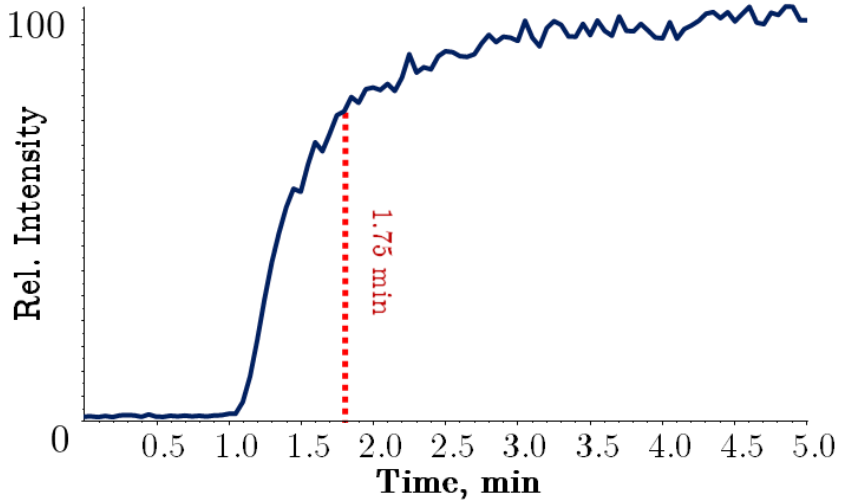

Figure 3-8. Total Ion Current of NLS scan of 58 Da in the negative ion mode. All ions with a loss of the acetone during MS/MS analysis were monitored, revealing the optimal length of PB reaction. *NLS*, neutral-loss scan; *MS/MS*, tandem mass spectrometry; *PB*, Paternò-Büchi.

MS/MS analysis on the PB adduct can elucidate isomeric lipids. After MS/MS is performed on the acetone adducted PC18:1 / 16:0, ions associated with the Δ9 lipid isomer were observed. The protonated PC18:1/16:0 is also present, representing the loss of the photochemically added acetone adduct. Similarly, this reaction can also be performed on fatty acids. Unlike the PB-MS/MS of PC, the highest fragment peak was the loss of the acetone adduct —m/z 281. Smaller peaks elucidating the C=C location was identified, representing the isomeric composition of the sample. Due to the high intensity of m/z 281 after PB-MS/MS analysis, this fragment ion is a strong candidate for subsequent fatty acid quantitative studies.

Afterwards PB reaction on rabbit whole blood was performed to identify unsaturated fatty acids by both PCTE and SFME (Figure 3-9). MS/MS was performed to ensure that the observed acetone-adducted oleic and linoleic acid peaks were accurate along with the differentiation of isomer quantities. It was observed that only a small portion of the reported FA18:1,18:2 peaks underwent a PB reaction. Based on the previous protocol, the efficiency of this method is around 30%. In both SFME and PCTE PB-reacted extracts, several peaks unrelated to unsaturated fatty acids were observed at a high concentration. Several small peaks associated with Δ9 and Δ11 FA 18:1 were observed in PCTE but not in SFME. This further emphasizes the stronger selectivity of PCTE for enriching lipids in comparison to the liquid-liquid approach by SFME. Throughout the spectra, numerous peaks were observed but were not analyzed for any relevance to FA18:2.

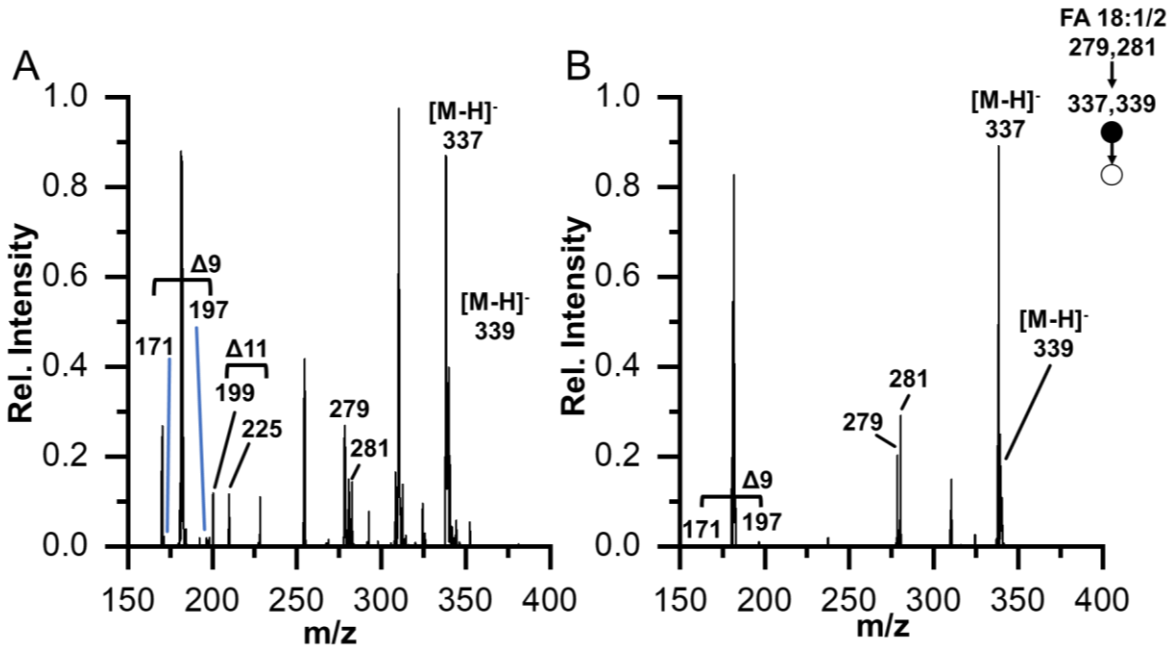

Figure 3-9. MS/MS spectra after PB reaction of whole rabbit blood using (a) PCTE and (b) SFME direct sampling ionization methods. *PCTE,* polymer coating transfer enrichment; *SFME,* slug-flow microextraction.

3.3.8 Lipid Biomarker Profiling for Type 2 Diabetes

As a preliminary investigation using a miniature MS instrument for fatty acid profiling using PCTE, several plasma samples were tested using the workflow shown in *Figure C-8.* Fatty acid distributions between healthy and T2D plasma samples were easily distinguished, revealing several quantitatively different FA when using full scan (Figure 3-10). In the healthy patient plasma, elevated levels of unsaturation of FA18:2/3 were present. However, T2D patients have a much higher intensity of oleic acid. Larger fatty acids such as FA20:4 were present in lower concentrations in healthy patients when compared to T2D patients. Overall, the fatty acid profile differences between two patients are immediately obvious using our miniature MS method. More detailed and thorough comparisons using a larger sample set would be beneficial and expand the applicability of our workflow for clinical use.

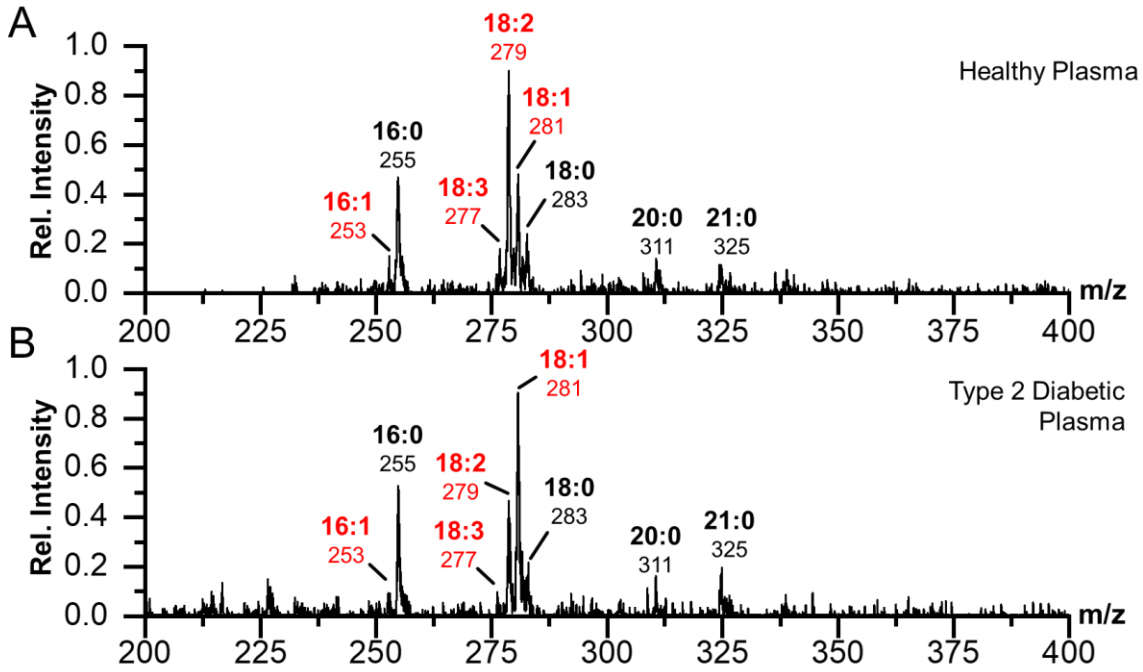

Figure 3-10. Full Scan MS comparison of fatty acid ratios between (a) healthy and (b) T2D patient serum. Human plasma—10 µL— was enriched using PCTE with ethyl acetate as the extraction solvent. *(red)* Labels indicate peak-intensity differences between the two fatty acid profiles. *T2D*, type-2 diabetes; *PCTE*, polymer-coating transfer enrichment.

3.4 Conclusion

In this study, PCTE was used in tandem with a miniature MS system to establish a workflow for potential lipid biomarker profiling in whole blood. PCTE was shown as a more efficient direct sampling method in comparison to SFME or other non-coated methods. A highly selective method for the enrichment of lipids and transfer to the extraction solvent was achieved. By using deuterated FA standards as an internal standard, background studies were performed to establish the capability of performing a high-coverage full scan MS analysis for relative quantitation. Online photochemical reactions were also used in tandem with our direct sampling miniature MS system to enable lipid structural analysis and MS/MS analysis for quantitative studies. As a result, a preliminary investigation was performed to compare the free fatty acid profiles between healthy and T2D plasma samples. Several fatty acids were highlighted to differentiate T2D that could be potentially used for disease diagnostics.

3.5 References

1. Fernandis, A. Z.; Wenk, M. R., Lipid-Based Biomarkers for Cancer. *J Chromatogr B Analyt Technol Biomed Life Sci* **2009,** *877* (26), 2830-5.
2. Larrouy-Maumus, G., Lipids as Biomarkers of Cancer and Bacterial Infections. *Curr Med Chem* **2019,** *26* (11), 1924-1932.
3. Bandu, R.; Mok, H. J.; Kim, K. P., Phospholipids as Cancer Biomarkers: Mass Spectrometry-Based Analysis. *Mass Spectrom Rev* **2018,** *37* (2), 107-138.
4. Loke, S. Y.; Lee, A. S. G., The Future of Blood-Based Biomarkers for the Early Detection of Breast Cancer. *Eur J Cancer* **2018,** *92*, 54-68.
5. Zarrouk, A.; Debbabi, M.; Bezine, M.; Karym, E. M.; Badreddine, A.; Rouaud, O.; Moreau, T.; Cherkaoui-Malki, M.; El Ayeb, M.; Nasser, B.; Hammami, M.; Lizard, G., Lipid Biomarkers in Alzheimer's Disease. *Curr Alzheimer Res* **2018,** *15* (4), 303-312.
6. Morrison, L. J.; Parker, W. R.; Holden, D. D.; Henderson, J. C.; Boll, J. M.; Trent, M. S.; Brodbelt, J. S., Uvlipid: A Uvpd-Based Hierarchical Approach for De Novo Characterization of Lipid a Structures. *Anal Chem* **2016,** *88* (3), 1812-20.
7. Poad, B. L.; Green, M. R.; Kirk, J. M.; Tomczyk, N.; Mitchell, T. W.; Blanksby, S. J., High-Pressure Ozone-Induced Dissociation for Lipid Structure Elucidation on Fast Chromatographic Timescales. *Anal Chem* **2017,** *89* (7), 4223-4229.
8. Ma, X.; Chong, L.; Tian, R.; Shi, R.; Hu, T. Y.; Ouyang, Z.; Xia, Y., Identification and Quantitation of Lipid C=C Location Isomers: A Shotgun Lipidomics Approach Enabled by Photochemical Reaction. *Proceedings of the National Academy of Sciences* **2016,** *113* (10), 2573-2578.
9. Macias, L. A.; Feider, C. L.; Eberlin, L. S.; Brodbelt, J. S., Hybrid 193 Nm Ultraviolet Photodissociation Mass Spectrometry Localizes Cardiolipin Unsaturations. *Anal Chem* **2019,** *91* (19), 12509-12516.
10. Zhang, J.; Yu, W.; Ryu, S. W.; Lin, J.; Buentello, G.; Tibshirani, R.; Suliburk, J.; Eberlin, L. S., Cardiolipins Are Biomarkers of Mitochondria-Rich Thyroid Oncocytic Tumors. *Cancer Res* **2016,** *76* (22), 6588-6597.
11. Fuchs, B.; Schiller, J., Maldi-Tof Ms Analysis of Lipids from Cells, Tissues and Body Fluids. *Subcell Biochem* **2008,** *49*, 541-65.
12. Wang, J.; Wang, C.; Han, X., Enhanced Coverage of Lipid Analysis and Imaging by Matrix-Assisted Laser Desorption/Ionization Mass Spectrometry Via a Strategy with an Optimized Mixture of Matrices. *Anal Chim Acta* **2018,** *1000*, 155-162.
13. Salivo, S.; Beccaria, M.; Sullini, G.; Tranchida, P. Q.; Dugo, P.; Mondello, L., Analysis of Human Plasma Lipids by Using Comprehensive Two-Dimensional Gas Chromatography with Dual Detection and with the Support of High-Resolution Time-of-Flight Mass Spectrometry for Structural Elucidation. *J Sep Sci* **2015,** *38* (2), 267-75.
14. Satomi, Y.; Hirayama, M.; Kobayashi, H., One-Step Lipid Extraction for Plasma Lipidomics Analysis by Liquid Chromatography Mass Spectrometry. *J Chromatogr B Analyt Technol Biomed Life Sci* **2017,** *1063*, 93-100.

15. Banerjee, S.; Zare, R. N.; Tibshirani, R. J.; Kunder, C. A.; Nolley, R.; Fan, R.; Brooks, J. D.; Sonn, G. A., Diagnosis of Prostate Cancer by Desorption Electrospray Ionization Mass Spectrometric Imaging of Small Metabolites and Lipids. *Proceedings of the National Academy of Sciences of the United States of America* **2017,** *114* (13), 3334-3339.

16. Sans, M.; Zhang, J.; Lin, J. Q.; Feider, C. L.; Giese, N.; Breen, M. T.; Sebastian, K.; Liu, J.; Sood, A. K.; Eberlin, L. S., Performance of the Masspec Pen for Rapid Diagnosis of Ovarian Cancer. *Clinical chemistry* **2019,** *65* (5), 674-683.

17. Zhang, J.; Katta, N.; Suliburk, J.; Rector, J.; Garza, K. Y.; Sans, M.; Zahedivash, A.; Ludolph, B.; Bensussan, A.; Giese, N.; Syed, A.; Yu, W.; Liu, J.; Nagi, C.; Young, J. H.; Eberlin, L. S.; Sorace, A. G.; Lin, J. Q.; DeHoog, R. J.; Milner, T. E., Nondestructive Tissue Analysis for Ex Vivo and in Vivo Cancer Diagnosis Using a Handheld Mass Spectrometry System. *Science Translational Medicine* **2017,** *9* (406), eaan3968-eaan3968.

18. Zou, R.; Cao, W.; Chong, L.; Hua, W.; Xu, H.; Mao, Y.; Page, J.; Shi, R.; Xia, Y.; Hu, T. Y.; Zhang, W.; Ouyang, Z., Point-of-Care Tissue Analysis Using Miniature Mass Spectrometer. *Analytical Chemistry* **2019,** *91* (1), 1157-1163.

19. Wang, H.; Liu, J.; Cooks, R. G.; Ouyang, Z., Paper Spray for Direct Analysis of Complex Mixtures Using Mass Spectrometry. *Angewandte Chemie* **2010,** *122* (5), 889-892.

20. Gómez-Ríos, G. A.; Pawliszyn, J., Development of Coated Blade Spray Ionization Mass Spectrometry for the Quantitation of Target Analytes Present in Complex Matrices. *Angewandte Chemie International Edition* **2014,** *53* (52), 14503-14507.

21. Bojko, B.; Gorynski, K.; Gomez-Rios, G. A.; Knaak, J. M.; Machuca, T.; Spetzler, V. N.; Cudjoe, E.; Hsin, M.; Cypel, M.; Selzner, M.; Liu, M.; Keshavjee, S.; Pawliszyn, J., Solid Phase Microextraction Fills the Gap in Tissue Sampling Protocols. *Anal Chim Acta* **2013,** *803*, 75-81.

22. Piri-Moghadam, H.; Alam, M. N.; Pawliszyn, J., Review of Geometries and Coating Materials in Solid Phase Microextraction: Opportunities, Limitations, and Future Perspectives. *Anal Chim Acta* **2017,** *984*, 42-65.

23. Zhang, W.; Chiang, S.; Li, Z.; Chen, Q.; Xia, Y.; Ouyang, Z., A Polymer Coating Transfer Enrichment Method for Direct Mass Spectrometry Analysis of Lipids in Biofluid Samples. *Angewandte Chemie International Edition* **2019**.

24. Liu, X.; Wang, X.; Bu, J.; Zhou, X.; Ouyang, Z., Tandem Analysis by a Dual-Trap Miniature Mass Spectrometer. *Analytical Chemistry* **2019,** *91* (2), 1391-1398.

4. FAST ANALYSIS OF MYCOTOXINS USING SLUG-FLOW MICROEXTRACTION WITH A MINIATURE MASS SPECTROMETRY SYSTEM

4.1 Introduction

Mycotoxins are secondary metabolites produced by filamentous fungi of the genera *Aspergillus*, *Penicillium*, and *Fusarium* that warrants global concern in foodstuff and feed safety. According to the Food and Agricultural Organization (FAO) of the United Nations, it is estimated that more than 25% of all agricultural products are contaminated with mycotoxins.[1] These metabolites adversely affect humans and animal cells to varying degrees—causing carcinogenic, hepatotoxic, estrogenic, mutagenic, and nephrotoxic effects.[2] The production of mycotoxins can occur in any various timepoint along the food chain—starting from pre-harvest to storage. Cereal crops are particularly susceptible to mycotoxin contamination, especially in tropical regions where temperature and humidity levels promote fungal growth. Poor agricultural practices, improper drying, or poor storage conditions are all factors that promote mycotoxin proliferation—resulting in mycotoxin accumulation to concentrations that can cause acute effects after consumption. Use of contaminated crops for animal feed or human consumption allows toxins to accumulate in processed and transformation products.

Several mycotoxins, including aflatoxins—B1 (AB1) and B2 (AB2) —, deoxynivalenol (DON) and zearalenone (ZEAR), are of interest due to their prevalence and severe effects on humans and animals alike.[3] Specific regulations and guidelines have been established across numerous countries to limit mycotoxin presence on stored cereal crops to be used for human and livestock consumption.[4] Aflatoxins have been classified as a human carcinogen, with chronic AB1 exposure being directly correlated to liver cancer.[5] DON, also known as vomitoxin, can cause impaired reproduction and growth in cases of chronic exposure.[6] According to a US Food and Drug (USFDA) report released in 2011, aflatoxin limits on corn and other grains for human and feed consumption are set to 20 ppb ($\mu g \cdot kg^{-1}$) and DON is set to 1 ppm ($mg \cdot kg^{-1}$).[7] Similarly, other countries have begun to regulate ZEAR due to its effect on animal reproduction and immune system, setting grain product limits to 60 ppb ($\mu g \cdot kg^{-1}$).[2, 8]

Quantitation of mycotoxins in foodstuffs and feed is a challenge due to the diversity and complexity of matrices, as well as its inherently low concentration. Different methods have been

utilized for mycotoxin analysis in food including thin layer chromatography[9], liquid chromatography (LC)[10], enzyme-linked immunosorbent assays[11], and immunoaffinity chromatography[12]. In recent years, on-site testing of mycotoxins has been of-interest, emphasizing simple, rapid, user-friendly, and cost-effective sampling techniques—including lateral flow assays and immunosensors.[13, 14] However, these assays are limited in quantitative capabilities and sensitivity, resulting in the inability to confirm low concentrations of mycotoxin presence.[15] LC with tandem mass spectrometry (MS/MS) —only be performed in analytical laboratories— remains the most utilized technique for mycotoxin quantitation based on its robust analysis and high sensitivity. [16]

Miniature MS systems have emerged as an alternative, combining the sensitivity and specificity of MS with the portability of point-of-care (POC) tests. Previously, we developed miniature MS instruments using a variety of direct sampling ionization methods for applications such as therapeutic drug monitoring[17], drugs of abuse screening[18], lipid profiling[19], and quantitation of peptides and proteins[20]. When combined with direct sampling methods, miniature MS systems with ambient ionization sources provide an easy-to-perform workflow that can be performed without significant technical expertise and minimal resources for analysis.[21] In this study, rapid testing and quantitation of mycotoxins in food was developed using a miniature mass spectrometer and slug-flow microextraction (SFME)[22] for direct sampling. A selection of mycotoxin with different chemical structures and properties were selected for analysis. Dried maize kernels were also used as the representative sample matrix for quantitation, along with several other different types of matrices, as a point of comparison to study matrix effects. Furthermore, SFME was adapted to perform surface analysis of mycotoxins on whole corn kernels. This workflow can enable direct testing of mycotoxin presence without any sample preparation and eliminates the possibility of sample carry over for use *in situ*.

4.2 Experimental Methods

4.2.1 Materials

HPLC-grade solvents including water, methanol, chloroform, dichloromethane (DCM), ethyl acetate (EA) and acetic acid (AA) were purchased from ThermoFisher Scientific (Bridgewater, NJ, USA). Four mycotoxin standards —AB1, AB2, DON, and ZEAR— were purchased from Alfa

Aesar (Haverhill, MA, USA). Due to the unavailability of deuterated forms of the selected mycotoxins, 2-ethylhexyl-4-hydroxybenzoate (2-EHB) and 6-methyl-4-phenyl-2-chromanone (6-MPC) were purchased for use as internal standards. Both 2-EHB and 6-MPC were selected based on their similarity in their partition coefficient —LogP— and molecular weight. All standards and internal standards were reconstituted using pure methanol to a concentration of 1000 ppm $1mg \cdot mL^{-1}$. β-cyclodextrin (β-CD) was purchased from Millipore Sigma (Billerica, MA, USA). 3% β-CD solution was prepared in water and heated to 30 ˚C to fully dissolve β-CD. Afterwards, the solution was stored at 4 ˚C to let β-CD precipitate and accumulate at the bottom of a 10 mL conical tube.

Borosilicate capillaries —0.86/1.5 mm, i.d. / o.d.— were purchased from Sutter Instruments (Novato, CA, USA) and used for SFME. The same glass capillaries were also used to fabricate nanoelectrospray (nESI) tips using a micropipette puller (Model P-1000, Sutter Instruments, CA, USA).

4.2.2 Standards and Sample Preparation

Mycotoxin standards were diluted to varying concentrations —ranging from 10 ppb to 1 ppm— in both methanol and 3% β-CD solutions. Methanol-diluted standards were analyzed directly through nESI by a miniature MS instrument. Mycotoxin standards in a β-CD matrix were first extracted by SFME. Afterwards, the extraction solvent was removed and 10 µL of methanol was added before analysis. Methanol was added to the extraction solvent to improve the ionization of mycotoxins when analyzed by MS. Compound 2-EHB was diluted to 200 ppb using methanol and used as the IS in negative ion mode. Compound 6-MPC was diluted to 500 ppb in methanol and used as the IS in the positive ion mode.

Dried corn kernels, corn starch and flour were purchased from the local supermarket as a real sample matrix. Dried corn kernels were ground in a coffee bean grinder for 10 s until the particulate diameter was relatively uniform to the visible eye. Ground samples were separated into 50 mg portions and placed into 1 mL centrifuge tubes for storage in the dark at room temperature. Both flour and corn starch were also measured into 50 mg portions, placed into 1 mL centrifuge tubes, and stored under the same conditions. All three matrices were spiked with 10 µL of the respective mycotoxin at different standard solution concentrations. AB1 standard solutions — 1 and 10 ppm— diluted in methanol were used to spike the food matrices with 100 and 200 ng of AB1,

respectively. ZEAR standard solutions —200 ppb, 1 ppm, and 10 ppm— were used to spike the food matrices with 5, 100, and 200 ng of ZEAR. Samples were subsequently dry-vortexed to mix the sample thoroughly and set out for 30 minutes to evaporate any remaining methanol.

Mycotoxin extraction of the mycotoxin-spiked 'real samples' —including, ground corn kernel, flour, and corn starch— was performed by adding 500 µL of 3% β-CD solution to the 50 mg ground sample and vortexed for 5 min. The sample was set aside for another 5 min for the particulates to settle at the bottom of the centrifuge tube and allowing for excess β-CD to precipitate and settle. Subsequently, 20 µL of the supernatant was removed and placed into the borosilicate capillary for SFME.

4.2.3 Slug-Flow Microextraction Protocol

SFME was performed using the borosilicate capillaries. The sample supernatant of 20 µL was first placed into the capillary, followed by 10 µL of extraction solvent. A liquid-liquid interface was formed at the intersection of both plugs due to the immiscibility of the sample and extraction solvent. Both plugs were cycled back and forth within the capillary by air pressure, implemented using a 10 µL pipette. Efficient diffusion of mycotoxins across the liquid interface was achieved, moving from the sample into the extraction solvent. During this step, capillary action cycles both sample and solvent plugs causing a comprehensive interaction of both sample and solvent to reach equilibrium in a reduced amount of time. After cycling both plugs for 30 s —approximately 60 cycles—, the extraction solvent was removed from the borosilicate capillary and placed into nESI tips. For mycotoxins analyzed in the negative ion mode, 10 µL of 2-EHB spiked methanol was added to the extraction solvent. In positive ion mode, the extraction solvent was first dried inside of the nESI tip by leaving it at room temperature for 5 min. Afterwards, 6-MPC spiked methanol was added into the nESI tip and cycled 5 to 10 times using the pipette to reconstitute the dried extraction solvent before ionization.

4.2.4 Miniature Mass Spectrometry Instrument Analysis

A miniature Mini β mass spectrometer (PURSPEC Technologies, Inc., West Lafayette, IN, US) equipped with a discontinuous atmospheric pressure interface (DAPI) was used for this experiment. Tandem MS (MS/MS) analysis using in-trap collision-induced dissociation (CID) was

performed to analyze all mycotoxin and IS peaks and to identify the major fragment peaks. Confirmation of the fragment ions was performed by collecting spectra on a Bruker Maxis Impact Q-ToF mass spectrometer (Bruker Daltonics, Bremen, Germany).

4.3 Results and Discussion

4.3.1 Mycotoxin Analysis using a Miniature MS Instrument

A single-ion trap miniature MS system was able to characterize several different mycotoxin standards using in-trap CID for MS/MS analysis. The mycotoxins in this study are varied based on its LogP value, which plays a role in the extraction efficiency using SFME. Both positive and negative ion modes were used to analyze AB1, AB2, ZEAR and DON. Limit of detections (LODs) and limit of quantitations (LOQs) were calculated based on the signal-to-noise ratio (SNR) of the lower concentration mycotoxin sample. The resulting analysis for all mycotoxins met or exceeded the standard limits established by food safety governing bodies. Results, along with specific analytical conditions are summarized in *Table D-1*. All four mycotoxin standards were diluted to a concentration of 1 ppm using methanol and analyzed by MS/MS to identify major fragment peaks (Figure 4-1). Protonated —$[M+H]^+$— AB1 and AB2 peaks were observed. AB2 had a significantly lowered ionization efficiency in comparison to AB1, resulting in a relatively poorer LOD. Peaks for sodium adducted—$[M+Na]^+$— ions were prominent in the full spectra. However, in-trap CID of these ions resulted in poor fragmentation efficiency, therefore MS/MS analysis was limited to protonated ions. A visible increase in SNR was observed when performing MS/MS after eliminating all sodium adducted mycotoxin ions from the linear ion trap. For the analysis of ZEAR, both negative and positive ion could be used. However, in comparison, negative ion mode resulted in better performance due to low chemical noise and efficient formation of fragment ion m/z 273. When analyzing DON, the ionizability of this mycotoxin was limited. This can be concluded due to the low total signal intensity of both the sodium adducted and protonated DON at high concentrations— greater than 1ppm. Due to this low ionizability, MS/MS analysis is also limited. Several previous papers have reported the analysis of DON by adding an acetate adduct and analyzing in the negative ion mode. By adding 1% AA to the ionization solution, acetate adducted DON peaks were observed in the negative ion mode. MS/MS of the acetate adduct resulted in the removal of acetate, revealing a charged DON fragment molecule as the major fragment ion.

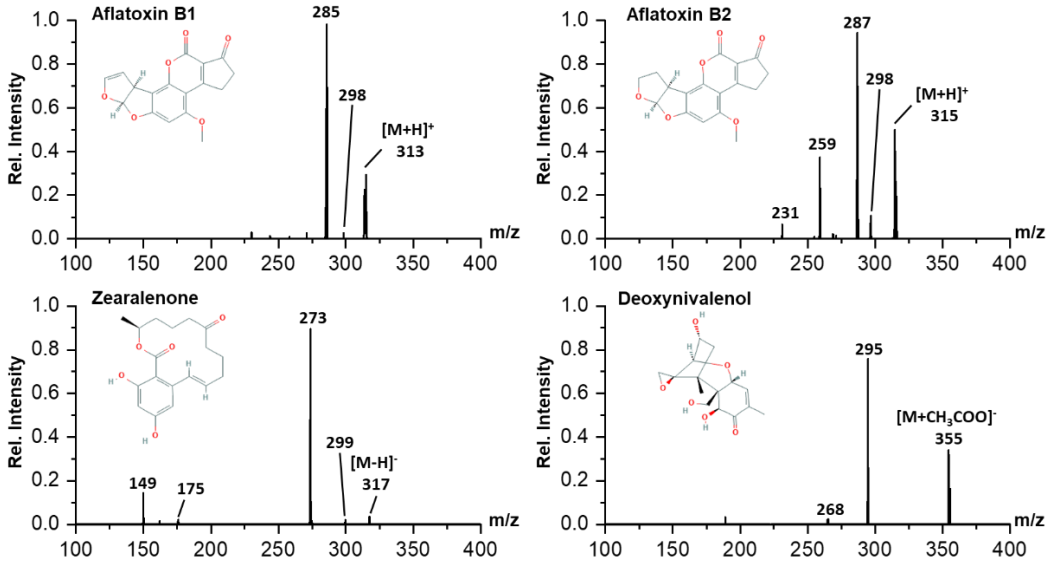

Figure 4-1. MS/MS spectra of different mycotoxins using standard solutions at a concentration of 1 ppm. (*top left*) AB1 and (*top right*) AB2 analyzed in the positive ion mode. (*bottom left*) Zearalenone and (*bottom right)* deoxynivalenol analyzed in the negative ion mode. Solutions were prepared in pure methanol except for deoxynivalenol which was prepared in a methanol: acetic acid solution (99/1; *v/v*).

For all four mycotoxins, the overall calculated RSD is elevated over other methods involving a miniature MS instrument. This can be attributed to the relatively increased instability of the ionization of mycotoxins when approaching the LOD. However, this can be trivialized when considering the established food safety limits for each mycotoxin —all of which are above the calculated LOD and LOQ.

4.3.2 Solvent Optimization for Mycotoxin Extraction and Ionization

Solvent optimization was performed to maximize the extraction and ionization efficiency of mycotoxins in a sample solution. One major criterion of SFME is that the extraction solvent selected must be immiscible with the sample solution to form the necessary liquid bridge. As a result, the selection of solvents is critical. The solvent used to reconstitute the ground solid samples—called *sample solvent*— must not mix with the *extraction solvent*. Conventional methods such as thin-layer chromatography perform sample pre-treatment by a ratio of acetonitrile:water (6/4; *v/v*) or methanol:water (1/1; *v/v*). However, the use of acetonitrile or methanol as the sample solvent will mix with commonly-used SFME solvents—EA, DCM, and chloroform. One option is the use of hexane as the extraction solvent. However, hexane has an

extremely poor ionizability and cannot mix with other ionizable solvents. A three-phase slug-flow microextraction using methanol:water (1/1; *v/v*) as the sample solvent, hexane as the solvent bridge, and EA as the extraction solvent also resulted in poor extraction efficiencies of the mycotoxins. As such, hexane was removed from the list of suitable solvents for mycotoxin extraction.

As a result, the only potential sample solvent to be used for SFME is water. Several different sample solutions were compared using water as the major solvent— deionized water and a 3% β-CD solution. β-CD was selected as a buffering molecule based on previous studies reporting that β-CD can form a polar complex with mycotoxins to help it remain in-solution rather than binding with sample surfaces. A comparison study between water and 3% β-CD solution as the sample solvent was performed, highlighting that the β-CD solution provided improved signal intensity ratios for both AB1 and ZEAR, as well as improved RSD (Figure 4-2). After selecting 3% β-CD as the sample solvent, solvent optimization for SFME was performed (Figure 4-3). Three common SFME solvents were chosen for analysis—chloroform, DCM, and EA. In the negative ion mode, all extraction solvents were similar in its calculated intensity ratio. However, EA was chosen as a compromise between intensity ratio and RSD when compared to DCM and chloroform. For positive ion mode, 6-MPC required a modification to the overall workflow due to its incompatibility to all extraction solvent. Due to its poor ionizability in these solvents, the signal intensity was extremely low and varied and resulting in low intensity ratios and large RSDs.

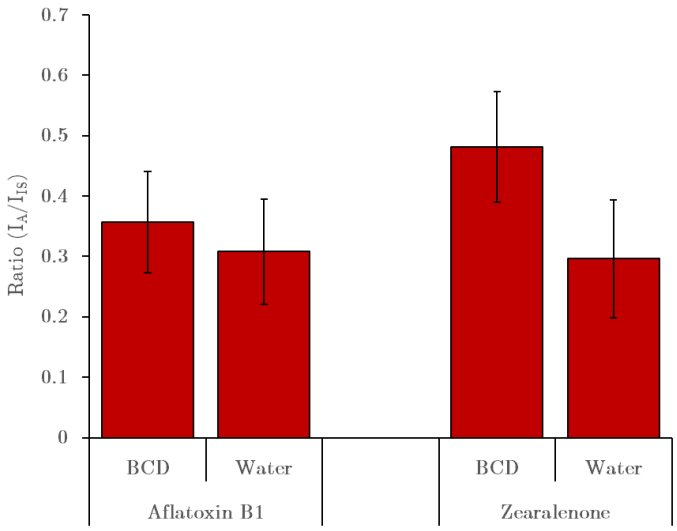

Figure 4-2. Comparison of 3% β-CD solution versus water as the sample solvent. Both zearalenone and aflatoxin B1 were evaluated for the improvement in extraction efficiency.

To improve the ionizability of the positive internal standard, the extraction solvent was first evaporated before the addition of 6-MPC spiked methanol at a concentration of 500 ppb. After introducing this protocol into the SFME miniature MS workflow, chloroform was chosen as the ideal extraction solvent (Figure D-1). In this case, intensity ratios were not as high as evaporated EA or DCM. However, the RSD was greatly improved.

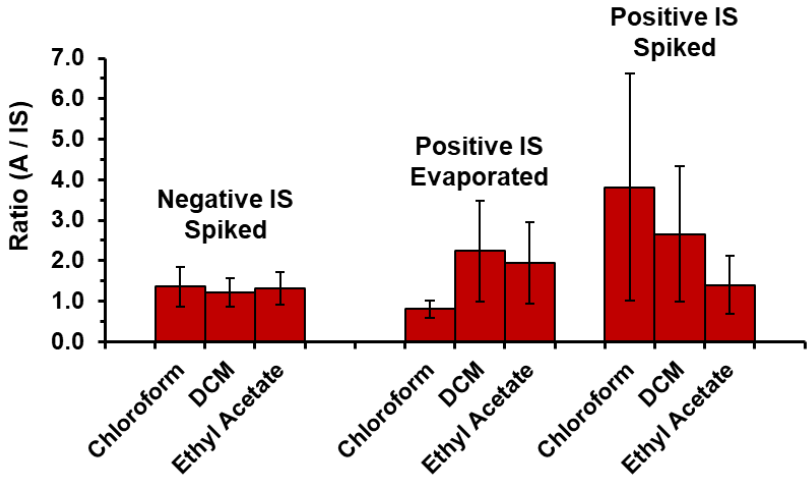

Figure 4-3. Intensity ratios of the analyte to internal standard for three different solvents in negative and positive ion mode. Analyte for negative ion mode was zearalenone and the analyte for the positive ion mode was aflatoxin B1. *IS*, internal standard; *DCM*, dichloromethane.

4.3.3 Matrix-matched Calibration Curves for Dried Corn Mycotoxin Analysis

The overall workflow combining SFME with the miniature MS system was evaluated for both AB1—positive ion mode— and ZEAR—negative ion mode (Figure 4-4). Mycotoxin samples were spiked into 3% β-CD solution at different concentrations for analysis by SFME. Internal standards were diluted in methanol and added to the extraction solvent after removal from the SFME capillary. Several calibration curves were formed using the β-CD samples. The AB1 calibration curve was drawn from a concentration range of 50 ppb to 1 ppm. Intensity ratios were calculated using the fragment ion peak signal intensity at m/z 285 over the fragment internal standard peak signal intensity at m/z 160 (Figure D-2,*left*). A strong linearity —$r^2 > 0.99$— was observed with RSDs less than 30% at every point. Two real samples were made by spiking 50 mg of dried corn kernels with 100 or 200 ng of AB1 with 500 µL of 3% β-CD solution. The resulting concentrations of each real sample are 200 ppb and 400 ppb, respectively. When plotted against the generated calibration curve, both AB1 ground corn kernel samples had less than 15 % error.

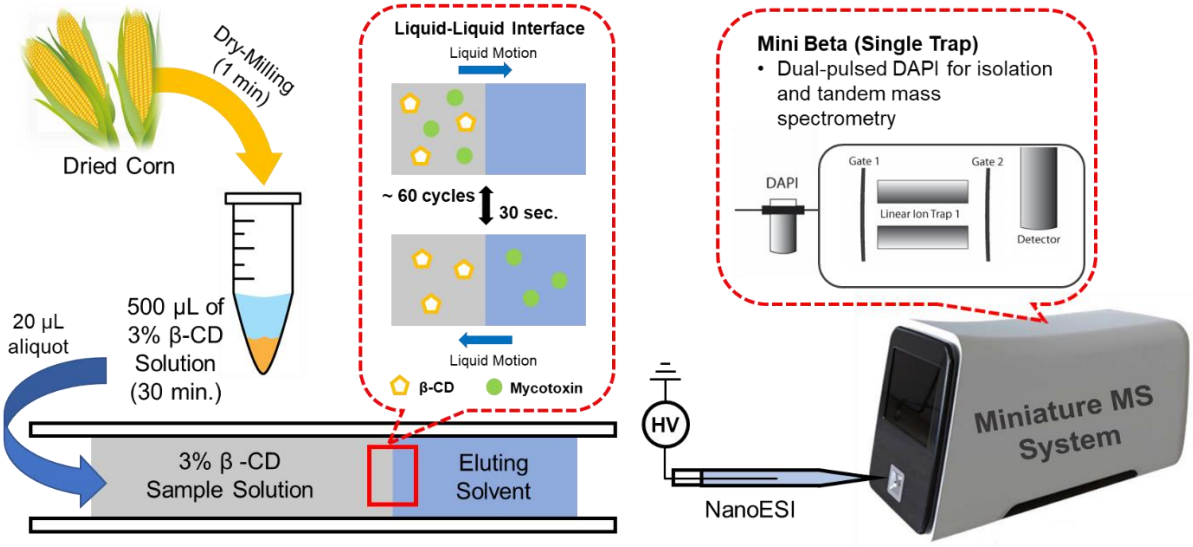

Figure 4-4. Schematic of the proposed SFME Miniature MS system workflow for mycotoxin analysis.

However, the 100 ng—200ppb— AB1 sample falls below the generated calibration curve due to the increased matrix effect at low AB1 concentrations (Figure 4-5, *left*).

Another calibration curve was drawn for ZEAR with a concentration range of 10 ppb to 1 ppm. Intensity ratios were calculated using the fragment ion peak signal intensity at m/z 273 over the fragment internal standard peak signal intensity at m/z 136 (Figure D-2,*right*). The calibration curve was linear— $r^2 > 0.99$— with RSDs less than 25% at each point. Real samples at different concentrations—20, 100, 200 ng— were synthesized and analyzed (Figure 4-5, *right*). All three samples had less than 10% error when plotted against the generated calibration curve, showing that mycotoxins can be quantified using a SFME and miniature MS instrument method.

The sample matrix is also another point-of-concern, especially due to the susceptibility of MS analysis to matrix effects. With especially complex samples, the matrix can contribute significantly to ion suppression, reducing the sensitivity and specificity of MS analysis. Several different matrices were used and compared to the ground corn sample to investigate the effects of different matrices using through the proposed workflow (Table D-2). In addition to ground corn kernels, both corn starch and flour were also used as a sample matrix. Both samples, measured to 50 mg each, were spiked with 100 ng of ZEAR and dried for 5 min before the addition of 500 µL of 3% β-CD solution. Intensity ratios were calculated for each sample matrix and compared to the calculated intensity ratio identified in ZEAR calibration curve. It was observed that the % error for all three matrices were under 11%. As a relatively low % error, the same calibration curve can be

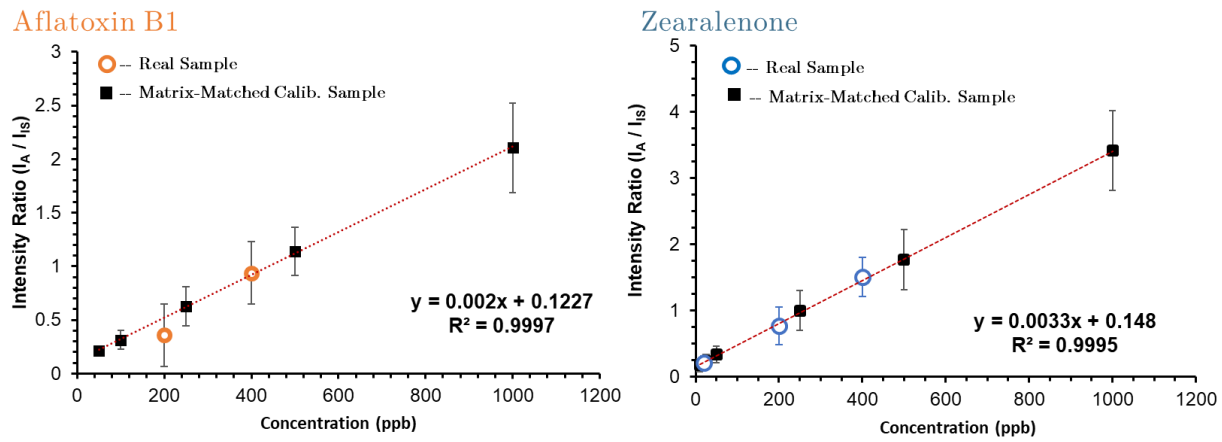

Figure 4-5. (*left)* AB1 matrix-matched calibration curve drawn from 50 ppb to 1 ppm. Two samples of AB1-spiked dried ground corn samples were plotted. (*right*) ZEAR matrix-matched calibration curve drawn from 10 ppb to 1 ppm. Three samples of ZEAR-spiked dried corn ground samples were plotted to test the calibration curve accuracy.

used for different sample matrices. This is a significant advantage in comparison to other conventional mycotoxin analytical methods since different sample matrices usually require a varying sample preparation for immunoassay or LC-MS methods.

4.3.4 Direct Surface Analysis of Mycotoxins using Slug-Flow Microextraction

Mycotoxin detection using conventional means requires large-batch sampling—allocating 1 kg of corn or other cereal grains— for laboratory analysis. During the analytical process, only several small samples are consumed; leaving a large amount of chemically processed grains. As a result, frequent sampling of stored grains can result in a significant loss. Furthermore, conventional sampling of stored foodstuffs can be hard to perform as a high-throughput method due to the involved sample preparation protocols. As a result, mycotoxin analysis is usually performed when necessary in contrast to continuous monitoring.

In this study, several direct surface analytical methods are proposed by adapting SFME in several methods. The first method involves using 100 µL of β-CD solution to cover a wide surface of a corn kernel (Figure 4-6, *left*). The solution is re-aspirated into the pipette after deposition and repeated for 30 s. The remaining solution is placed into a borosilicate glass capillary to perform SFME. However, one significant drawback of this method is the loss of β-CD solution. The corn kernel absorbs a significant amount of solution or is otherwise lost during the aspiration procedure.

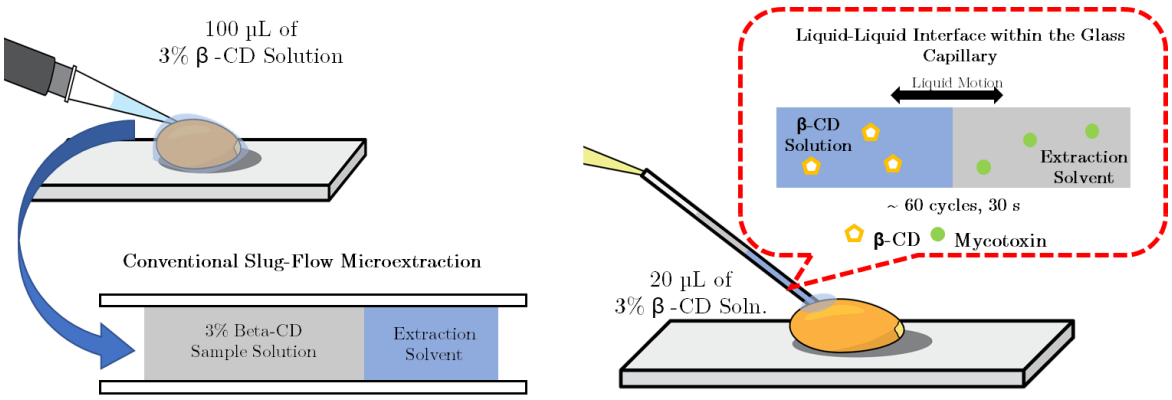

Figure 4-6. Surface SFME workflows using corn kernels with 200 ng of AB1 spiked onto the surface. (*left)* 100 µL of β-CD deposited throughout the entire kernel. *(right)* SFME-prepared capillary tilted onto the surface of a corn kernel for analysis.

This loss of solution directly affects the resulting signal intensity, as less mycotoxins were extracted from the surface of a corn kernel. A different method was proposed to overcome the loss of mycotoxins during solution deposition (Figure 4-6, *right*). A capillary pre-loaded with 10 µL of extraction solvent with 20 µL of β-CD solution is used to interact with the corn kernel surface. By carefully moving the sample solvent —β-CD solution— to the end of the capillary, the sample solvent can directly interact to a small area on the sample surface. A 10 µL pipette was used to ensure that only the sample solvent exited the capillary, while capillary action ensures that both solvent plugs are cycled. While the β-CD solution acts as a carrier to capture and carry mycotoxins on the sample surface, SFME is also performed simultaneously. Thus, mycotoxins are captured and transferred to the extraction solvent in a single cycle. This method results in a five-fold increase in signal intensity as observed in Figure D-3.

Further evaluation of the method identified in *Figure 4-6,right* was performed on various locations within a corn kernel where mycotoxins could be present. Three different kernel locations were chosen —surface, base, and interior (Figure 4-7). Each of these areas have different physical characteristics. The surface of the corn kernel is smooth with a skin-like layer, resulting in minimal losses of sample solution. The base —area connected to the corn cob— is extremely fibrous which can easily absorb solution. Finally, the interior —called *endosperm*— is crumbly and is the most complex surface of the three options. Each of these locations are spiked with 5 ng of ZEAR onto the three different surfaces on different corn kernels to prevent sample crossover. It was observed that the kernel endosperm has a high signal RSD in comparison to the base or surface. This is likely due to the prevalence of matrices such as lipids and metabolites within a corn kernel.

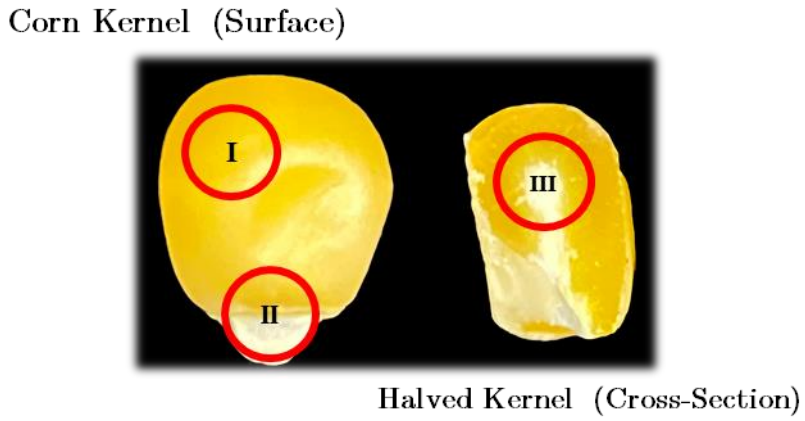

Figure 4-7. Three different sampling locations of the corn kernel spiked with ZEAR: *(I)* Corn surface, *(II)* base, and *(III)* endosperm. *ZEAR*, zearalenone.

The full scan MS spectrum of the kernel endosperm spiked with ZEAR shows various interfering peaks with the ZEAR precursor ion peak (Figure D-4, *left*). However, MS/MS analysis still shows a clean spectrum with a prominent m/z 273 fragment ion peak of ZEAR with the m/z 136 fragment internal standard peak for quantitation (Figure D-4, *right*). The three different areas of the corn kernel were compared to a blank sample. The blank was created by performing surface SFME onto the endosperm with no spiked ZEAR. A comparison of each of the corn kernel areas results shows a difference in signal intensity ratios to the blank with acceptable RSDs (Table 4-1). As a result, this method shows good performance and can be easily adapted to perform *in situ* analysis of corn with visible traces of fungi or a continuous monitoring of ensilaged cereal crops without sample consumption.

Table 4-1. Calculated intensity ratios using surface SFME. Samples were spiked with 5 ng of ZEAR placed onto the three different kernel locations and compared to a blank from the corn kernel endosperm.

Kernel Location	Intensity Ratio (I_A/I_{IS})	RSD
(I) Surface	0.202	20.5%
(II) Base	0.266	26.0%
(III) Endosperm	0.257	35.2%
Blank	0.114	26.2%

4.4 Conclusion

In this work, a workflow using SFME and a miniature MS system was combined to analyze mycotoxins from various food samples. The workflow presented uses a single ion trap miniature MS system to provide strong LOD and LOQs for the detection and quantitation of ZEAR and AB1 in ground corn samples, corn starch and flour. An adaptation of SFME was also shown to analyze mycotoxins on various surfaces of a single corn kernel. It was observed that the different surfaces had little effect on the analysis of ZEAR. Similarly, the matrix effect was trivial across the different types of solid samples. Thus, it was concluded that various samples types can be analyzed using our workflow without any significant impact onto the analysis of mycotoxins. The addition of internal standards into our workflow enables mycotoxin quantitation in both powdered, ground, and surface samples with LODs less than 20 ppb and 5 ng for ZEAR. Due to the variety of different mycotoxins that exist and its potential to contaminate various types of grains, mycotoxins pose a significant threat to the global food supply. As an initial foray into food safety, this study shows an immense potential that can be expanded to analyze a variety of other toxins and foodstuffs. With the ability to perform quantitative surface analysis in complex mixtures, the developed workflow in this study can be easily used for direct in-field analysis of mycotoxins with minimal sample preparation.

4.5 References

1. Marin, S.; Ramos, A. J.; Cano-Sancho, G.; Sanchis, V., Mycotoxins: Occurrence, Toxicology, and Exposure Assessment. 2013.
2. Abrunhosa, L.; Morales, H.; Soares, C.; Calado, T.; Vila-Chã, A. S.; Pereira, M.; Venâncio, A., A Review of Mycotoxins in Food and Feed Products in Portugal and Estimation of Probable Daily Intakes. *Critical Reviews in Food Science and Nutrition* **2016**.
3. Sforza, S.; Dall'Asta, C.; Marchelli, R., Recent Advances in Mycotoxin Determination in Food and Feed by Hyphenated Chromatographic Techniques/Mass Spectrometry. John Wiley & Sons, Ltd: 2006; Vol. 25, pp 54-76.
4. Van Egmond, H. P. In *Worldwide Regulations for Mycotoxins*, 2002; Kluwer Academic/Plenum Publishers: 2002; pp 257-269.
5. Barrett, J. R., Liver Cancer and Aflatoxin: New Information from the Kenyan Outbreak. *Environmental Health Perspectives* **2005,** *113* (12), A837-A837.
6. Pestka, J. J., Deoxynivalenol: Mechanisms of Action, Human Exposure, and Toxicological Relevance. Springer: 2010; Vol. 84, pp 663-679.
7. Association, N. G. a. F., A Guide for Grain Elevators, Feed Manufacturers, Grain Processors and Exporters. *FDA Mycotoxin Regulatory Guidance* **2011**.
8. Riedel, M., China ' S Maximum Levels for Mycotoxins in Foods. *Global Agricultural Information Network* **2014,** (GB 2761-2011), 1-8.
9. Welke, J. E.; Hoeltz, M.; Dottori, H. A.; Noll, I. B., Quantitative Analysis of Patulin in Apple Juice by Thin-Layer Chromatography Using a Charge Coupled Device Detector. *Food Additives and Contaminants - Part A Chemistry, Analysis, Control, Exposure and Risk Assessment* **2009,** *26* (5), 754-758.
10. Cho, S.; Lee, C.; Jang, M.; Son, Y.; Lee, S.; Choi, I.; Kim, S.; Kim, D., Aflatoxins Contamination in Spices and Processed Spice Products Commercialized in Korea. *Food Chemistry* **2008,** *107* (3), 1283-1288.
11. Hendrickson, O. D.; Chertovich, J. O.; Zherdev, A. V.; Sveshnikov, P. G.; Dzantiev, B. B., Ultrasensitive Magnetic Elisa of Zearalenone with Pre-Concentration and Chemiluminescent Detection. *Food Control* **2018,** *84*, 330-338.
12. Rahmani, A.; Jinap, S.; Soleimany, F., Qualitative and Quantitative Analysis of Mycotoxins. *Comprehensive Reviews in Food Science and Food Safety* **2009,** *8* (3), 202-251.
13. Ren, Y.; Zhang, W.; Lin, Z.; Bushman, L. R.; Anderson, P. L.; Ouyang, Z., In-Capillary Microextraction for Direct Mass Spectrometry Analysis of Biological Samples. *Talanta* **2018,** *189*, 451-457.
14. Wu, S.; Liu, L.; Duan, N.; Wang, W.; Yu, Q.; Wang, Z., A Test Strip for Ochratoxin a Based on the Use of Aptamer-Modified Fluorescence Upconversion Nanoparticles. *Microchimica Acta* **2018,** *185* (11), 1-8.

15. Mahmoudi, T.; de la Guardia, M.; Shirdel, B.; Mokhtarzadeh, A.; Baradaran, B., Recent Advancements in Structural Improvements of Lateral Flow Assays Towards Point-of-Care Testing. *TrAC Trends in Analytical Chemistry* **2019,** *116*, 13-30.

16. Hidalgo-Ruiz, J. L.; Romero-González, R.; Martínez Vidal, J. L.; Garrido Frenich, A., A Rapid Method for the Determination of Mycotoxins in Edible Vegetable Oils by Ultra-High Performance Liquid Chromatography-Tandem Mass Spectrometry. *Food Chemistry* **2019,** *288*, 22-28.

17. Li, L.; Chen, T.-C.; Ren, Y.; Hendricks, P. I.; Cooks, R. G.; Ouyang, Z., Mini 12, Miniature Mass Spectrometer for Clinical and Other Applications—Introduction and Characterization. *Analytical Chemistry* **2014,** *86* (6), 2909-2916.

18. Ma, Q.; Bai, H.; Li, W.; Wang, C.; Cooks, R. G.; Ouyang, Z., Rapid Analysis of Synthetic Cannabinoids Using a Miniature Mass Spectrometer with Ambient Ionization Capability. *Talanta* **2015,** *142*, 190-6.

19. Zou, R.; Cao, W.; Chong, L.; Hua, W.; Xu, H.; Mao, Y.; Page, J.; Shi, R.; Xia, Y.; Hu, T. Y.; Zhang, W.; Ouyang, Z., Point-of-Care Tissue Analysis Using Miniature Mass Spectrometer. *Analytical Chemistry* **2019,** *91* (1), 1157-1163.

20. Chiang, S.; Zhang, W.; Farnsworth, C.; Zhu, Y.; Lee, K.; Ouyang, Z., Targeted Quantification of Peptides Using Miniature Mass Spectrometry. *Journal of Proteome Research* **2020,** *19* (5), 2043-2052.

21. Pu, F.; Chiang, S.; Zhang, W.; Ouyang, Z., Direct Sampling Mass Spectrometry for Clinical Analysis. *The Analyst* **2019,** *144* (4), 1034-1051.

22. Ren, Y.; McLuckey, M. N.; Liu, J.; Ouyang, Z., Direct Mass Spectrometry Analysis of Biofluid Samples Using Slug-Flow Microextraction Nano-Electrospray Ionization. *Angewandte Chemie International Edition* **2014,** *53* (51), 14124-14127.

5. CONCLUSION AND FUTURE PROSPECTS

5.1 Summary of Work

Miniature mass spectrometry (MS) systems have the potential to be an ideal solution for implementing clinical-level biomedical testing at the point-of-care (POC). The main object of this dissertation was to expand the applicability of miniature MS systems by establishing direct sampling ionization workflows for convenient POC biomedical testing. Proteins and peptides were quantified using immunoaffinity enrichment with miniature MS instrument (*Chapter 2*). Similarly, profiling of different lipid biomarkers (*Chapter 3)* is shown using novel polymer coating for high coverage enrichment of lipids in biofluids. Finally, exogenous metabolites that pose a global threat to human health were extracted by slug-flow microextraction for analysis by a miniature MS system. These three studies further expand the versatility of fast, direct sampling miniature MS system workflows for biomedical testing of various biomolecules.

In *Chapter 2*, a new miniature MS instrument was characterized to understand the advancements and its applications for high mass analysis. Several notable advancements include the introduction of an external gas inlet and the addition of a secondary linear ion trap for improved resolution, accuracy, and sensitivity necessary for proteomic analysis. Improvements to electronics were sufficient to enable mass accuracy within 0.1% and eliminate any concerns with scan-out RF linearity. Mass scan-out can also be slowed sufficiently to enable unit resolution spectra in the high-mass range—greater than 1,500 Da. Furthermore, both beam-type and in-trap collision-induced dissociation (CID) are available for peptide analysis. This enables a quick transition between low and high energy CID modalities for tandem MS (MS/MS) analysis. Certain molecules favor a high energy CID method to produce a major fragment, whereas low energy CID methods results in a richer fragmentation profile. Overall, these advancements were used to develop a peptide multiplexing workflow, characterizing two *Met* peptide sequences in the same sample run. Each of these advancements help establish the basis for the quantitation of peptides and proteins. Furthermore, development of a miniature MS method for quantitation of the *Met* peptide was completed. The *Met* peptide was analyzed using MS/MS and MS^3, identifying and characterizing the significant b_5 peptide fragment at m/z 633. The resulting method had a strong linear range starting from 50 nM and a limit of detection (LOD) / limit of quantitation (LOQ) of 10 and 20 nM,

respectively. Finally, a quantitative method was developed for the analysis of digested *Met* protein, a tyrosine kinase receptor associated with invasive cancer phenotypes and poor patient prognosis. Overall validation of the workflow was performed by quantifying the *Met* peptide in an immunoaffinity enriched sample of SKBR3 cell lysate.

However, even with the current advancements to miniature MS, further improvements to sensitivity is needed to detect low concentration biomarkers. SKBR3 cells represent a low-expression level of *Met* peptide, resulting in a concentration outside of defined linear range, but within the detectable range. Increases to the initial amount of starting cell lysate would be beneficial to bring the final concentration level of *Met* peptide to a detectable level. Further studies into the ionization of *Met* peptide at low concentrations using the positive ion mode—similar to the conventional LC-MS/MS methods— would be beneficial. Identifying the component behind the poor ionization of the *Met* peptide in positive ion mode would also further improve the overall method and transition the use of miniature MS towards a large-scale sample analysis.

In *Chapter 3*, polymer coating transfer enrichment (PCTE) was transferred for use with a miniature MS system to profile lipids in whole blood. Although several improvements are still necessary to fully realize lipid profiling—especially with lipid classes such as PC and PE—preliminary investigations using full scan MS was performed. Comparative spectra between an enrichment modality with the polymer coating and without were performed, highlighting the efficacy of the polymer coating for high-coverage lipid enrichment. A wide coverage of free fatty acids was identified using both SFME—no polymer coating— and PCTE using full scan MS and a miniature MS instrument. Background studies were performed to validate whether quantitation using full scan MS could be performed between the same sample without significant variations in the free fatty acid profile. Similarly, photochemical reactions were performed on both lipid standards and whole blood to realize lipid structure elucidation. The relevant fragment peaks associated with PC isotopes and FA were easily identified. Finally, a photochemical reaction was performed on whole blood to irradiate all free fatty acids and forming acetone-adducted FA peaks. After isolation and MS/MS analysis on FA18:1/18:2, diagnostic ions revealing the C=C position were identified at low peak intensities. However, in-trap CID on the peaks also result in the removal of an acetone molecule to reveal the original FA peak. Further development of a neutral loss scan for a dual linear ion trap instrument would be the next step in quantifying free fatty acids in biofluid samples.

Studies focused on utilizing the dual linear ion trap miniature MS instrument is an important step in potential lipid biomarker profiling. Neutral loss scans and precursor ion scans are extremely helpful in elucidating not only photochemically reacted free FA peaks, but also with lipids. Many lipids—after MS/MS analysis— reveal or lose its characteristic molecule at its substitution site. Precursor ion scans have been used to identify the peaks that produce a specific molecular —i.e. m/z 185 for phosphatidylcholine lipids. However, these methods are conventionally limited to triple quadrupole MS instruments. New developments to the dual linear ion trap miniature MS instrument have shown the implementation of both neutral loss scan and precursor ion scan. The use of these scan modes in a miniature MS system for lipid profiling should be attempted in the future to advance the capabilities of elucidating lipid profiles. Similarly, free FA profiling between diseased and healthy serum samples were attempted to explore the capabilities of miniature MS instruments in identifying novel lipid profile biomarkers.

Finally, Chapter 4 addresses different types of metabolites—mycotoxins— for biomedical testing. In this work, slug-flow microextraction (SFME) was used as the direct sampling method with a miniature MS instrument to analyze mycotoxins from various food samples. The workflow presented was able to quantify zearalenone and aflatoxin B1 in ground corn kernels, corn starch and flour. An adaptation of SFME was also presented to analyze mycotoxins from various surfaces without any sample consumption. Similarly, the matrix effect was minimal when analyzing different matrices through our workflow, thus concluding that different sample types can be analyzed without any significant effect on mycotoxin analysis. The addition of a pre-spiked internal standard enables a streamlined workflow for mycotoxin quantitation in both powdered and surface samples. With the ability to perform quantitative surface analysis in complex mixtures, the developed mycotoxin workflow in this study can be translated to continuously monitor stored or ensilaged grains. As a result, direct sampling ionization with miniature MS systems is a versatile tool in analyzing potentially harmful exogenous metabolites on various surfaces and unique matrices.

5.2 Future Prospects and Directions

In conclusion, direct sampling ionization coupled to miniature MS instruments were demonstrated in the scope of three different classes of biomarkers. Based on the promising results presented within this dissertation, miniature MS systems have proven to be a versatile biomedical

testing tool—mirroring its more mature counterpart, MS. Although miniature MS systems are unlikely—nor meant to— supplant MS, it fills a gap in the healthcare pathway to eliminate diagnostic delays by a significant fraction. However, the work in this dissertation only explores a small fraction of the entire potential of miniature MS systems. Numerous biomolecules and potential biomarkers have unique characteristics that provide various diagnostic values. The translation of existing MS-compatible techniques, adaptation of direct sampling ionization techniques, or even the development of new POC methods are all potential solutions to expand miniature MS systems for biomedical testing. As such, future POC implementation of miniature MS systems hinges largely upon the creativity and dedication in research focused towards innovating complementary POC direct sampling ionization techniques.

Another key area necessary for the implementation of miniature MS systems is the development of automated devices regarding direct sampling ionization methods for high-throughput analysis. Automated or easy-to-use interfaces are necessary for POC use, especially for more involved techniques such as PCTE or SFME. Direct sampling ionization methods such as paper spray and paper capillary spray have already begun to introduce automated workflows and cartridges—both of which represent a significant step in advancing direct sampling ionization miniature MS systems. The next step would be to automate SFME and PCTE, both of which cover a wide range of biomolecules that cannot be analyzed by paper spray. The eventual automation and device development of these methods will enable high-throughput direct sampling ionization where only several miniature MS systems are sufficient to handle POC sampling in an outpatient center.

The final hurdle for direct sampling ionization with miniature MS systems is a familiar challenge that also hinders the implementation of MS in clinical laboratories. Even with the improved sensitivities or specificities in their respective settings, there is a significant laboratory-to-laboratory variability and non-standardization of protocols. In part, this stems from the late regulations and recommendations established by the FDA, where most—if not, all— LC-MS/MS methods are developed in-house and evaluated by a case-to-case basis.[1] As a result, methods are scattered and can differ significantly between laboratories and other standardized FDA tests. For laboratories that perform relative quantitation or qualitative experiments without internal standards, the resulting data cannot be shared or data-mined in large-scale cohort studies. The Clinical Laboratory Improvement Act (CLIA) has established guidelines for toxicology, steroid analysis,

and several other types of biomolecules.[2] However, it would be impossible to establish a comprehensive coverage of all molecules analyzable by MS and in extension, miniature MS instruments. For example, protein quantitation and protein biomarker analysis by MS is not approved by the FDA, stemming from the large variability in its operation from lab-to-lab.[3] Furthermore, the market for MS instruments is diverse along with different types of MS instruments. All current MS instruments have their own figures of merit—whether it is higher/lower sensitivity, specificity, tandem MS capabilities, integrated photochemical reactions, etc. For the current state of miniature MS instruments, this is not a pressing issue. However, the future of miniature MS as a POC biomedical testing tool is promising enough where other types of miniature MS instruments being developed and marketed is not inconceivable. Thus, early device, automation, and protocol development of these direct sampling ionization methods to be paired with a standardized miniature MS instrument can play a significant role in emphasizing the unification and adoption of miniature MS as a biomedical testing tool. With these key points in mind, an integrated miniature MS system using direct sampling ionization methods for biomedical testing can be easily expected in the future, following its eventual implementation in a POC setting.

5.3 References

1. Schniedewind, B.; Meyer, E. J.; Christians, U., Long-Term Performance of Laboratory-Developed Liquid Chromatography-Tandem Mass Spectrometry Tests and a Food and Drug Administration-Approved Immunoassay for the Therapeutic Drug Monitoring of Everolimus. *Ther Drug Monit* 2020, 42 (3), 421-426.
2. Lynch, K. L., CLSI C62-A: A New Standard for Clinical Mass Spectrometry. *Clinical Chemistry* 2016, 62 (1), 24-29.
3. Lathrop, J. T.; Jeffery, D. A.; Shea, Y. R.; Scholl, P. F.; Chan, M. M., US Food and Drug Administration Perspectives on Clinical Mass Spectrometry. *Clinical Chemistry* 2016, 62 (1), 41-7.

APPENDIX A. INTRODUCTION SUPPLEMENTAL FIGURES

Table A-1. List of therapeutic and illict drugs that have been analyzed by PSI-MS. Da, Dalton; LogP, partition coefficient; LOD, limit of detection; LOQ, limit of quantitation. Reproduced from *Chiang, et. al.* [1]

Analyte	Drug Class	Molecular Weight (Da)	LogP	LOD / LOQ (ng/mL)
Acetaminophen	Pharmaceutical	151.16	0.5	250
Amitriptyline	Pharmaceutical	277.41	4.92	1
Amphetamine	Illicit	135.21	1.76	1
Anabasine	Pharmaceutical	308.37	3.57	0.1
Atenolol	Pharmaceutical	266.34	0.57	50
Benzethonium	Pharmaceutical	412.637	3.13	0.02
Benzoylecgonine	Metabolite	289.33	1.71	1
Buprenorphine	Illicit	467.64	4.98	1.6
Citalopram	Pharmaceutical	324.39	3.5	0.1
Cocaine	Illicit	303.12	2.3	0.05
Cotinine	Metabolite	176.219	0.07	3,2,5
Cyclophosphamide	Pharmaceutical	261	0.8	11
Cyclosporine	Pharmaceutical	1202.63	3.64	5
Dextromorphan	Pharmaceutical	271.4	3.6	0.6
Docetaxel	Pharmaceutical	807.88	2.4	13
Heroin	Illicit	369.41	1.58	125
Hydralazine	Pharmaceutical	160.176	1	16
Ibuprofen	Pharmaceutical	206.28	3.97	500
Imatinib	Pharmaceutical	493.6	3	9
Irinotecan	Pharmaceutical	586.67	3.2	13
Lidocaine	Pharmaceutical	234.34	2.44	4
MDMA	Illicit	193.24	1.65	0.04
Methamphetamine	Illicit	149.23	2.07	0.3
Morphine	Pharmaceutical /Illicit	285.34	0.89	12
Nicotine	Toxic Alkaloid	162.23	1.17	1
Oxycodone	Illicit	315.36	0.3	16
Paclitaxel	Pharmaceutical	853.9	3	12,15
Pazopanib	Pharmaceutical	437.52	3.59	0.5
Proguanil	Pharmaceutical	253.73	2.53	0.08
Simvastatin	Pharmaceutical	418.57	4.68	50

Sirolimus	Pharmaceutical	914.19	4.3	0.5
Sitamaquine	Pharmaceutical	343.51	5.11	5
Sunitinib	Pharmaceutical	398.47	5.2	0.1
Tacrolimus	Pharmaceutical	804.01	3.3	0.2
Tamoxifen	Pharmaceutical	371.51	7.1	8
Telmisartan	Pharmaceutical	514.62	7.7	0.3
THC	Illicit	314.46	5.65	4
Topotecan	Pharmaceutical	421.45	0.8	17
Verapamil	Pharmaceutical	454.6	3.79	3, 0.75, 0.1

[1] Chiang, S.; Zhang, W.; Ouyang, Z., Paper spray ionization mass spectrometry: recent advances and clinical applications. *Expert Rev Proteomics* 2018, 15 (10), 781-789.

Table A-2. Criteria and optimal values for the development of a novel POC-TB diagnostic test in comparison to the values of current technologies. *POC*, point-of-care; *TB*, tuberculosis; *PET*, positron emission tomography; *CT*, computer tomography; *MTB/RIF*, mycobacterium tuberculosis/rifampicin. * indicates the current gold-standard values for TB diagnostics.

Criteria	**Bacterial Culture**	**Chest X-Ray**	**PET/CT**	**Xpert-MTB/RIF**	**Smear Microscopy**	**Optimal Values**	**Minimum Values**
Sample Type	Sputum/Serum	Visual	Visual	Sputum	Sputum	Minimal to Non-invasive	Sputum
Sensitivity	95-99%*	92%	71-96%	68-88%	52.8%	$> 95\%$ compared to culture	$> 80\%$
Specificity	99%*	63%	40-50%	98%	98.6%	$> 99\%$ compared to culture	$> 97\%$
Time to Result	4-5 Days	$<$ 10 min.	$<$ 60 min.	$<$ 120 min.	$<$ 60 min.	$<$ 20 min.	$<$ 180 min.
Sample Processing	Manual	Manual	Injection	Automated	$<$ 5 Steps	Automated	$<$ 5 Steps
Electronics	Visual / Integrated	Separate	Separate	Separate	None	None / Integrated Device	Separate
Detection	Visual	Visual	Quantitative	Semi-quantitative	Visual	Quantitative	Semi-quantitative
Treatment Monitoring	Yes	No	No	No	No	Yes	No
Reagents	Many	N/A	Radioactive	Integrated	$<$ 4 reagents	Consumables	$<$ 4 external reagents

APPENDIX B. TARGETED PROTEIN AND PEPTIDE QUANTITATION STUDY

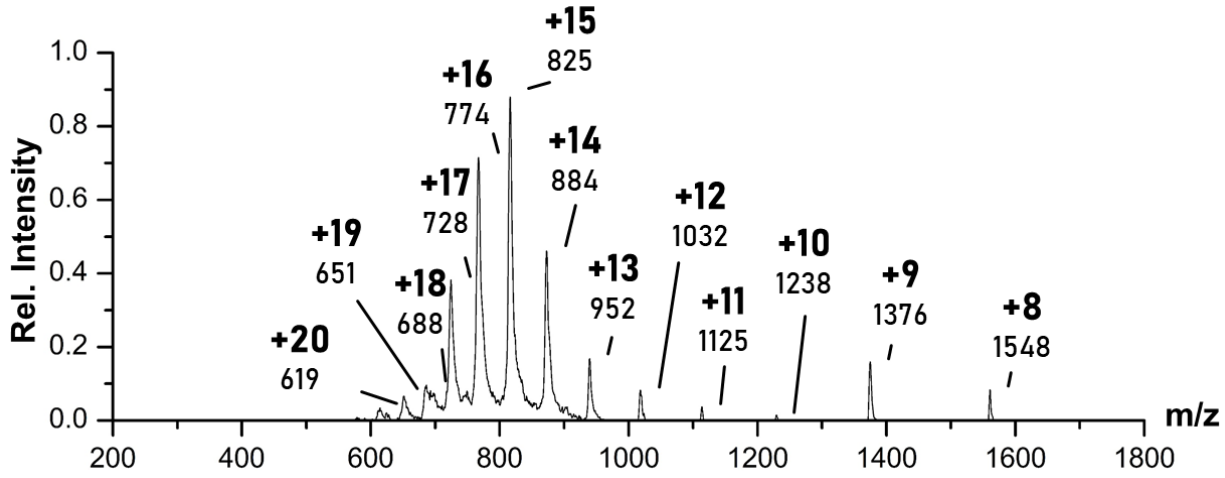

Figure B-1. Cytochrome C —12 kDa, 10 µM— in methanol:water (1/1;*v/v*; 0.5% formic acid) was ionized by nESI and analyzed by our miniature MS instrument. *nESI*, nano-electrospray ionization.

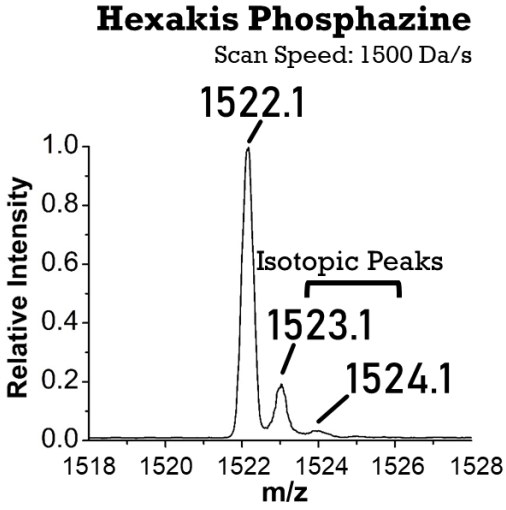

Figure B-2. High-resolution analysis of HEX using a scan speed of 1500 Da/s. Isotopic peaks are clearly resolved from each other illustrating greater than unit resolution. *HEX*, Hexakis(1H, 1H, 5H-octafluoropentoxy)-phosphazine.

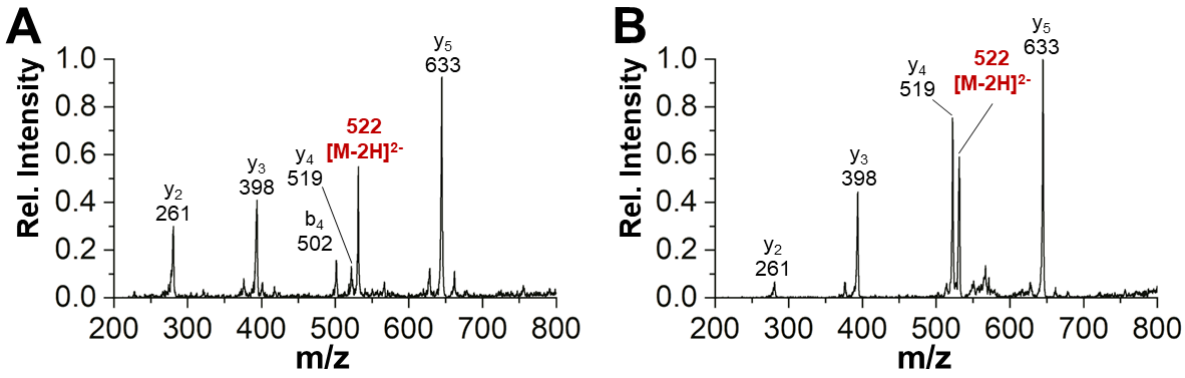

Figure B-3. (a) Beam-type and (b) in-trap CID of *Met* peptide —Sequence: YVNDFFNK. *CID*,collision-induced dissociation.

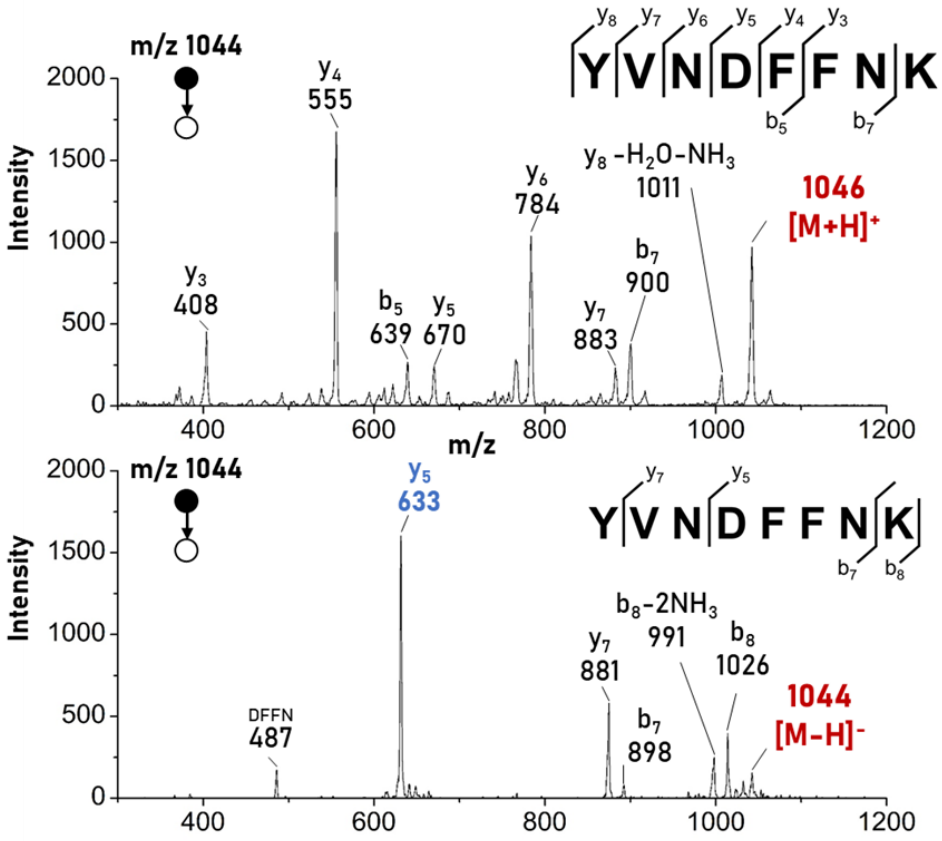

Figure B-4. MS/MS analysis of the *Met* peptide was performed in positive(*top)* and negative (*bottom)* ion modes to highlight the difference in fragmentation pattern. The targeted peptide fragment for quantitation was based upon overall ion intensity and signal-to-noise ratio of the respective spectra. *MS/MS*, tandem mass spectrometry.

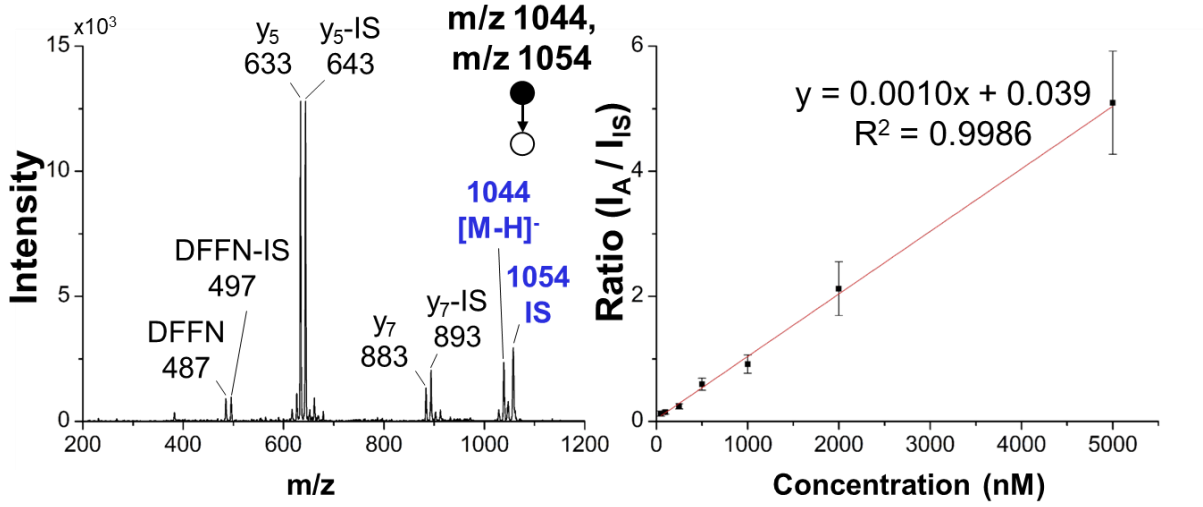

Figure B-5. *Met* peptide and its internal standard in a 10ppm background solution of trypsin-digested mouse liver protein (*left)*. Matrix-matched quantitation curve from 10 nM to 5 µM of *Met* peptide and 1 µM internal standard. (*right)*.

APPENDIX C. POLYMER COATING TRANSFER ENRICHMENT LIPID STUDY

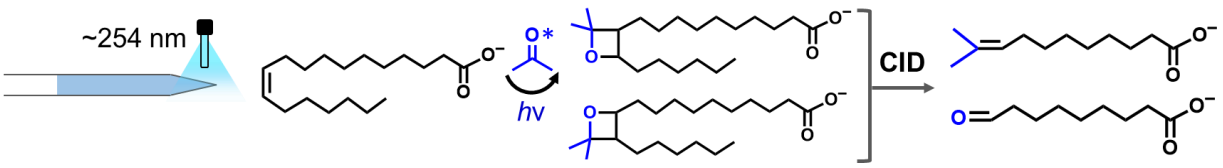

Figure C-1. Schematic of the Paternò-Büchi reaction denoting the acetone addition and the two MS/MS products after performing collision-induced dissociation.

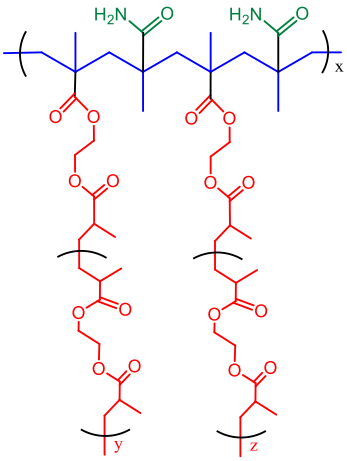

Figure C-2. Chemical structure of polymer for PCTE. Acrylamide backbone (*blue*) forms the base structure of the polymer. Amide groups (*green*) decrease the hydrophobicity of the polymer to improve sample interaction with the polymer. Aliphatic bore *(red)* forms a complementary chemical structure to the fatty acid chains in all classes of lipids.

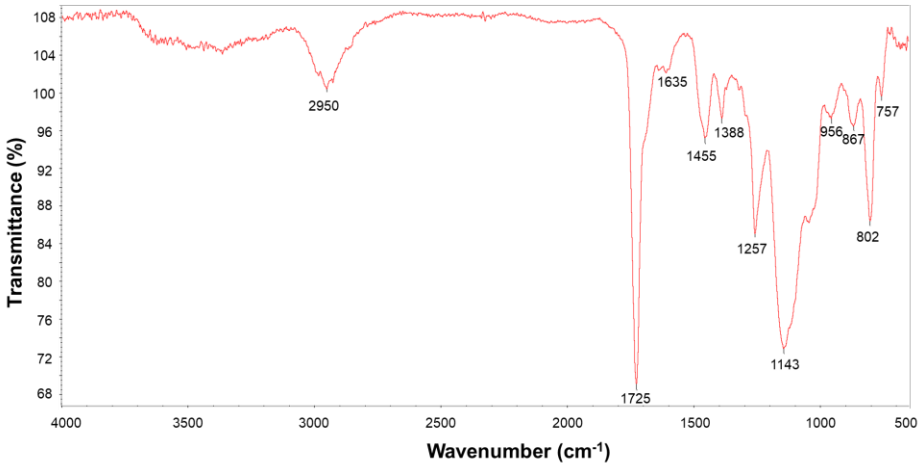

Figure C-3. IR spectroscopy of the formed polymer coating to characterize the chemical composition.

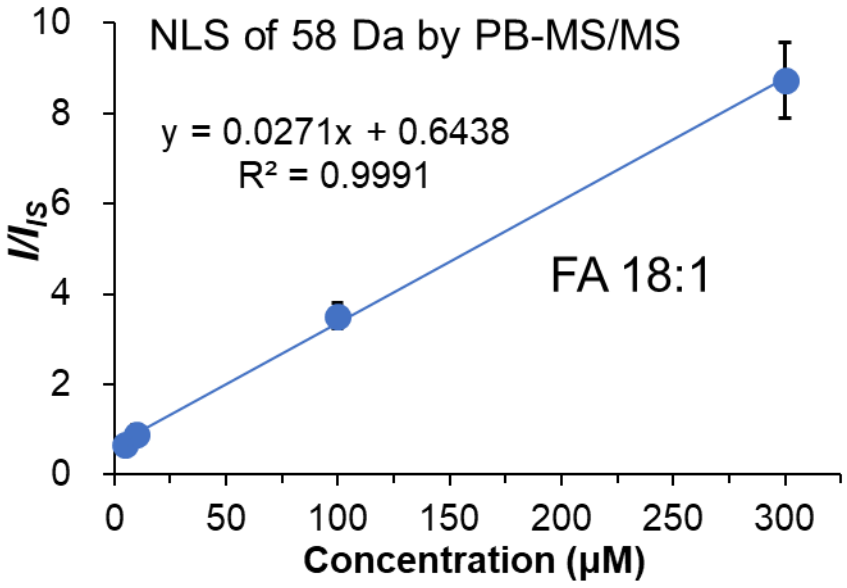

Figure C-4. Quantitation curve of FA 18:1 drawn by monitoring the loss of 58 Da by PB-MS/MS.

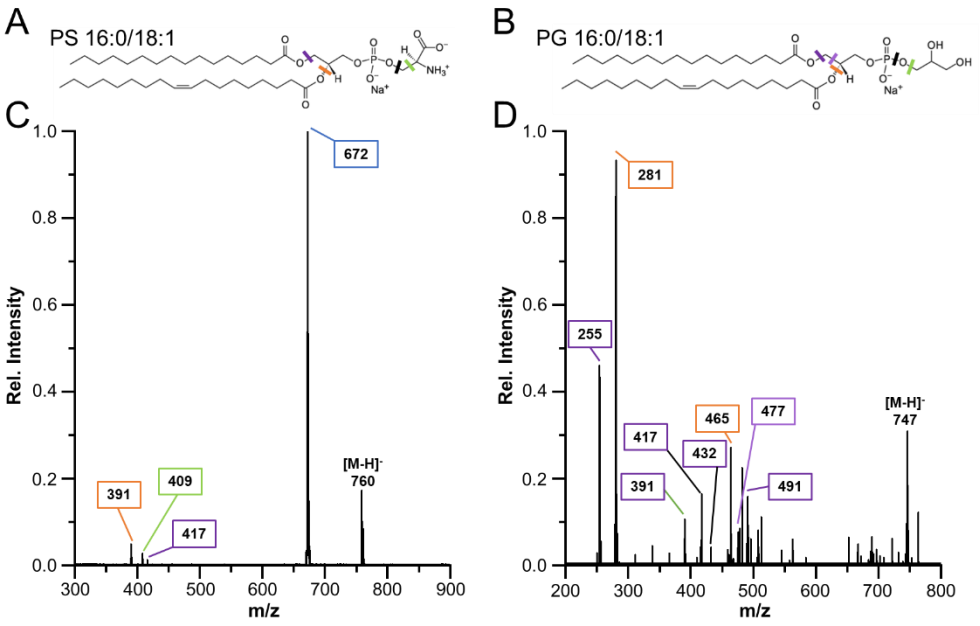

Figure C-5. (a, c) Phosphatidylserine 16:0 / 18:1 chemical structure and its MS/MS spectrum. (b,d) Phosphotidylglycerol 16:0 / 18:1 chemical structure and its MS/MS spectrum. Both lipid standards were analyzed in the negative ion mode. Colored boxes correlate with the bond cleavages denoted by the colored lines on the chemical structures.

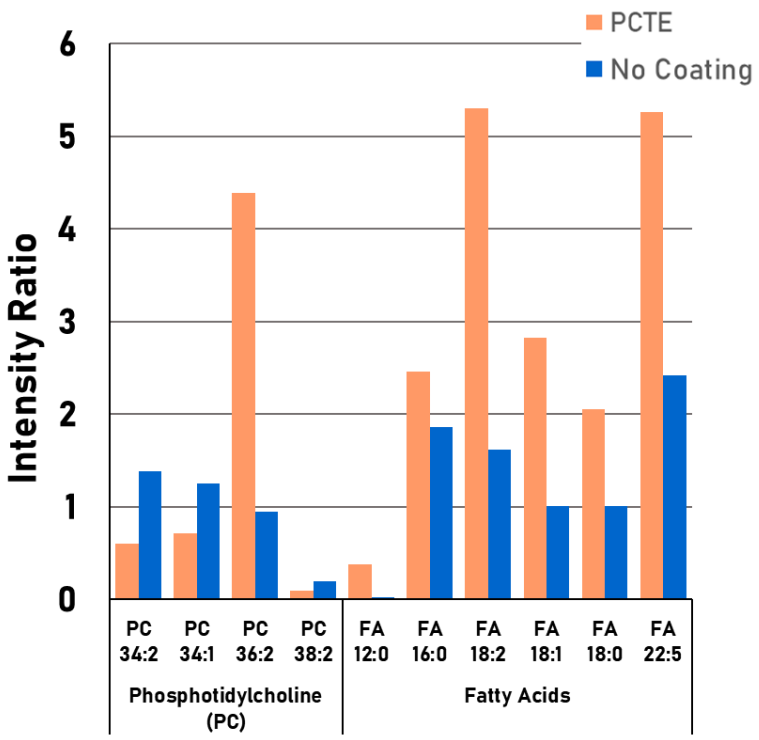

Figure C-6. Intensity ratios between PCTE and no coating—SFME. Intensity ratios were calculated by identifying the peak signal intensity over the highest background peak intensity.

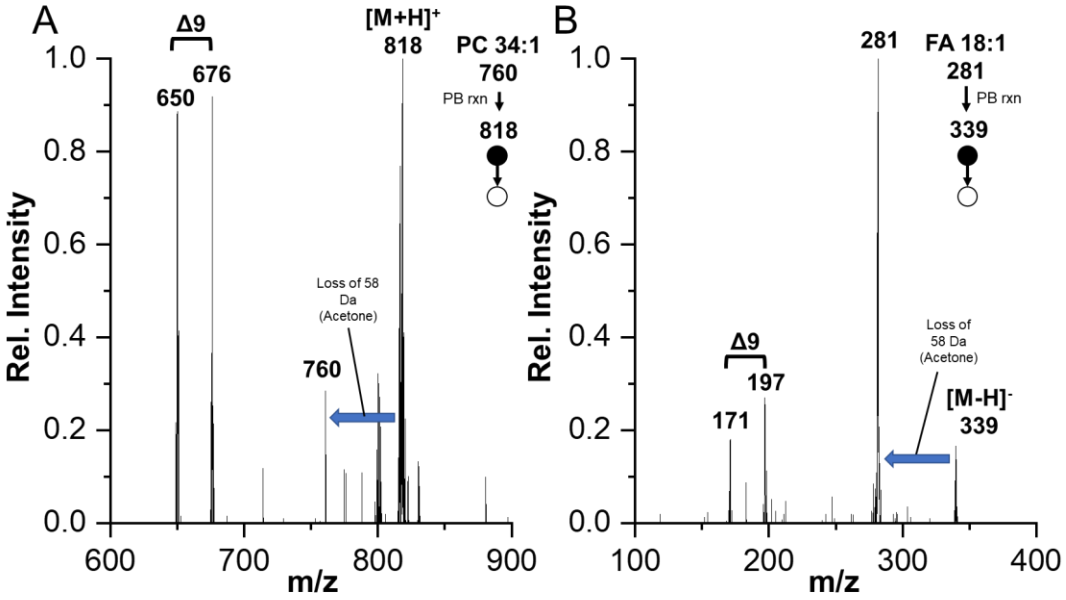

Figure C-7. MS/MS spectra after PB reaction of (a) PC 16:0 / 18:1 and (b) FA 18:1 at a concentration of 10 ppm.

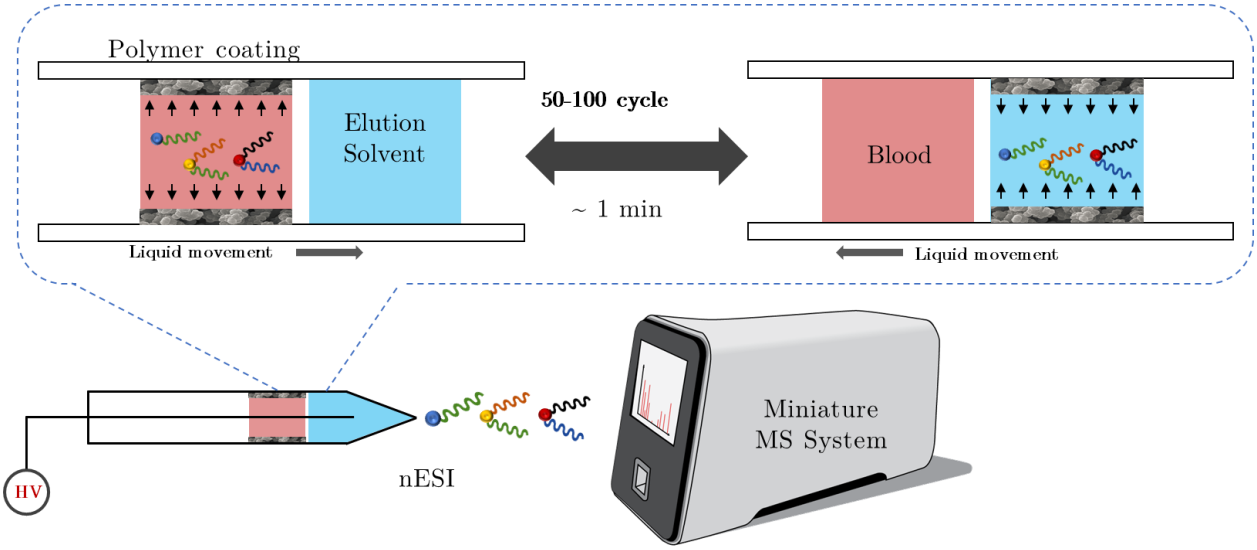

Figure C-8. Sample workflow incorporating the direct sampling ionization method—PCTE— paired to the miniature MS system. *PCTE*, polymer-coating transfer enrichment; *MS*, mass spectrometry.

APPENDIX D. MYCOTOXIN ANALYSIS BY A MINIATUURE MS SYSTEM STUDY

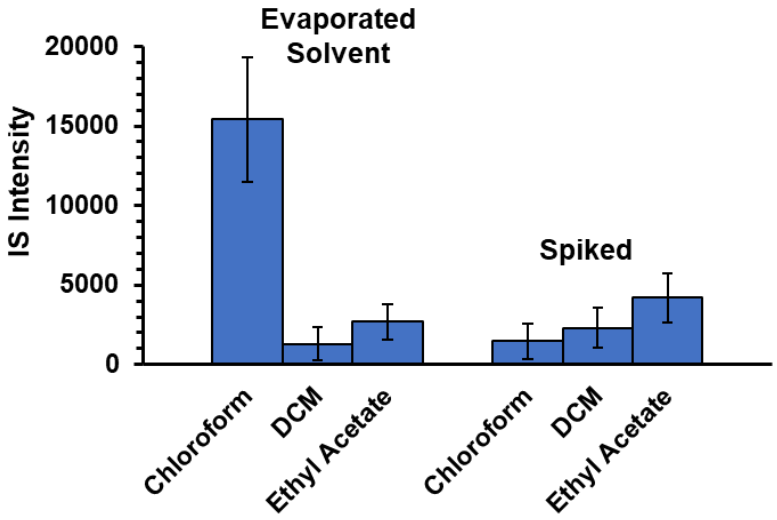

Figure D-1. Average signal intensity for the positive internal standard when extraction solvent is either evaporated or spiked into the internal standard solution. *IS,* internal standard; *DCM,* dichloromethane.

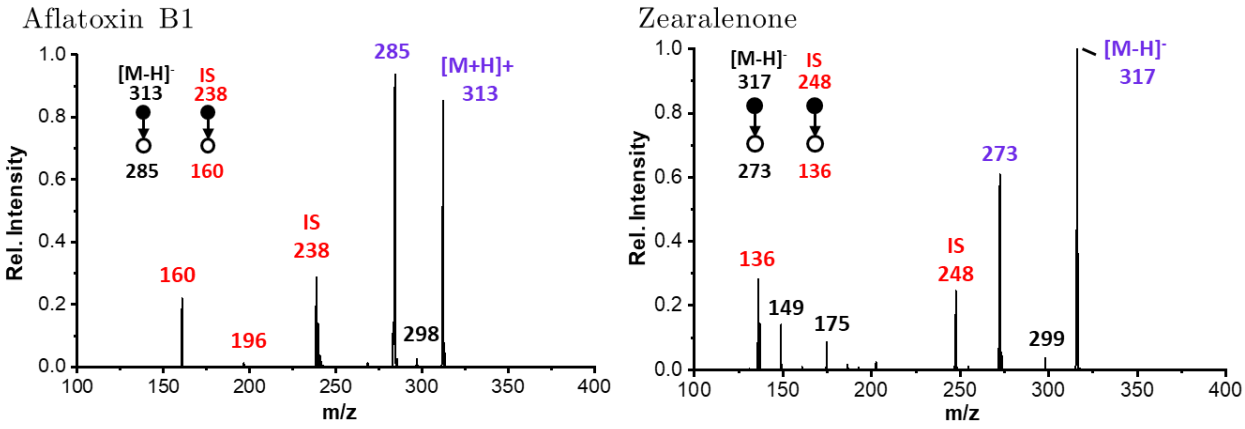

Figure D-2. MS/MS spectra of (*left*) aflatoxin B1 and *(right)* zearalenone along with their respective internal standards.

Table D-1. Selected mycotoxin characteristics, extraction conditions, and analytical results when analyzed in a β-CD matrix by SFME and a miniature MS system. *β-CD*, β-cyclodextrin; *SFME*, slug-flow microextraction; *MS*, mass spectrometry; *LogP*, partition coefficient; *LOD*, limit-of-detection; *LOQ*, limit-of-quantitation; *RSD*, relative signal deviation; *MeOH*, methanol; *AA*, acetic acid; *EA*, ethyl acetate.

Mycotoxin	LogP	Ion Mode	Precursor Ion (m/z)	Product Ion (m/z)	Extraction Solvent	Ionization Solvent	LOD (ppb)	LOQ (ppb)	RSD
Aflatoxin B1 (AB1)	1.6	Pos.	$[M+H]^+$ 313	285	Chloroform (evaporated)	MeOH	20	50	19.7 %
Aflatoxin B2 (AB2)	1.3	Pos.	$[M+H]^+$ 315	287	Chloroform (evaporated)	MeOH	100	200	20.9%
Deoxynivalenol (DON)	- 0.7	Neg.	$[M+CH_3COO]^-$ 355	295	Ethyl Acetate	MeOH w/ 1% AA (mixed with EA)	250	500	20.5%
Zearalenone (ZEA)	3.6	Neg.	$[M-H]^-$ 317	273	Ethyl Acetate	MeOH (mixed with EA)	5	10	27.1%

Table D-2. Analysis of different sample matrices spiked with Zearalenone. % error calculated based on intensity ratio to the intensity ratio calculated from the generated calibration curve.

Matrix	Intensity Ratio (I_A/I_{IS})	RSD	% Error
Dry Milled Corn	0.764	36.6 %	5.35
Corn Starch	0.56	30.4 %	10.89
Flour	0.720	29.1 %	6.43

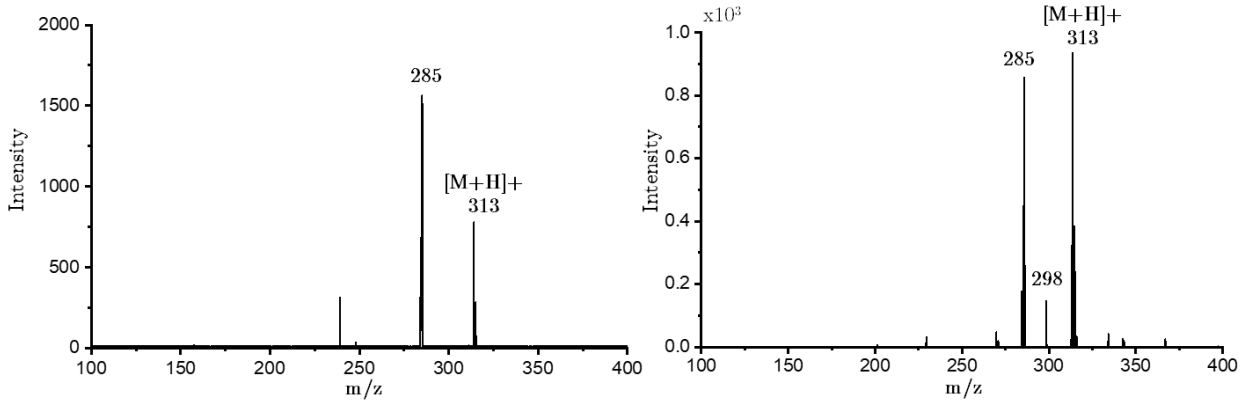

Figure D-3. Resulting spectra of 100 ng of AB1 deposited onto the surface of a corn kernel. (*left*) Surface analysis by depositing 100 µL of β-CD solution throughout the kernel surface. *(right)* Surface analysis of pre-loaded SFME capillary. The overall signal intensity is increased by five-fold when compared directly.

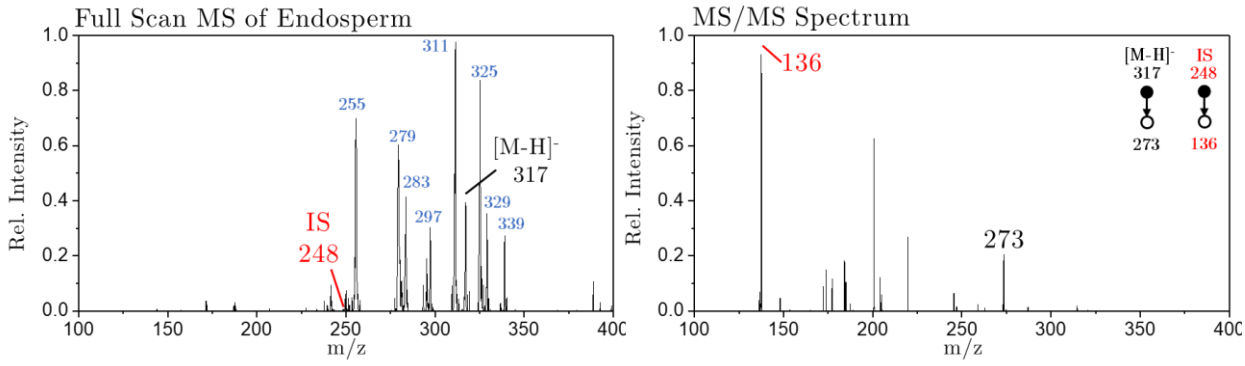

Figure D-4. (*left*) Full scan MS and *(right)* MS/MS spectrum of corn endosperm spiked with 5 ng of ZEAR.

PUBLICATIONS

Articles

1. **Chiang, S.**; Zhang, W.; Farnsworth, C.; Zhu, Y.; Lee, K.; Ouyang, Z., Targeted Quantification of Peptides Using Miniature Mass Spectrometry. *J Proteome Res* 2020, 19 (5), 2043-2052.
2. **Chiang, S.**; Zhang, W.; Ouyang, Z., Paper spray ionization mass spectrometry: recent advances and clinical applications. *Expert Rev Proteomics* 2018, 15 (10), 781-789.
3. Pu, F.; **Chiang, S.**; Zhang, W.; Ouyang, Z., Direct sampling mass spectrometry for clinical analysis. *Analyst* 2019, 144 (4), 1034-1051.
4. Ren, Y.; **Chiang, S.**; Zhang, W.; Wang, X.; Lin, Z.; Ouyang, Z., Paper-capillary spray for direct mass spectrometry analysis of biofluid samples. *Anal Bioanal Chem* 2016, 408 (5), 1385-90.
5. Zhang, W.; **Chiang, S.**; Li, Z.; Chen, Q.; Xia, Y.; Ouyang, Z., A Polymer Coating Transfer Enrichment Method for Direct Mass Spectrometry Analysis of Lipids in Biofluid Samples. *Angew Chem Int Ed Engl* 2019, 58 (18), 6064-6069.
6. Zhou, X.; Liu, X.; **Chiang, S.**; Cao, W.; Li, M.; Ouyang, Z., Stimulated Motion Suppression (STMS): a New Approach to Break the Resolution Barrier for Ion Trap Mass Spectrometry. *J Am Soc Mass Spectrom* 2018, 29 (8), 1738-1744.
7. **Chiang, S.**; Zhang, W., Ren, Y.; Ouyang, Z. Rapid Analysis of Mycotoxins using Direct Sampling Ionization with Miniature Mass Spectrometry Systems. *(In progress)*

Textbook Chapter

1. **Chiang, S.**; Zhang, W.; Ouyang, Z.; Chapter 5: Mass Spectrometry and Applications. *Henry's Clinical Diagnostics and Management by Laboratory Methods 24th ed, Elsevier*. *(In progress)*